Cbx7 Represses Cancer Stem Cell Phenotype in Tera2 Through Inhibition of Wnt Signaling

by
André Rashad Kydd

A dissertation submitted to Johns Hopkins University in conformity with the requirements for the degree of Doctor of Philosophy

Baltimore, Maryland
March, 2014

(Intended to be Left Blank)

Abstract

Epigenetics has been defined as heritable changes in cell phenotypes and attendant gene expression patterns that do not directly alter the nucleic acid base sequence. Several interdependent processes are currently classified as epigenetic, such as DNA methylation, nuclear positioning and covalent modifications of histone proteins, interaction with non-coding RNA species, and higher order organization of nucleic acid in the nucleus. This thesis centers on the activities of key players in maintenance of epigenetic imposition of gene silencing, the repressive Polycomb group proteins and DNA methylation. Both mechanisms serve as major regulators of normal developmental processes and have interactive roles in cancer as potential mediators of abnormal gene silencing and associated altered DNA methylation of normally unmethylated regions such gene promoter CpG islands. Our lab has previously reported on the polycomb complex, PRC1, and specifically the protein CBX7, and its role in initiating DNA methylation at cancer-specific genes in Tera2 embryonal carcinoma cells. Tera2 has been shown to differentiate to neuronal cells in response to exposure to all-*trans* retinoic acid (ATRA), but in CBX7-overexpressing Tera2, a small "outgrowth" subpopulation exhibits retinoid resistance after 3 weeks of ATRA exposure. When withdrawn from ATRA exposure and subsequently re-exposed, the majority of Cbx7 outgrowth cells again show sensitivity to the differentiating effects of ATRA, but again forms a retinoid resistant subpopulation. The CBX7 and CBX7 outgrowth populations exhibit reduced tumorigenicity in NOD/SCID mice. We link CBX7 overexpression to suppression of both canonical and non-canonical Wnt signaling pathways, owing in part to transcriptional repression and

associated DNA methylation of the LEF1 enhancer protein and cJUN transcription factor. In the above Tera2 model, the unresponsiveness of the Wnt pathway induced by CBX7 may represent an altered epigenetic state associated with a less tumorigenic state with a new pattern of cancer-specific promoter CpG island DNA hypermethylation.

First Reader/Advisor: Stephen B. Baylin, M.D.

Second Reader: Robert A. Casero, Ph.D.

Acknowledgements

I would like to thank Stephen B. Baylin for the opportunity to work under his mentorship. Our discussions of the literature and experimental design played an invaluable role in my growth as a researcher. I am grateful to the contributions of my Thesis Committee Members, Dr. Robert Casero, Dr. Saul Sharkis, and Dr. David Berman. Their regular insights helped to propel me forward on this project and other areas of research.

There are many people within the Tumor Biology Department that provided invaluable support to this project. First and foremost, I have to thank Dr. Cynthia Zahnow, who provided valuable feedback and guidance for the xenograft experiments, as well as members of her lab- James Shin, Kirsten Harbom, and Robert Beaty- that helped conduct the xenografts experiments. I am also grateful to the faculty members of the Tumor Biology Department that have also provided valuable insight into my projects. I would not have been able to reach this point without their mentorship, guidance, teaching, and support that I received on a regular basis from the fellow graduate students, postdocs, and staff in all of the labs of the Department. Many thanks to Ray-Whay Yen for management and overseeing many aspects of the Department's cell culture operations. I also have to thank Tina Largent for ordering supplies and lab management. I have to thank the wonderful administrators of the department, Kathy Bender and Tammy Means, for all the work they perform to support the functioning of the lab. In addition, I think them for years of wonderful memories during my time in the lab.

Table of Contents

List of Tables

List of Figures

(Intended to be left blank)

Chapter 1

Introduction

Epigenetics Overview

Epigenetics has been defined as heritable changes in DNA structure that do not directly alter the nucleic acid base sequence (1). Several processes are currently classified as epigenetic, such as DNA methylation, nuclear positioning and covalent modifications of histone proteins, interaction with non-coding RNA species, and higher order organization of nucleic acid in the nucleus. These interconnected processes work to regulate normal development, differentiation, and responses to environmental stress and stimuli, while abnormalities in these systems contribute to cellular dysfunction and disease (2).

Histone Modifications and Polycomb Group Proteins

Histone modifications play a major role in epigenetic regulation. Histone core octamers- 2 units each of the H2A, H2B, H3, and H4 protein- are encircled by approximately 150 base pairs of helical DNA to form nucleosomes (3-5). The linear arrangement of histones along DNA, and their degree of density, correlates with level of expression. Regions of DNA with highly condensed nucleosomes correlate with heterochromatin, while areas with sparse nucleosomes- open chromatin- are transcriptionally competent. The N-terminal end of histone peptides, often known as histone "tails," extend away from the octamer core. The side groups of amino acids on histone tails are subject to a wide range of covalent modifications, including methylation, acetylation, ubiquitination, and phosphorylation (6). The effect of each modification is

dependent on the relative position of the modified amino acid in the histone's peptide sequence. The addition and removal of these histone marks are catalyzed by enzyme complexes that "write" or "erase" these modifications in a regulated fashions at different locations throughout the epigenome (7-9).

One major histone mark is the acetylation of lysine side chains. Histone acetylation is typically found in areas of open chromatin, and often associated with active transcription or enhancer elements (10-14). Unmodified lysine residues on histone tails counteract the negative charge of phosphate groups in the backbone of DNA. It is believed that the addition of neutral acetyl groups eliminates these positive charges, making compaction of negatively-charged DNA more difficult (15). Given the need for accessible chromatin with transcription, histone acetyltransferases (HAT), most notably P300, are often associated with transcriptional co-activators (16-17). On the other hand, removal of acetyl groups by various histone deacetylases (HDACs) is often associated with the repression of transcription (18, 19).

Another major class of modifications is histone lysine methylation. The effects of histone methylation are dependent upon both the position of the modified lysine residue, as well as the number of methyl groups added to that lysine (20). For example, di and tri-methylation of lysine 4 of H3 (H3K4) is typically associated with actively transcribed genes (21), while H3K4 monomethylation is commonly found at enhancer elements (22, 23). H3K27 and H3K9 methylation are associated with repressed chromatin (20), but methylation of H3 lysine 36 found within the gene body of active genes, promotes transcriptional elongation, and blocks abnormal initiation of cryptic transcription within genes (24, 25). The histone lysine methyltransferase and demethylase enzymes are

typically associated with protein complexes that contribute to their recruitment to the proper genomic locations, help to refine the specificity of enzymatic action, and facilitate the activating or inhibitory functions of the complexes (26, 27). For example, regulatory complexes with repressive effects on transcription can recruit histone lysine demethylases that remove modifications associated with active transcription (28), while also associating with methyltransferases that catalyze the addition of repressive lysine methylation (29-31).

These histone marks are specifically bound by several proteins with conserved protein motifs. The functional consequences of any of these marks are often defined by chromatin-associated proteins that "read" histone modification, i.e. their binding affinity with histone tails is altered. For example, proteins with the chromodomain or bromodomain protein motif bind methylated lysines or acetylated lysines, respectively (7, 9, 32). Minor sequence differences within chromodomain motifs allow a distinction between modifications that should lead toward that transcriptional repression *versus* activation of the underlying genetic material (8). These differences are crucial for the divergent effects of active histone methylation, such as H3K4, and repressive marks, such as H3K9 and H3K27 (2). The composition of the protein complexes- including catalytic subunits that deposit or remove modification and components that recruit other chromatin modifiers- lead to the downstream effects on local epigenetic landscape and gene expression.

In addition to histone tail modifications, the location and density of nucleosomes along the DNA molecule has a significant impact on transcription. Regions of DNA with dense, highly-ordered nucleosomes- termed "heterochromatin"- typically have low

expression of the genes encoded in these areas. In contrast, areas with more sparse arrangement of nucleosomes have a greater degree of accessibility for transcription factors- termed "euchromatin"- are often associated with genes with higher levels of expression (or the greater ability to induce these genes in response to signaling or other stimuli) (6). Proteins that bind repressive histone marks, such as the HP1 family, can facilitate the condensation of nucleosomes and drive the formation of heterochromatin (7, 8). The recruitment of chromatin-remodeling complexes can also alter the nucleosome landscape to either promote or suppress transcriptional activity (13). Some of these remodeling complexes, such as Swi/SNF, require energy in the form of ATP hydrolysis to carry out these functions (2, 33).

The Polycomb group proteins demonstrate a major class of histone modifying proteins whose repressive function highlights the critical role for epigenetic regulation during development. The founding member of the group, Polycomb, was discovered as a mutant leading to alteration of *Drosophila melanogaster* body segmentation patterns, manifested as in increase in the number of sex combs on the Drosophila leg. This phenotype was attributed to alteration of homeotic gene clusters (Hox genes) responsible for anterior-posterior body planning in *Drosophila* (34). The various Polycomb proteins act in complexes (35), and are typically divided into two groups: Polycomb Repressive Complex (PRC) 1 and PRC2. PRC1 contains Ring1A/B, Ph, Pc/Cbx (homologs of dRing, Posterior Sex Combs [Psc], Polyhomeotic [Ph], and Polycomb [Pc]), while PRC2 contains Ezh2, Eed, Suz12, RbAp48 and RbAp46. Ezh2 (and Ezh1) of PRC2 contains histone methyltransferase activity against lysine 27 of Histone 3 (H3K27), while Ring1B contains ubiquitin ligase activity against lysine 119 of Histone 2A (H2A-K119) (36).

PRC1 components subsequently bind to the H3K27me3 site via the chromodomain of a Polycomb homolog, where it catalyzes the ubiquitination on H2A (36), which might interfere with nucleosome position or RNA polymerase function. Other reports suggest that PRC1 can also block transcriptional elongation. Biochemical data from *Drosophila* also suggests that PRC1 can in fact condense nucleosomes, even in the absence of histone tails, suggesting an additional mechanism to promote transcriptional repression (36). Both PRC1 and PRC2 associate with HDACs, which also promote chromatin condensation and repressive function (37). A variant of PRC2 – PRC4 – may also contain the SirT1 histone deacetylase, and may have different histone targets from the PRC2 complex (38). In vertebrates, several core Polycomb group proteins contain many related paralogs, potentially increasing the complexity of regulation achievable by different Polycomb complexes (39). Importantly, Polycomb group proteins have been shown to regulate a wide range of developmental regulators in a wide range of organisms (29, 40, 41).

Canonical models of Polycomb-mediated repression state that PRC2 is initially recruited to a site of silencing and catalyzes the trimethylation on H3K27 (H3K27me3). In Drosophila, a defined consensus DNA sequence – the Polycomb Response Element (PRE)- has been shown to play a major role in promoting the recruitment of the Polycomb complexes. While no such sequence has been identified in mammalian cells, several other mechanisms have been proposed. Some DNA motifs within the HoxC cluster have been identified as recruiters of Polycomb complexes (42). One particular protein- Polyhomeiotic (Pho) directly binds DNA at a defined sequence (43). Numerous long non-coding RNAs have been demonstrated to bind to PRC2 and PRC1 complexes.

The Xist/Tsix double-stranded RNA contributes to the recruitment of Polycomb complexes during random X-inactivation in mammalian female homozygotes (44, 45). HOTAIR, an antisense transcript from the mammalian HOXC cluster, binds PRC2 components Suz12, and facilitates silencing of the HOXD cluster in *trans* (46, 47). Other long non-coding RNAs, such as ANRIL (at the p16 locus) and MOV10 have been shown to interact with members of the PRC1 (48-50).

DNA Methylation

In mammalian cells, the majority of DNA methylation occurs at the 5-position of cytosine bases, most often in the context of 5'-CpG-3' dinucleotide sequences (51). This reaction is catalyzed by DNA methyltransferase (DNMT) enzymes, which utilize S-adenosylmethionine as the donor for the methyl group. In mammalian cells, the primary DNMTs are DNMT1 and DNMT3a/b. DNMT3a and DNMT3b are considered be "*de novo*" methyltransferases, as they have a greater ability to add methyl groups to unmethylated CpG dinucleotide targets. DNMT1 is considered the "maintenance" DNMT, as it has far greater methyltransferase activity on hemimethylated CpG sites than unmethylated sites (52). However, additional studies suggest that there is significant overlap in maintenance and *de novo* DNA methylation functions between DNMT1 and DNMT3b (53). CpG dinucleotides are often clustered at or near the promoters of many genes- known as "CpG islands" and in repetitive sequences (52, 54). Most cytosine bases within CpG islands are unmethylated, but CpG methylation is found within the open reading frame of genes (55). On the other hand, many repetitive elements (e.g. Long

Interspersed Repetitive Elements, LINES) within the human genome contain dense methylation and exist within heterochromatin (56). There is also evidence for non-CpG cytosine methylation (e.g. CpHpG, CpHpH, where "H" represents C, A, or T nucleotides) in mammalian embryonic stem cells, which is predominantly found in gene exons and introns and decreases upon differentiation. While non-CpG methylation is more common in plants (57, 58), the mechanism(s) for maintaining this form of methylation and its functional role in stem cells remain to be elucidated (51).

While DNA methylation has long been considered a highly stable mark over time, the discovery of active DNA demethylation and additional covalent modifications of cytosine nucleotides has altered our view of DNA methylation. Most demethylation is thought to occur passively, when DNA methylation patterns are not maintained over several rounds of DNA replication and cell division. DNA demethylases, such as members of the Ten-Eleven Translocase (TET) family, catalyze the oxidation of 5-methyl cytosine, and, to a lesser extent, 5-formylcytosine and 5-carboxylcytosine (59). It is believed that the oxidation products of 5-methylcytosine (5-hydroxymethylcytosine, 5-formylcytosine, 5-carboxycytosine) are targets of base-excision repair, leading to their replacement with an unmodified (unmethylated) cytosine base (60). In embryonic stem cells, TET proteins are enriched at developmental regulators and appear to facilitate normal DNA methylation patterns in conjunction with DNMTs (61). The exact mechanisms that promote this repair process and any unique function(s) of these cytosine bases with more extensive oxidation are also under intense investigation.

Despite the wealth of knowledge about DNA methylation, the process(es) that initiate aberrant *de novo* DNA methylation patterns in mammalian cells are an area of

active research study. DNMTs are not considered to have intrinsic sequence specificity. In other organisms, non-coding RNA/ double-stranded RNA and histone modifications have been causally linked to DNA methylation (52, 57). Interaction between the histone modifications and DNA methylation machinery remains a central theory of the field. The enzyme G9a, which catalyzes the methylation of lysine 9 on histone 3 (H3K9), has been shown to promote the recruitment of DNMT3a and 3b during differentiation, linking this repressive mark to *de novo* DNA methylation (62). Given their importance in the repression of developmental regulators, Polycomb group proteins are regarded as playing in important role in this process. Some studies have suggested a role for the PRC2 catalytic component Ezh2 in recruitment of DNMT1 (63), and additional studies have strengthened the link between methylation of H3K27 and DNA methylation (64, 65). However, other studies have suggested that additional factors mediate this process (66, 67). Ohm et al. have previously shown that genes that are prone to DNA methylation in adult cancers are highly enriched for "bivalent" genes, which typically exhibit relatively low levels of expression and carry both repressive H3K27 methylation and the active H3K4 di and tri-methylation modifications in the vicinity of their transcriptional start site (68, 69). Transcription factors and other developmental regulators are highly enriched among bivalent domains, and during the course of differentiation and lineage commitment, these regulators resolve into a "monovalent" histone pattern- either harboring the active H3K4 methylation pattern alone, or the repressive H3K27 methylation. Further studies in our lab have highlighted the tendency for such bivalent genes to gain promoter hypermethylation in cancer (70).

Epigenetics and Cancer

Epigenetic dysregulation, both with respect to DNA methylation and histone modifications, has been shown to play a role in many diseases, most notably in cancer. Cancer cells typically exhibit significant shifts in DNA methylation. Many genes, particular tumor suppressors, show increased methylation in CpG islands within promoter regions, while showing hypomethylation of CpG dinucleotides in many areas of the genome away from CpG islands. This promoter hypermethylation strongly correlates with transcriptional repression of the gene, but only occurs in a small portion of CpG islands (2). In some cases, loss of gene function by promoter hypermethylation in one allele is accompanied by genetic abnormalities, such as point mutation or chromosomal deletion, of the second allele (55). While other researchers have highlighted the role of prominent "driver" mutations that occur with high frequency in cancer (71), several of these genes actually show a frequency of DNA hypermethylation higher than genetic defects (72). However, many defects observed in cancer affect both the genome and epigenome. Hypermethylation of some DNA repair factors promote genomic instability, leading to both more genetic abnormalities (73), as well as sensitivity to chemotherapeutic agents that generate DNA damage (55, 74). In addition, some mutations directly impact the epigenome, as proteins involved in epigenetic regulations are themselves targeted for mutation (75). Interestingly, neomorphic mutations of the Isocitrate Dehydrogenase 1 and 2 (IDH1 and IDH2) enzymes lead to a hypermethylation phenotype in leukemia (76). Mutant IDH1/2 generate 2-hydroxyglutarate instead α-ketoglutarate, a necessary co-factor for the the enzymatic activity of TET2 and other

histone lysine demethylases (26, 76). These studies link both abnormal active DNA demethylation and cellular metabolic abnormalities to the promoter hypermethylation observed in cancer and blocks in differentiation.

Members of our lab have also shown the link between inflammation and promoter hypermethylation. There is a well-known link between chronic inflammation/infections and carcinogenesis (77). In addition to the wide range of viral products that drive cellular growth, inflammation also targets the epigenome. DNA damage is frequently generated from reactive oxygen species (ROS) from immune system cells. O'Hagan et al. were able to demonstrate the recruitment of PRC4 components and DNA methyltransferases to the site of an induced double-strand break (78). In response to oxidative damage from hydrogen peroxide, there were global shifts in PRC4 members and DNMT1 and DNMT3b to GC-rich areas of the genome, with increases in DNA methylation in the promoters of genes with low overall levels of expression (79). Berman et al. have also linked the nuclear lamina localization of genes to genome-wide shifts in DNA methylation. Partially methylated domains, which represent large regions of hypomethylated DNA with spikes of DNA hypermethylation at CpG islands, show significant overlap with lamina-associated domains and regions of DNA that replicate later in S phase during mitosis in colorectal cancer cells when compared with normal colon (80).

The role of epigenetics in defining cellular phenotype has taken on renewed interest in light of the "cancer stem cell" theory of tumorigenesis. Traditionally, tumors have been thought to emerge as a clonal population as cells sequentially acquire mutations. However, researchers have gained a greater understanding of the

contributions of both genetic and epigenetic aberrations to tumor heterogeneity. In recent years, increasing evidence has shown that small subsets of tumor cells – termed "cancer stem cells" or "tumor-initiating cells"– were responsible for these properties of tumors (81, 82). Studies on numerous tumors have demonstrated the ability to isolate minor subpopulations that are able to regenerate the cellular heterogeneity exhibited by the tumor of origin in serial xenograft models (83, 84). In this sense, they match two cardinal features of stem cells – the ability to both self-renew and to differentiate. Furthermore, these subpopulations tended to resemble – in expression of embryonic and early developmental signaling pathways, morphology, and surface markers (68, 82, 85, 86) - more primitive and/or undifferentiated cells of that tissue of origin. This finding led researchers to propose that these tumor initiating cells might, in fact, be derived from adult stem cells and/or other undifferentiated/primitive cell types through mutations or epigenetic alterations. In addition, the "cancer stem cell" theory helped to explain the clinical behavior of many tumors (87). Many chemotherapeutics target cancer cells by active cellular processes such as DNA replication or mitosis. While such drugs could destroy terminally differentiated or actively-dividing cells, cancer stem cells may be relatively quiescent. Therefore, they would remain less susceptible to such cytotoxic agents. Given their nature as stem cells, they would be capable of differentiation, leading to the re-emergence of tumors, as well as self-renewal.

Despite this evidence, there are still multiple arguments against the "cancer stem cell" hypothesis. Kern et al. highlight the difficulties in identifying and accurately measuring the precise proportion of tumor cells within a given tumor, the inaccuracies in using surface markers, and tumorigenic potential of "non-stem" cells (88). In addition, it

is usually impossible to isolate truly pure populations of stem cells with commonly used markers. Reduced but measureable levels of tumor formation in "non-stem cell" fractions of heterogenous populations suggest that presence of multiple determinants of a cell's ability to form tumors, which may not neatly coincide with the presence of known markers (88).

Dysregulation of the Polycomb group proteins further support the cancer stem cell hypothesis. It is believed that the gene expression changes caused by Polycomb dysregulation contribute to the undifferentiated phenotype that is a hallmark of cancer. Abnormal control of Polycomb contributes to blocks in differentiation that increase tumorigenicity (43), and many individual Polycomb components are overexpressed in cancer (89-91). Along the same lines, other studies have demonstrated the selection of drug-resistant populations, facilitated by epigenetic regulators. These cells, in turn, are left to regenerate the tumor, ultimately leading to clinical relapse (87) (and references therein). Sharma et al. have demonstrated the development of chemotherapy-resistant cell lines (e.g. EGFR and MET kinase inhibitors, RAF inhibitors), which required higher levels of the histone demethylase Jarid1A (KDM5A), as well as IGF-1R signaling (92). In some cases, these subpopulations were also enriched for the CD133 tumor marker. As previously mentioned, the re-distribution of Polycomb proteins in the context of cellular stress appears to increase promoter DNA methylation of susceptible targets, particularly those with low levels of expression (79).

The major contributions of epigenetic regulation of cellular dysfunction represent an opportunity for clinical application of drugs that modify the epigenome. The elimination of these stem cells may be achieved by impairing the abnormal epigenetic

programs that sustain these subpopulations of cells (87, 93). Demethylating agents, such as the nucleotide analogs 5-aza-cytidine and 5-aza-2'-deoxycytidine (94), have already been approved by the FDA for use in treating myelodysplastic syndrome (95). The application of demethylating agents and HDAC inhibitors in solid tumors, either alone or as a sensitization agent for other chemotherapies, is already underway (55, 96). Exploring how the various systems of epigenetic regulation not only provides greater understanding of the dynamic working of cells, but also provides exciting opportunities for improving cancer care and treatment.

Chapter 2

CBX7 Reduces Tera2 Tumorigenicity

Abstract (Chapter 2)

Past research has demonstrated a strong association between histone modifications catalyzed by the Polycomb group complexes and cancer-associated DNA hypermethylation. Our previous studies in Tera2 have demonstrated increases in DNA methylation with the overexpression of CBX7 in the Tera2 teratocarcinoma cell line. Despite cancer-specific patterns of promoter hypermethylation, Tera2 cells with CBX7 overexpression exhibit resistance to retinoic acid-mediated differentiation, but increased latency of subcutaneous tumor formation and decreased frequency of tumor formation. We have linked this to promoter hypermethylation and repression of JUN and LEF1, the downstream DNA-binding effectors of the canonical and non-canonical Wnt signaling. Although we have demonstrated the repression and DNA methylation of CD44, an important stem cell marker and transcriptional target, we show that repression of this specific target may not be solely responsible for the reduced tumorigenicity. Lentiviral knockdown of CD44 reduces *in vitro* sphere formation, but does not reduce tumorigenicity in xenograft studies. We hypothesize that other targets of the Wnt pathway, or other signaling pathways important for tumorigenicity and/or stem cell phenotype, may be responsible for these effects. However, the unresponsiveness of the Wnt pathway induced by CBX7 may represent an altered epigenetic state associated with a less tumorigenic state with a new pattern of cancer-specific promoter CpG island DNA hypermethylation.

Introduction

Despite the long history of research on the Polycomb Group proteins, many aspects of Polycomb Repressive Complex (PRC) function remain unclear. There is significant conservation between the Polycomb complexes expressed in Drosophila and those found in mammalians cells. The PRC4 complex as previously been defined as a variant of the canonical PRC2 complex. The PRC4 variant complex has been defined as one that contains the SirT1 class III histone deacetylase, as well as novel isoform of the Eed accessory protein, which utilizes an alternative translational start site (38).

More recently, there have been new discoveries in the role of variations in PRC1 composition. Gao et al. have shown unique PRC1-like complexes: every complex contains Ring1b, which catalyzes the ubiquitination of H2A, but other accessory components of PRC1- such as the Polycomb group Ring Fingers (PCGF homologs), chromobox (i.e. Cbx) family, and RYBP- bind in a mutually exclusive pattern and localize to unique clusters of genes (97). Among mouse Cbx family members, there are also differences in binding affinities to RNA and methyl-lysines (H3K9 and H3K27) (98). Several papers from the Kerpolla lab have demonstrated varying binding affinities of Cbx fusion proteins to chromatin (99, 100). During embryonic stem cell differentiation, members of the Cbx family show a mutually-exclusive association with core PRC1 members. In mouse embryonic stem cells, Cbx7 appears to be the predominant Cbx member associated with Ring1b, and Cbx7 is localized at the promoters of Cbx2, 4, and 8 and represses their expression (101, 102). When exposed to retinoic

acid, these embryonic stem cells differentiate and endogenous Cbx7 expression declines. The removal of transcriptional repression by Cbx7 allows a rise in expression in these Cbx members. O'Loghlen et al. (101) highlight the role of miRNA regulation in this autoregulatory Cbx system utilized during the differentiation of embryonic stem cells. Although these studies have shown unique patterns of recruitment of these variants of the canonical PRC1, the exact mechanisms of recruitment and full understanding of their functional significance remain to be elucidated.

CBX7 was highlighted as a gene that promotes a bypass of replicative senescence in prostatic epithelial cells by repression of p16 (103). Non-coding RNA, ANRIL, and H3K27me3 both contribute to the recruitment of CBX7 to the p16 locus (49). Despite this role in suppressing p16, a common target for dysfunction in cancers, there are conflicting data on the role of CBX7 in carcinogenesis. CBX7 accelerates B-cell lymphoma formation in the context of c-Myc overexpression, an effect that is dependent on p16 repression (104). Pallente et al. have also shown an association between reduced expression of CBX7 in thyroid cancer, and reduced growth with CBX7 overexpression in thyroid cancer cell lines (105). CBX7 expression and recruitment has also been demonstrated to increase E-cadherin expression in thyroid cancer (106). In contrast, overexpression of CBX7 in Tera2 embryonal carcinoma cells reduces E-cadherin expression and leads to promoter hypermethylation (107).

Our lab has previously reported on PRC1 and its role in initiating DNA methylation at cancer-specific genes in Tera2 embryonal carcinoma cells (107). The Tera2 human embryonal carcinoma cell line is derived from a metastatic testicular tumor. Similar to normal embryonic stem cells, Tera2 has been shown to differentiate to

neuronal cells in response to exposure to all-*trans* retinoic acid (ATRA) (108-110). However, none of the aforementioned studies on PRC1 combinatory diversity have considered changes in DNA methylation. In addition to the links between PRC2 member Ezh2 and its H3K27 methylation mark, PRC1 member CBX7 interacts with the DNA methyltransferase 1 (DNMT1), DNMT3a, and DNMT3b and H3K9 methyltransferase G9a. In addition to its role in DNA methylation, overexpression of CBX7 in Tera2 also generates a small subpopulation that exhibits resistance to ATRA after several weeks of exposure (107).

Epigenetic regulation and signaling pathways contribute to normal stem cell function and differentiation (41, 82, 111). The Wingless-Integration site (Wnt) signaling pathway represents one such circuit that mediates the balance of stem cell phenotype and lineage differentiation. Members of the LEF/TCF family are constitutively bound to DNA at distant enhancer elements, and bind transcriptional co-repressors, such as Groucho and HDAC1, in the absence of soluble Wnt ligands. Long-range chromatin interaction between these repressors and transcription factors near transcriptional start sites ensure negligible expression of Wnt target genes (23). Without ligand, the transmembrane Wnt receptors LRP and Frizzled do not associate. The β-catenin destruction complex (Glycogen Synthase Kinase 3β [GSK-3β], Axin1, Axin2, Casein Kinase) phosphorylates β-catenin. This phosphorylation event promotes the ubiquitination and proteasomal degradation of β-catenin. The presence of soluble Wnt ligand promotes the physical association of Frizzled and LRP, which increases the activity of Dishevelled. The Dishevelled protein destabilizes the destruction complex and reduces the kinase activity of GSK-3β, leading to a reduction in β-catenin

19

phosphorylation and an increase in β-catenin protein levels. Stable β-catenin translocates to the nucleus of Wnt-activated cells and binds to LEF/TCF proteins, which displaces co-repressors from LEF/TCF proteins. The complex of β-catenin and LEF/TCF recruits transcriptional co-activators, which drives Wnt target genes, such as c-Myc and CD44 (112, 113).

In addition to this canonical pathway, Wnt ligands have also been shown to drive gene expression changes through non-canonical pathway via calcium/Protein Kinase C signaling/Cam KII signaling and through activation of Rac/JUN N-terminal kinase (JNK) and Rho/ROCK signaling (112). Phosphorylation of JUN by JNK increases transcriptional activity of JUN, and can drive gene expression changes in response to numerous stimuli (114, 115). Unphosphorylated JUN binds HDAC3 and MBD3/NuRD, but JNK-mediated phosphorylation reduces the affinity between these co-repressors and JUN (116, 117). However, there is considerable cross-talk between these two branches, as JUN can bind to its own promoter (118), and common targets with both AP-1 and LEF1/TCF binding sites exhibit increased activity with JUN phosphorylation (112). This interaction of LEF1 and JUN has also been demonstrated for CD44, osteopontin, c-Myc, and matrix metalloprotease 7 (MMP7) (119). Similar to its effect on β-catenin, GSK3β-mediated phosphorylation of JUN protein facilitates binding of E3 ligase Fbw7 and subsequent proteasomal degradation (120, 121).

Despite extensive research, controversy remains about the role of the Wnt signaling pathway in embryonic stem cell regulation. Wnt signaling has been shown to be important for maintaining human embryonic stem cells (122, 123) and in induced pluripotent stem cell (iPS cell) formation (124, 125). On the other hand, numerous

20

papers have demonstrated that inhibition of GSK3β, which increases β-catenin protein levels, can promote differentiation of embryonic stem cells (126, 127). Other studies in embryonal carcinoma cells show increases in Wnt activity with retinoid-induced differentiation (128).

To gain greater insight into the consequences of CBX7 overexpression and the associated DNA hypermethylation, we performed xenograft studies of our empty vector control Tera2, CBX7-overexpressing Tera2, and CBX7 Outgrowth populations. This information was also particularly important given the CBX7-mediated increases in DNA methylation in genes commonly methylated in adult cancers (107). We link CBX7 overexpression to a suppression of both canonical and non-canonical Wnt signaling pathways, owing in part to the repression and DNA methylation of the LEF1 enhancer protein and cJUN transcription factor. These data suggest that Wnt may be important for maintaining tumor stem cell function in the context of teratocarcinomas.

Materials and Methods

Cell Culture. Tera2 cells were cultured in McCoy's 5A (Gibco) supplemented with 15% fetal bovine serum (FBS) by volume (Gemini Bio-Products, Atlanta Biologicals). The generation of Tera2 with CBX7 has been previously described (107). Empty vector, CBX7, and CBX7 Outgrowth Tera2 were maintained under constant puromycin selection. All-*trans* retinoic acid (ATRA) was purchased from Sigma. Cells were exposed to 1uM ATRA, with fresh media added with each splitting of cells or every three days. All cells were grown at 37C in humidified 5% CO_2 atmosphere.

Western Blotting. Whole cell lysates were generated by 30-second vortexing followed by 30 minute rotation at 4C in modified RIPA buffer (50mM Tris-HCl, pH 7.5, 150mM NaCl, 0.25% SDS) supplemented with Complete protease inhibitor (Roche) and AEBSF (Pefabloc, Roche). Cell lysates used for detection of phosphorylated proteins were also supplemented with PhosStop phosphatase inhibitor (Roche). Protein concentrations were calculated by BCA protein assay (Pierce Thermo Scientific).

Luciferase Assays. Tera2 cells were seeded at 25K cells in 24well dishes. Firefly luciferase vectors (TOPFLASH/FOPFLASH; Promega) were transfected in a 10:1 mass ratio with pTK-RL *Renilla* luciferase constitutive control vector for normalization (Promega). Samples were co-transfected with either β-catenin, LEF1, or with excess

pIRES to normalize total DNA transfected. All vectors were transfected with Lipofectamine2000 at a 2.5:1 ug DNA:ul ratio (Invitrogen). Cells were lysed with Passive Lysis Buffer (Promega) 48 hours after transfection. Firefly and *Renilla* luciferase activity in lysates were measured according to Dual Luciferase Reporter Assay System (Promega) according to manufacturer's protocol on a Monolight 2010 luminometer (Analytic Luminescence Laboratory).

Tumor Sphere Formation. Tera2 sphere formation was performed as described in (129). Cells were dissociated with PBS-based Cell Dissociation buffer. 5000 cells were incubated in 1ml of DMEM:F12 supplemented with 10ng/ml EGF (Invitrogen), 20ng/ml FGF2 (Invitrogen), and 20ng/μl heparin (StemCell Technologies) in Ultra-Low Attachment 24-well Plates (Corning Costar). Cells were seeded on plates without prior rehydration of wells. Spheres were counted on day 10 of incubation and photographed on AxioCam software. Only spheres larger than 50μm were included in the count. Two biological replicates were performed, each performed in quadruplicate.

cDNA Synthesis, Real-time PCR, and Gene Expression Microarray. Sample mRNA was isolated from cell pellets by Qiagen RNeasy kit according to manufacturer's protocol (Qiagen) and quantified by NanoDrop. 2μg RNA was digested with DNaseI according to manufacturer's protocol (Invitrogen), followed by First-Strand cDNA Synthesis reaction (Invitrogen). Real-time PCR reactions were run with Qiagen 2x SYBR Green mix, with 10nM final primer concentration. PCR reactions were performed on ABI (machine specs) with StepOne v2.1 software. Fold changes were calculated by $2^{-\Delta\Delta Ct}$ method, with

normalization to GAPDH. All data represents at least 2 biological replicates, each run in triplicate. Primers were ordered from Integrated DNA Technologies. Primer sequences are listed in Table 2.1. Global gene expression studies were performed by Agilent Human Gene Expression 4x44K microarray. Cell pellets for empty vector Tera2, CBX7-overexpressing Tera2, and CBX7 Outgrowth populations were provided to the Johns Hopkins Sidney Kimmel Cancer Center Microarray Core. RNA isolation and quality control was performed by the Microarray Core facility.

Lentiviral Transduction. Anti-CD44 shRNA lentiviral constructs were purchased from Sigma, custom ordered for insertion into the pHGK promoter and neomycin selection gene. Twenty-thousand Tera2 cells/well in 24-well plates were seeded, and cells (empty vector, CBX7, and CBX7 outgrowth) were transduced at a multiplicity of infection (MOI) of 1 with 8μg/ml Polybrene (Sigma). Media without antibiotics was changed the following morning (approximately 16hours). Dual selection (0.5ug/ml puromycin, 100μg/ml geneticin for empty vector Tera2 and CBX7-overexpressing, 0.5ug/ml puromycin, 200ug/ml geneticin for CBX7 Outgrowth) was started on day 2 and maintained during all experiments. Sequences targeted by lentivirus shRNA are listed in Table 2.3.

Flow Cytometry. Samples for flow cytometry were dissociated with Enzyme-free dissociation buffer (Invitrogen/Gibco). 5×10^5 cells were used for each negative control and experimental branch. Cells were blocked with 0.5% FBS/PBS for 10 minutes at room temperature. Primary antibody diluted in 0.5% FBS/PBS was incubated for 10 minutes at

4C. For cell surface staining only, cells were washed with 2ml 1xPBS. For subsequent intracellular staining, cells were fixed with freshly prepared 4% formaldehyde (from paraformaldehyde powder), permeabilized with 0.2% Triton-X for 10 minutes. For unconjugated primary antibodies, cells were then incubated with secondary antibody (1:400, 100ul total volume per tube) for 10 minutes at room temperature, washed with 2ml 1xPBS. For CD44 staining, unconjugated mouse anti-CD44 (1:10 dilution, Meridian Life Sciences) was used as the primary antibody, with 1:400 donkey anti-mouse Alexa Fluor 647 secondary antibody. PerCP-Cy5.5-conjugated anti-Oct4 (BD Biosciences) was used for intracellular staining. Samples were analyzed on FACSCalibur flow cytometer with FASCComp software (BD Biosciences).

Chromatin Immunoprecipitation. Chromatin Immunoprecipitation was performed as previously described (66). Briefly, actively growing Tera2 cells in 15cm plates were rinsed with 1xPBS and cross-linked with 1% formaldehyde in 1xPBS for 10 minutes at room temperature, followed by quenching with 125mM glycine. After rinsing, cells were dissociated with 0.05mM trypsin for 5 minutes at room temperature, and neutralized with 10%FBS/1xPBS. Cells were then scrapped and centrifuged. Cell pellets were rinsed twice with 1xPBS supplemented with Complete protease inhibitor (Roche) and 1mM AEBSF (Pefabloc; Roche). Cytoplasmic extraction was performed by lysis with Cytoplasmic Extraction Buffer (CEB: 10mM HEPES Buffer pH 7.8, 10mM KCl, 1.5mM MgCl$_2$, 0.34M sucrose, 10% glycerol) with 0.2% NP-40, followed by rinse with CEB (without NP-40). Nuclei were resuspended in SDS Lysis Buffer (Millipore) and sonicated for 15 pulses of 10 seconds at 2.5 output level, 40% duty cycles, with 20 seconds of

25

pause between each pulse on a Sonifier 450 (Branson). The sheared nuclei were centrifuged at top speed for 10 minutes at room temperature. Chromatin was quantified, and master mix of 80ug of chromatin was diluted to 400ul SDS Lysis Buffer, and diluted to 4ml in ChIP Dilution Buffer (Millipore). 50µl aliquot (approximately 1ug chromatin) of diluted chromatin was stored overnight at -20C as input. Each immunoprecipitation was incubated with respective antibodies overnight at 4C on rotator: normal rabbit IgG (Upstate), 1µl; anti-HA (Covance), 5µl; DNMT3B (custom antibody, as previously described (130)), 0.3ul; DNMT1 (Sigma), 5µl; JUN (Cell Signaling Technologies), 5µl; LEF1 (Cell Signaling Technologies), 5µl; H3K4me3 (Upstate), 5µl; H3K27me3 (Upstate), 5ul; H3 (Abcam), 1.5µl. 5ul Protein A and 15ul Protein G-coated magnetic Dynabeads (Dynal/ Invitrogen) were rinsed twice with Blocking Reagent (0.5% BSA/1xPBS, Invitrogen) and blocked overnight in fresh Blocking Reagent, rotating overnight (approximately 16hrs) at 4C. After incubation, 100ul of blocked magnetic bead mixture was added to each immunoprecipitation and incubated at 4C on rotator for 3 hours. Following incubation, magnetic beads were rinsed four times with Low Salt Buffer (Millipore), followed by two rinses with High Salt Buffer (Millipore). Immune complexes and beads were incubated with 105ul Elution Buffer (50mM Tris-HCl pH 8.0, 10mM EDTA, 1% SDS) and heated at 65C for 15 minutes, with vortexing every two minutes. Beads were spun for 1minute at maximum speed (~15000g), and supernatant was transferred to a new 1.5ml tube. Aliqouted input sample was mixed with 50ul Elution buffer. Elutant was incubated overnight at 65C with rotation. The following morning, 100ul of 1xPBS was added to the samples, and treated with RNaseA (200ug/ml final concentration; Amersham) for 1 hour at 37C, followed by 2 hour treatment with

Proteinase K (200ug/ml final concentration; Invitrogen) at 55C. DNA was mixed with 1ml Buffer PB (Qiagen) and loaded on columns on vacuum manifold (Qiagen PCR Cleanup Kit), and rinsed with 750ul Buffer PE. DNA was eluted with 2x 50ul Buffer EB (Qiagen). All samples were diluted 1:2 in Buffer prior to quantitative real-time PCR. Input samples were diluted 1:10 in Buffer EB.

Xenograft Studies. Cells were trypsinized, counted, and injected 3-5million cells in 100ul of 1:1 mixture of chilled 1xPBS/MatriGel (Becton Dickinson). NOD/SCID mice were injected subcutaneously bilaterally. Tumor incidence was noted at the first palpable of subcutaneous tumor. Per protocol guidelines, tumors were dissected when reached 2cm in any dimension, or when animals exhibited extreme distress. Dissected tumors were sectioned and preserved in 4% formaldehyde overnight. Fresh 4% formaldehyde was prepared by dissolving paraformaldehyde (Sigma) in distilled deionized water. Paraformaldehyde was heated to 60C, and depolymerization was catalyzed by addition of 10ul 1M NaOH in fume hood, and 0.22um filtered. Tumor fixation into formalin and sectioning onto slides was performed at the Johns Hopkins Mouse Phenotyping Core. Immunohistochemistry for lineage markers and slide scanning was performed at the Johns Hopkins Kimmel Cancer Center Tissue Microarray Core Facility. Marker expression was analyzed by Aperio ImageScope, using the Positive Pixel Count v9 algorithm. All studies involving mice were performed according to the rules and ethics of Institutional Review Board and Institutional Animal Care Use Committee (IACUC).

Results

CBX7 Outgrowth Formation and Tumor Formation in Tera2-CBX7

Previous research in our lab has shown that Tera2 cells overexpressing CBX7 differentiate over the course of about three weeks of ATRA exposure. However, unlike empty vector control Tera2 cells, which only express the puromycin selection gene, a small subpopulation of CBX7-overexpressing Tera2 cells emerges starting at approximately 20 days of exposure to 2uM all-*trans* retinoic acid (ATRA)- the CBX7 "Outgrowth" population (107). This population, which was withdrawn from ATRA exposure after 30 days, has been kept continually growing in culture. When re-exposed to ATRA, the CBX7 Outgrowth population once again appears to differentiate in a similar manner as Tera2 cells upon their first exposure to ATRA (Figure 2.1). However, upon second exposure to ATRA (at least 5 passages after withdrawal from ATRA), the vast majority of CBX7 Outgrowth population differentiated, and once again, a small population of retinoid-resistant cells begin to grow after approximately 15 days, a few days earlier than CBX7 Tera2 during their first exposure to ATRA. There are examples of retinoid-resistant Tera2 cells caused by genetic defects, such as the loss of retinoic acid receptor gamma (RARγ) (131). However, we believe that the behavior of the CBX7 Outgrowth population was inconsistent with the selection for a small number of cells with genetic defect(s) leading to retinoid resistance, as the majority of cells in the bulk CBX7 Outgrowth population would have to revert back to retinoid sensitivity in order to

differentiate upon a second exposure to ATRA. This observation suggested that the CBX7 population resembles a "cancer stem cell," as suggested by a maturation defect in the cells and through its ability to regenerate phenotypic heterogeneity (the re-establishment of ATRA-sensitive cells in the bulk population of CBX7-overexpressing cells), and/or other epigenetically defined drug-resistant subpopulations (92, 132).

Embryonal carcinoma cells, such as Tera2, are generally believed to be the undifferentiated "stem cell" population within malignant testicular cancers (108). Given the existence of a retinoid-resistant subpopulation, we believed that CBX7 overexpression would accentuate this "cancer stem cell" population(s) and generate teratocarcinomas more rapidly and/or with a higher frequency of tumor incidence than empty vector Tera2. Multiple studies have shown that CBX7 has the potential to block maturation by repressing transcription factors involved in lineage differentiation (101, 102). However, CBX7 Tera2 cells exhibit lower overall frequency of tumor formation and higher latency than EF1 tumors, suggesting that CBX7 has tumor-suppressor function (Figure 2.2). Surprisingly, the CBX7 Outgrowth population (generated by Helai Mohammad, with one single 30-day exposure to ATRA followed by continued growth in ATRA-free media) developed no tumors in NOD/SCID mice.

One hypothesis for the reduced tumorigenicity in the CBX7-overexpressing cells and CBX7 Outgrowth population was that these cells exhibited abnormal differentiation potential. As previously noted, xenografted Tera2 cells can differentiated into all three germ layers (endoderm, mesoderm, ectoderm) (108, 110). Immunohistochemistry (IHC) was performed on formalin-fixed sections empty vector Tera2 and CBX7-overexpressing Tera2 tumors were examined for a number of lineage markers to evaluate for any change

in the lineages found within the tumors, as represented by the degree of positive staining for each marker. The empty vector and CBX7-overexpression Tera2 showed no significant differences in staining for several lineage markers (CD34, CK18, desmin, GFAP, chromogranin, S100), which argues against an *in vivo* shift in differentiation potential (Figure 2.3). Despite the reduced tumorigenicity of CBX7-overexpressing cells and the CBX7 Outgrowth population, these cell populations maintained their levels of the stem cell transcription factor Oct4 and stem cell marker CD133 *in vitro*, as measured by flow cytometry (Figure 2.4). Although Tra-1-60, a surface marker of undifferentiated embryonic stem cells, showed a reduction in the CBX7 cells, the CBX7 Outgrowth population, which formed no xenograft tumors *in vivo*, had Tra-1-60 levels comparable to empty vector controls (Figure 2.4).

Reduction in CD44 and CD44-associated signaling

Given the reduction *in vivo* xenograft formation, we hypothesized that CBX7-overexpressing cells had other gene expression changes, possibly due to promoter DNA methylation, that reduce the tumorigenicity of these cells. We were particularly mindful of changes in interaction of the cells with the extracellular matrix (ECM) and in stem cell gene programs. We hypothesized that ECM interactions might be critical for stem cell niche interaction and xenograft tumor formation as assayed *in vivo*, a defect not as evident during *in vitro* 2D cell culture. Our lab has previously linked cancer-specific hypermethylation of ECM targets in colon cancer, albeit such changes could be used to predict worse prognosis (72). In fact, a review of gene expression data from our Tera2-

CBX7 system (107) suggested that a number of ECM targets were reduced in the CBX7 system (Table 2.4). We found that CD44, a well-known mediator of both cell-ECM interaction and stem cell phenotype (133), was significantly reduced by real-time PCR and flow cytometry (Figure 2.5). Both the CBX7 and CBX7 Outgrowth populations showed increases in methylation throughout the CD44 CpG island compared to control empty vector Tera2 cells (Figure 2.6). This repression in CD44 could be reactivated with short term exposure to the DNA demethylating agent 5'-deoxy-2-azacytidine (DAC-72hrs, 1uM; Figure 2.7). In addition to CD44, a number of integrins associated with CD44 expression – integrins β1, β2, α7- showed reduction as well (Figure 2.8). These integrins did not show any increase in promoter hypermethylation. Other integrins, however, showed no statistically significant change or modest increases. Osteopontin, a secreted ECM component shown to act in a feedback loop with CD44 and important in integrin-related signaling (116, 134), was also reduced (Figure 2.8). One of the downstream targets of CD44 activation, the c-Src kinase, also showed reduced activity (as measured by phosphorylation), in the CBX7 and CBX7 Outgrowth populations (Figure 2.9).

In order to detect dysregulated signaling pathways in CBX7 and CBX7 Outgrowth cells, we performed by MetaCore analysis on global gene expression data from Agilent 4x44K gene expression microarray. This analysis indicated a disruption of the Wnt signaling pathway, as CD44, JUN, and LEF1 showed reduced expression in CBX7 and CBX7 Outgrowth populations (Figure 2.10). The role of the Wnt signaling pathway in adult cancer has been well demonstrated. Genetic mutations in colorectal cancer, such as mutation of the APC destruction complex member, significantly reduce

the activity of GSK3β and allow increased accumulation of β-catenin protein expression irrespective of the presence of Wnt ligand. In addition, numerous reports have demonstrated the epigenetic silencing of inhibitory components of this pathway, such as the secreted Frizzled-related proteins and Sox17 (135, 136). Given this body of knowledge, we hypothesized that dysregulation of the Wnt pathway may be relevant to the reduction in tumorigenicity exhibited in CBX7-overexpressing Tera2. Several studies have demonstrated the links between Wnt signaling, JUN, and CD44 (137, 138). We confirmed that both JUN and LEF1 mRNA are significantly reduced in CBX7 and CBX7 Outgrowth cells compared to empty vector EF1 Tera2 cells (Figure 2.11). These changes are also observed at the protein level (Figure 2.11). Both LEF1 and JUN show an increase in promoter DNA methylation in the CBX7 and CBX7 Outgrowth cells. The CpG island at the LEF1 promoter extends from 1kb upstream from the transcriptional start site to 1.5kb downstream. The downstream portion includes the first exon of LEF1 and partially into the first intron. Interestingly, the DNA methylation increases do not occur at the transcriptional start site, but rises only at the downstream edge of the LEF1 promoter CpG island (Figure 2.12). Other members of the LEF/TCF family- TCF1, TCF3, and TCF4 (i.e. TCF7L2) showed no change at the mRNA level, and slight increases at the protein level (data not shown). To further evaluate the activity of the Wnt/β-catenin signaling pathway, we used the TOPFLASH luciferase reporter system. This reporter vector harbors two inverted triplets of multimerized consensus TCF/LEF binding sites upstream of a minimal Herpes Simplex Virus (HSV) Thymidine Kinase (TK) minimal promoter, which drive expression of the firefly luciferase. The FOPFLASH vector, which carries mutated LEF/TCF binding sites, is transfected in place

of TOPFLASH as a negative control. In many contexts, the activity of the TOPFLASH vector, but not FOPFLASH is enhanced by co-transfection of β-catenin. As shown in Figure 2.13, CBX7 and CBX7 Outgrowth cells show both reduced basal signaling and response to co-transfection of β-catenin. With co-transfection of LEF1 and β-catenin, both CBX7 and CBX7 Outgrowth show increases in reporter activity, though still significantly less than control Tera2 cells (Figure 2.14). We used Western blot to measure the phosphorylation status of GSK3β, which correlates with the activity of this kinase. We detected no differences in phosphorylation status of the kinase between empty vector, CBX7, and CBX7 Outgrowth populations (Figure 2.15)

Chromatin Changes at Wnt Pathway Genes

To further probe this pathway, we used chromatin immunoprecipitation (ChIP) to study the localization of CBX7 and DNA methylation machinery. We have previously shown that the recruitment of overexpressed CBX7 to promoters that gain DNA methylation (107). However, we also discovered that repressive complexes, even those capable of recruiting DNA methyltransferases, possess the ability to repress gene expression even without increases in methylation (139). Consistent with their reduction in expression in the CBX7 and CBX7 Outgrowth populations, we found significant decreases in the active mark H3K4me3, with modest gains in the repressive mark H3K9me3, near the CD44 transcriptional start site (Figure 2.16). We also detected enrichment of DNMT1 and DNMT3B within the gene body of CD44 in areas that also show increased DNA methylation (Figure 2.17, Figure 2.18). There was a loss in active

H3K4me3 modification and a decrease in repressive H3K27me3 at the JUN and LEF1 transcription start sites (Figure 2.19, Figure 2.21). At JUN, we observed recruitment of HA-CBX7 and DNMT1 (in CBX7 Tera2 only; Figure 2.20). For LEF1, we observed HA-CBX7 only in CBX7 cells (not CBX7 Outgrowth), as well as a modest enrichment of DNMT1 (Figure 2.22). We did observe enrichment in DNMT3B in the CBX7 Outgrowth cells in areas that gained DNA methylation (Figure 2.23).

Validation of CD44 effect in Reduction of Tera2 Tumorigenicity

To validate our findings, we used lentiviral shRNA to knockdown expression of CD44. With stable selection (greater than 3 weeks), we were able to confirm reduction in CD44 mRNA (Figure 2.24). Flow cytometry revealed that two of the shRNAs with the greatest knockdown (The RNAi Consortium [TRC] #308110 and 296191, labeled as shCD44-3 and shCD44-5, respectively) also exhibited reduced expression of surface CD44 (Figure 2.25). Empty vector cells with reduced CD44 produced about 50% fewer spheres than empty vector control cells with scrambled-sequence negative control lentivirus on *in vitro* sphere formation ability (Figure 2.26). Though the active shRNA constructs all induced an increase in Src phosphorylation, this phosphorylation was blunted in the cells with effective CD44 knockdown (shCD44-3) vs. another shRNA that was ineffective at reducing CD44 surface expression (TRC #57563, "shCD44-1"; Figure 2.27).

Given the results of the *in vitro* sphere formation assay, we hypothesized that we would observe reduced tumorigenicity- i.e. increased tumor latency and/or decreased

34

tumor frequency- in CD44 knock-down cells. Therefore, we performed a xenograft study to assay the tumorigenicity of Tera2 cells transduced with lentivirus with scrambled sequence, ineffective CD44 knockdown (shCD44-1), and effective CD44 (shCD44-3). Surprisingly, the empty vector Tera2 cells with effective CD44 knockdown showed no increase in latency in tumor formation. In fact, the cell line with ineffective CD44 knockdown, which had not exhibited any difference in CD44 surface expression, showed an increase in latency (Figure 2.28).

We attempted to address the role of CD44 with greater knockdown with wild-type Tera2 cells. The previous xenograft experiment required double antibiotic selection: puromycin to ensure continued expression of the tagged CBX7-HA construct, and geneticin for selection for cells with incorporation of shRNA lentivirus particles. The use of wild-type Tera2 cells, which had not been previously exposed to any antibiotic treatment, would allow for high antibiotic concentration for single selection. Theoretically, this might allow for selection of cells with that had achieved greater knockdown of CD44 (and the accompanying antibiotic resistance gene). We repeated selection for the same panel of lentiviruses with shRNA constructs targeting CD44. As seen in transduction into the empty vector cells, the greatest CD44 knockdown was achieved with lentiviruses shCD44-3 and shCD44-5, as measured by mRNA (Figure 2.29) and by protein levels (Figure 2.30) compared to the non-targeting (negative) control (shNTC).

Upon injection of NOD-SCID with transduced Tera2 cells, surprisingly, neither CD44 construct demonstrated a statistically significant change in tumor latency (Figure 2.31). However, tumors derived from cells tranduced with shCD44-5 (effective CD44)

demonstrated a statistically significant decrease in tumor volume compared to negative control cells. Tumors derived from shCD44-3-transduced cells did not show any difference in tumor growth (Figure 2.32). These divergent results prompted us to question the mechanism by which these two lentiviral constructs, which both showed similar reductions in CD44 mRNA and surface expression prior to injection *in vitro*, could generate different growth characteristics *in vivo*. One hypothesis for the difference in behavior between these two lentiviral strains was a difference in the persistence in CD44 knockdown between these two constructs. Once injected, the transduced Tera2 cells were no longer under antibiotic selection for the anti-CD44 shRNA lentiviral constructs. We compared mRNA expression of CD44 levels at between 9 and 10 weeks after injection, a time-point at which xenografted tumors in the non-targeted control and shCD44-3 treatment group reached the maximum tumor size permissible under institutional rules governing animal experiment protocols (tumor diameter of 2cm). At this time point, both effective CD44 treatments revealed that CD44 knockdown was maintained relative to the non-targeting control (Figure 2.33). In fact, the shCD44-3 maintained levels of CD44 even lower than shCD44-5. Therefore, a difference in CD44 knockdown persistence could not account for the differences in tumor growth.

Discussion

In this study, we were able to demonstrate CBX7-mediated reduction in tumorigenicity of Tera2 embryonal carcinoma cell lines. This phenotype emerged despite the fact that the protein induces the emergence of a retinoid-resistant population and produces cancer-specific patterns of promoter DNA hypermethylation and gene silencing. These results extend findings about the cellular response to this cancer-related DNA methylation abnormality in terms of the cancer phenotypes associated with such changes.

Colleagues in the Baylin lab have shown the strong correlation between the marking of genes with "bivalent" chromatin in ESC, which are a subset of genes highly enriched for transcriptional/developmental regulation, and genes which acquire the above abnormal, promoter CpG island DNA methylation in cancer (68, 70). Notably for the present study, key genes which manifested this change, and or had decreased expression in cells with CBX7 over-expression, LEF1, cJUN, and CD44, are all listed as bivalent genes in human embryonic stem cells. While Polycomb-marked genes with low basal expression may be upregulated, as exemplified by the activation of bivalent genes, this is less likely to occur when abnormal DNA methylation is present in the promoter region. This latter fact has been well studied for repression of the GATA4 in the Tera2 cells versus colon cancer cells (140). The promoter of this gene is normally bivalently marked in Tera2, but without DNA methylation, and the gene is in a poised transcription state (140). Increased expression is readily induced by retinoic acid and the gene assumes an

active transcription state by chromatin marking (140). In contrast, when GATA4 is DNA hypermethylated in colon cancer cells, basal transcription is fully repressed and tight, long-distance chromatin looping envelopes the gene (140). GATA4 is one of the genes which undergoes decreased expression and evolves promoter DNA hypermethylation in our initial studies of CBX7 over-expression in Tera2 cells (107). In these latter studies, association of CBX7 and DNMTs appeared to drive the switch from Polycomb-based to DNA methylation-based repression.

Hypotheses for the tumor phenotypes observed

General considerations

As alluded to above, we were surprised in our study to find that CBX7 over-expression induced a less aggressive tumor phenotype despite also inducing a cancer-specific pattern of DNA methylation abnormalities and gene silencing. In retrospect, our observed switches in Tera2 cells for genes with bivalent promoter chromatin and Polycomb occupancy to DNA hypermethylation may reflect certain clinical findings in some adult cancers. A cancer cell phenotype has been defined, first in colon cancers and later other tumors, termed the CpG Island Methylator Phenotype (CIMP+) (73, 141, 142). The CIMP phenotype in colorectal cancer was associated with proximal colon tumors, mutations in BRAF, and hypermethylation and silencing of the MLH1 DNA repair protein and associated microsatellite instability (MSI) (73, 141, 142). CIMP+ versus CIMP- tumors, including for colon cancer as well as for breast tumors and brain gliomas,

are typically associated with a more, rather than less, favorable clinical status (73, 141, 142-144). On the other hand, some tumors show worse outcomes for tumors with CIMP+ status (145).

Perhaps, then, there are then analogies to phenotypes for certain adult cancers and the phenotypes we now observe as a consequence of CBX7 overexpression in Tera2. In the present work, and our previous study (107), CBX7 appears to target a wide range of bivalent genes for hypermethylation and to induce a less aggressive tumor phenotype. The hypermethylation initiated by CBX7 in embryonal carcinoma cells and the mechanisms that direct the establishment of the CIMP+ status may reflect that, in some instances, epigenetic abnormalities like promoter DNA hypermethylation can be associated with restriction of cell phenotypes to less adept tumorigenic states. If so, a key question is how the methylation changes induced may operate to drive the phenotypes. Possibilities inherent to our data are discussed below.

Role of changes in CD44

One change of potential functional importance in our present Tera2 studies concerns the DNA hypermethylation and associated silencing of the cell surface protein CD44. In considering this, it needs to be discussed that the functions for this protein seem to be extremely context dependent. This single-pass CD44 transmembrane protein is a commonly known interactor with the extracellular matrix (ECM) (146). CD44 is a receptor for hyaluronic acid, as well as Osteopontin (OPN; aka Secreted Phosphoprotein,

SPP1), collagen, fibrin, and integrins (116). Association with specific combinations of alpha and beta integrins also reinforces the role of crosstalk for CD44 with the extracellular environment. Larger isoforms of CD44, which are included via alternative splicing, also contain attachment for heparin sulfate, which has been shown to bind various growth factors, such as Fibroblast growth factor (FGFs), epidermal growth factors (EGF), and hepatocyte growth factor (HGF)/scatter factor (SF) (116). More recently, high expression of CD44 (along with other surface markers) has served as a marker of subpopulations of cancer cells with increased tumor-forming potential, termed cancer stem cells (CSCs) (133), as determined by tests such as in vitro tumor sphere formation and in vivo xenograft assay for both liquid and solid tumors (133, 147-149). The well-recognized role for CD44 lends support that this protein helps cancer stem cells (and, by proxy, normal adult progenitor cells) maintain protein connections with the respective stem cell niche and proper microenvironment, in addition to its role in increasing the local concentration of growth factors (133, 150). Further studies of CD44 have revealed that this protein can also participate in various signaling pathways that may also promote an undifferentiated progenitor state (148). In addition to integrin signaling, CD44 has been linked to HGF and its signaling through c-Met (133). Higher molecular weight CD44 has also been linked to testicular cancer formation (151). Overexpression of CD44 has also been linked to epithelial-mesenchymal transition (EMT) (152). Epithelial cells that have undergone EMT exhibit increased CD44 expression, as well as more aggressive and therapy-resistant tumors. CD44 has also been shown to be a target of Wnt/β-catenin signaling (137, 153), and loss of CD44 reduces colon carcinogenesis (154).

In contrast to the above studies of CD44, our present results associate decreased expression of this protein with reduced tumorigenicity. However, as shown in Figure 2.31 and Figure 2.33, effective and persistent knockdown of CD44 may not be sufficient to alter the latency of xenografted Tera2, and, therefore, cannot fully explain the effect of CBX7 overexpression on reduced tumorigenicity. However, our CD44 knockdown studies to date with lentivirus shCD44-5 may not be robust enough to induce reduced tumor volumes in the mouse studies performed or increased latency for tumor appearance. More work will be required to sort out these possibilities.

Role of changes in the Wnt pathway

One of the DNA hypermethylation paradigms in cancer, particularly in colon tumors, involves alterations of signaling for the Wnt pathway. Our lab and others have shown epigenetic repression to frequently involve silencing of the secreted Frizzled Related Proteins (sFRPs) which are a family of proteins that normally serve as negative regulators of the Wnt pathway (107, 135). Also, SOX17, a nuclear protein inhibitor of WNT signaling is also very frequently simultaneously silenced (136). These methylation changes are, thus, associated with activation of canonical WNT pathway signaling that drives tumorigenesis (135, 136). These epigenetic changes, in colon cancer, augment effects of genetic mutation of *APC* (71) and together inhibit β-catenin degradation and force constitutive Wnt activity (135, 136).

41

In contrast to the above activation of the canonical WNT pathway in association with abnormal promoter DNA methylation, in our present study, the decreased expression of LEF1 and JUN is associated with a constitutive *loss* of canonical Wnt signaling. Importantly, non-canonical WNT signaling is actually associated with cellular differentiation and lineage commitment (155-157). Thus, the reduction in tumorigenicity may be attributable to the loss of JUN and/or LEF1. The JUN proto-oncogene was originally identified as the human homolog of the avian sarcoma virus v-Jun gene (121). JUN is part of the activator-protein 1 (AP-1) complex, which is typically composed of members of the Jun family (JUN, JUNB, JUND) and Fos family (FOS, FOSB, FRA1, FRA2), and ATF. Phosphorylation of JUN by members of the JUN N-terminal kinase family (JNK) leads to reduced binding of co-repressors (116) and drives increased transcriptional activity of the JUN protein. JNK-mediated phosphorylation also allows cells to respond to cellular stress, including DNA damage. Furthermore, JNK signaling via JUN also drives the expression of pro-angiogenic factors and ECM modifiers (133). In subcutaneous tumor explants, cells are particularly subjected to hypoxia prior to the recruitment of murine vessels to the injection site, an effect not observable in *in vitro* cell culture (158).

We tried to address the potential role of JUN and LEF1 in our Tera2 system by lentivirus-mediated shRNA knockdown. For these studies, transduction with anti-LEF1 and anti-JUN lentiviral shRNA resulted in increased expression in empty vector Tera2 for these genes using multiple targeting sequences in independent transduction experiments (data not shown). We did not evaluate whether these changes also occurred in CBX7 and CBX7 Outgrowth populations transduced with these constructs, and did not characterize

any further cellular changes in these cells. The mechanism for the increased JUN and LEF1 expression in empty vector is not clear, and requires further investigation.

Role of epithelial to mesenchymal transition

Another hypothesis is that the anti-tumorigenic effect of CBX7 is mediated by pathways other than Wnt that are aberrantly regulated in CBX7-overexpressing Tera2 cells. Notably, our MetaCore analysis revealed that the CBX7 and CBX7 Outgrowth populations exhibit genome-wide patterns of TGFβ-dependent Epithelial-Mesenchymal Transition (EMT) (Figure 2.35). EMT represents a spectrum of reversible gene expression changes that alters intercellular interactions during the course of normal development. This process generates mesenchymal cells with reduced connections between cells and greater mobility, which is essential for the initial stages of organogenesis. Ultimately, the majority of such cells undergo the reciprocal process- mesenchymal-to-epithelial transition (MET)- for the formation of the fully-differentiated adult organs (159). EMT requires epigenetic reorganization of large sections of the genome, but with no additional changes in DNA methylation (160). For many adult systems, the EMT has been associated with an increase in progenitor/stem cell populations, as well as in increase in tumor aggressiveness and/or metastatic potential. External signaling, such as via TGF-β, and hypoxia (161), via HIF1α signaling (162), has both been shown to drive EMT. A number of transcription factors, such as Twist1, Snail (i.e. SNAI1), Slug (i.e. SNAI2), ZEB1, and ZEB2 (163) are downstream effectors of the gene expression programs that drive EMT (161, 162). These transcription factors serve

to repress structural components of adherens junctions, most notably E-cadherin and occludins, which are crucial mediators of strong interactions between cells and cell polarity. These factors also drive alterations in gene expression via miRNAs (164, 165) and alternative splicing of critical genes (166). EMT has previously been shown to generate cells with increased tumorigenicity (152).

CBX7 overexpression in Tera2 may show reduced tumorigenicity in part due to an Epithelial-Mesenchymal Transition. Many solid tumors that undergo an EMT are thought to select for population with *greater* tumorigenic potential (152). Also, adult epithelial cells that undergo EMT have been linked to *higher* expression of CD44 (148, 152, 167). On the other hand, embryonic stem cells and other similar pluripotent cells (iPS cells, embryonal carcinoma cells) may actually require the close cell-cell interaction normally associated with an epithelial phenotype (159, 168). Embryonic stem cells lose this epithelial phenotype as they differentiate and gain mesenchymal characteristics during this process (159). During the formation of induced pluripotent stem (iPS) cells, cells must undergo a *mesenchymal-epithelial transition* to return to a pluripotent state (169, 170). Studies on Tera2 from the Baylin lab have previously demonstrated a reduction in expression and hypermethylation of E-cadherin with CBX7 overexpression (107). While the majority of cells of xenografted cells ultimately differentiate once injected, a small portion must remain undifferentiated to sustain a teratocarcinoma. If CBX7 forces pluripotent embryonal carcinoma cells to undergo an Embryonic-Mesenchymal Transition, such as due to the loss of E-cadherin or abnormal Wnt signaling, these cells may lose the ability to maintain this subpopulation. Furthermore, just as CBX7 leaves Tera2 cells unresponsive to changes in Wnt signaling, CBX7 may

restrict cells to a single state with regards to epithelial *or* mesenchymal phenotype (a partial EMT), leaving them unable to perform a dynamic process of either EMT or MET (159). As discussed by Nieto (159), the cancer stem cells from adult tumors may not need to reach an epithelial-like phenotype characteristic of embryonic stem cells/iPS cells. This may explain why EMT reduces tumorigenicity in Tera2 cells, while increasing tumorigenicity in many other adult cancers.

Morphologically, CBX7 and CBX7 Outgrowth cells appear to have a more fibroblast-like appearance, a common hallmark of EMT (Figure 2.1). In addition, there is preliminary evidence that CBX7 and CBX7 Outgrowth exhibit greater mobility than empty vector cells as determined by *in vitro* scratch test (data not shown). Given the importance of the EMT process, additional study of this pathway in Tera2 and perturbations caused by CBX7 expression into the potential links of Polycomb repression and tumorigenicity is warranted.

Conclusions

As previously stated, our results have led us to the conclusion that the increased DNA methylation initiated by Cbx7 overexpression in Tera2 reflects the formation of a less tumorigenic state, despite induction of widespread promoter hypermethylation. Many of the cellular changes that occur during carcinogenesis- the "Hallmarks of Cancer"- represent a shift to a restricted state of autonomous and uncontrolled cell growth and lack of responsiveness to external signals (171, 172). Promoter hypermethylation is viewed as one the central mechanisms that promotes such

tumorigenic states, e.g. by inactivating tumor suppressors that allow constitutively active Wnt pathway (135). However, as we have discussed, promoter hypermethylation associated with the CpG Island Methylator Phenotype (CIMP) in many solid tumors, including breast, gastric and colorectal cancer, suggests alternative consequences of this mechanism of gene silencing. The Wnt and EMT pathways allow cellular plasticity, leading to global changes in gene expression, cellular behavior, intercellular interaction, and differentiation. While many cancers direct these pathways into a restricted and *active* state, the reduced tumorigenicity observed in embryonal carcinoma cells with Cbx7 overexpression demonstrates that these tumorigenic pathways could also be reduced in certain contexts. At the level of chromatin, embryonic stem cells have relatively open chromatin and require a dynamic turnover of chromatin proteins (173). Cbx7 overexpression may not only stabilize protein complexes that contain DNA methyltransferases, leading to the observed hypermethylation (107), but may also prevent this open chromatin conformation that maintains stem cell expression and pluripotency and allows full developmental potential (173). This could explain why embryonal carcinoma cells, like embryonic stem cells, might be particularly susceptible to restrictions on plasticity.

The ability to distinguish scenarios where epigenetic changes accelerate tumorigenecity from those where the consequences may be a less aggressive cancer state is of great clinical significance. There is currently an increasing interest in the concept of epigenetic therapies for a wide range of solid tumors (174). Future research will require a greater understanding of the mechanisms that correlate hypermethylation signatures to changes in the aggressiveness of individual tumors. If the reduced tumorigenicity in

CIMP+ tumors indicates that there are other mechanisms other than promoter hypermethylation that drive individual tumor types, inducing DNA demethylation may have minimal impact on a patient's clinical course. Research by the Baylin lab has shown the ability for long-term benefit in a cohort of patients extensively treated with other chemotherapy agents after short-term epigenetic therapy with a combination of HDAC inhibitors and DNA demethylating agents (96). While some patients showed remarkable responses to epigenetic therapy, others exhibited stable disease or progressive disease. Ongoing research is required in order to distinguish which patients would most benefit from epigenetic therapy. In cases where promoter hypermethylation limits the tumorigenic potential of cancer, the administration of demethylating agents could allow the re-expression of genes that promote tumor progression or reduces tumor cell responsiveness to other treatments (175). For some patients, targeting Polycomb-mediated repression (or components of the epigenetic machinery) might represent a better strategy.

Ongoing research in cancer strongly suggests that the heterogeneity of tumors for properties such as metastatic ability and/or chemotherapy resistance, as well as the ability of cancer cells to regenerate that heterogeneity, makes the eradication of cancer a difficult challenge. This principle has already been demonstrated *in vivo* for drug-tolerant states, which can be re-sensitized with small molecule inhibitors (92). While we were able to manipulate Polycomb genes via direct transfection, developing clinically applicable methods that restrict the phenotypes into less tumorigenic or less metastatic states by altering the function of Polycomb group proteins may represent a major mode of

treatment for cancer. In this regard, potent new inhibitors of Polycomb action have recently been developed and are now just entering clinical trials (174, 176-178).

References

1. Riggs AD, Martienssen RA, Russo VEA. Introduction. In: Russo VEA, editor. Epigenetics Mechanisms of Gene Regulation. Cold Spring Harbor, NY: Cold Spring Harbor Laboratory Press; 1996. p. 1-4.

2. Baylin SB, Jones PA. A decade of exploring the cancer epigenome - biological and translational implications. Nat Rev Cancer. 2011 Sep 23;11(10):726-34.

3. Kornberg RD. Chromatin structure: A repeating unit of histones and DNA. Science. 1974 May 24;184(4139):868-71.

4. Kornberg RD, Thomas JO. Chromatin structure; oligomers of the histones. Science. 1974 May 24;184(4139):865-8.

5. Luger K, Mader AW, Richmond RK, Sargent DF, Richmond TJ. Crystal structure of the nucleosome core particle at 2.8 A resolution. Nature. 1997 Sep 18;389(6648):251-60.

6. Jenuwein T, Allis CD. Translating the histone code. Science. 2001 Aug 10;293(5532):1074-80.

7. Paro R, Hogness DS. The polycomb protein shares a homologous domain with a heterochromatin-associated protein of drosophila. Proc Natl Acad Sci U S A. 1991 Jan 1;88(1):263-7.

8. Eissenberg JC, James TC, Foster-Hartnett DM, Hartnett T, Ngan V, Elgin SC. Mutation in a heterochromatin-specific chromosomal protein is associated with suppression of position-effect variegation in drosophila melanogaster. Proc Natl Acad Sci U S A. 1990 Dec;87(24):9923-7.

9. Owen DJ, Ornaghi P, Yang JC, Lowe N, Evans PR, Ballario P, et al. The structural basis for the recognition of acetylated histone H4 by the bromodomain of histone acetyltransferase gcn5p. EMBO J. 2000 Nov 15;19(22):6141-9.

10. ALLFREY VG, FAULKNER R, MIRSKY AE. Acetylation and methylation of histones and their possible role in the regulation of rna synthesis. Proc Natl Acad Sci U S A. 1964 May;51:786-94.

11. Hebbes TR, Thorne AW, Crane-Robinson C. A direct link between core histone acetylation and transcriptionally active chromatin. EMBO J. 1988 May;7(5):1395-402.

12. Hebbes TR, Thorne AW, Clayton AL, Crane-Robinson C. Histone acetylation and globin gene switching. Nucleic Acids Res. 1992 Mar 11;20(5):1017-22.

13. Ito T, Ikehara T, Nakagawa T, Kraus WL, Muramatsu M. p300-mediated acetylation facilitates the transfer of histone H2A-H2B dimers from nucleosomes to a histone chaperone. Genes Dev. 2000 Aug 1;14(15):1899-907.

14. Jeppesen P, Turner BM. The inactive X chromosome in female mammals is distinguished by a lack of histone H4 acetylation, a cytogenetic marker for gene expression. Cell. 1993 Jul 30;74(2):281-9.

15. Chandy M, Gutierrez JL, Prochasson P, Workman JL. SWI/SNF displaces SAGA-acetylated nucleosomes. Eukaryot Cell. 2006 Oct;5(10):1738-47.

16. Ogryzko VV, Schiltz RL, Russanova V, Howard BH, Nakatani Y. The transcriptional coactivators p300 and CBP are histone acetyltransferases. Cell. 1996 Nov 29;87(5):953-9.

17. Grunstein M. Histone acetylation in chromatin structure and transcription. Nature. 1997 Sep 25;389(6649):349-52.

18. Taunton J, Hassig CA, Schreiber SL. A mammalian histone deacetylase related to the yeast transcriptional regulator Rpd3p. Science. 1996 Apr 19;272(5260):408-11.

19. Rundlett SE, Carmen AA, Kobayashi R, Bavykin S, Turner BM, Grunstein M. HDA1 and RPD3 are members of distinct yeast histone deacetylase complexes that regulate silencing and transcription. Proc Natl Acad Sci U S A. 1996 Dec 10;93(25):14503-8.

20. Rea S, Eisenhaber F, O'Carroll D, Strahl BD, Sun ZW, Schmid M, et al. Regulation of chromatin structure by site-specific histone H3 methyltransferases. Nature. 2000 Aug 10;406(6796):593-9.

21. Strahl BD, Ohba R, Cook RG, Allis CD. Methylation of histone H3 at lysine 4 is highly conserved and correlates with transcriptionally active nuclei in tetrahymena. Proc Natl Acad Sci U S A. 1999 Dec 21;96(26):14967-72.

22. Heintzman ND, Stuart RK, Hon G, Fu Y, Ching CW, Hawkins RD, et al. Distinct and predictive chromatin signatures of transcriptional promoters and enhancers in the human genome. Nat Genet. 2007 Mar;39(3):311-8.

23. Jin F, Li Y, Ren B, Natarajan R. Enhancers: Multi-dimensional signal integrators. Transcription. 2011 Sep-Oct;2(5):226-30.

24. Hon G, Wang W, Ren B. Discovery and annotation of functional chromatin signatures in the human genome. PLoS Comput Biol. 2009 Nov;5(11):e1000566.

25. Xie L, Pelz C, Wang W, Bashar A, Varlamova O, Shadle S, et al. KDM5B regulates embryonic stem cell self-renewal and represses cryptic intragenic transcription. EMBO J. 2011 Mar 29.

26. Cloos PA, Christensen J, Agger K, Helin K. Erasing the methyl mark: Histone demethylases at the center of cellular differentiation and disease. Genes Dev. 2008 May 1;22(9):1115-40.

27. Pasini D, Cloos PA, Walfridsson J, Olsson L, Bukowski JP, Johansen JV, et al. JARID2 regulates binding of the polycomb repressive complex 2 to target genes in ES cells. Nature. 2010 Jan 14.

28. Shi Y, Lan F, Matson C, Mulligan P, Whetstine JR, Cole PA, et al. Histone demethylation mediated by the nuclear amine oxidase homolog LSD1. Cell. 2004 Dec 29;119(7):941-53.

29. Pietersen AM, van Lohuizen M. Stem cell regulation by polycomb repressors: Postponing commitment. Curr Opin Cell Biol. 2008 Apr;20(2):201-7.

30. Pasini D, Hansen KH, Christensen J, Agger K, Cloos PA, Helin K. Coordinated regulation of transcriptional repression by the RBP2 H3K4 demethylase and polycomb-repressive complex 2. Genes Dev. 2008 May 15;22(10):1345-55.

31. Herranz N, Dave N, Millanes-Romero A, Morey L, Diaz VM, Lorenz-Fonfria V, et al. Lysyl oxidase-like 2 deaminates lysine 4 in histone H3. Mol Cell. 2012 May 11;46(3):369-76.

32. Dhalluin C, Carlson JE, Zeng L, He C, Aggarwal AK, Zhou MM. Structure and ligand of a histone acetyltransferase bromodomain. Nature. 1999 Jun 3;399(6735):491-6.

33. Cote J, Quinn J, Workman JL, Peterson CL. Stimulation of GAL4 derivative binding to nucleosomal DNA by the yeast SWI/SNF complex. Science. 1994 Jul 1;265(5168):53-60.

34. Lewis EB. A gene complex controlling segmentation in drosophila. Nature. 1978 Dec 7;276(5688):565-70.

35. Jones CA, Ng J, Peterson AJ, Morgan K, Simon J, Jones RS. The drosophila esc and E(z) proteins are direct partners in polycomb group-mediated repression. Mol Cell Biol. 1998 May;18(5):2825-34.

36. Wang H, Wang L, Erdjument-Bromage H, Vidal M, Tempst P, Jones RS, et al. Role of histone H2A ubiquitination in polycomb silencing. Nature. 2004 Oct 14;431(7010):873-8.

37. Tie F, Furuyama T, Prasad-Sinha J, Jane E, Harte PJ. The drosophila polycomb group proteins ESC and E(Z) are present in a complex containing the histone-binding protein p55 and the histone deacetylase RPD3. Development. 2001 Jan;128(2):275-86.

38. Kuzmichev A, Margueron R, Vaquero A, Preissner TS, Scher M, Kirmizis A, et al. Composition and histone substrates of polycomb repressive group complexes change during cellular differentiation. Proc Natl Acad Sci U S A. 2005 Feb 8;102(6):1859-64.

39. Kerppola TK. Polycomb group complexes--many combinations, many functions. Trends Cell Biol. 2009 Dec;19(12):692-704.

40. Bracken AP, Dietrich N, Pasini D, Hansen KH, Helin K. Genome-wide mapping of polycomb target genes unravels their roles in cell fate transitions. Genes Dev. 2006 May 1;20(9):1123-36.

41. Lee TI, Jenner RG, Boyer LA, Guenther MG, Levine SS, Kumar RM, et al. Control of developmental regulators by polycomb in human embryonic stem cells. Cell. 2006 Apr 21;125(2):301-13.

42. Woo CJ, Kharchenko PV, Daheron L, Park PJ, Kingston RE. A region of the human HOXD cluster that confers polycomb-group responsiveness. Cell. 2010 Jan 8;140(1):99-110.

43. Bracken AP, Helin K. Polycomb group proteins: Navigators of lineage pathways led astray in cancer. Nat Rev Cancer. 2009 Nov;9(11):773-84.

44. Plath K, Fang J, Mlynarczyk-Evans SK, Cao R, Worringer KA, Wang H, et al. Role of histone H3 lysine 27 methylation in X inactivation. Science. 2003 Apr 4;300(5616):131-5.

45. Silva J, Mak W, Zvetkova I, Appanah R, Nesterova TB, Webster Z, et al. Establishment of histone h3 methylation on the inactive X chromosome requires transient recruitment of eed-Enx1 polycomb group complexes. Dev Cell. 2003 Apr;4(4):481-95.

46. Gupta RA, Shah N, Wang KC, Kim J, Horlings HM, Wong DJ, et al. Long non-coding RNA HOTAIR reprograms chromatin state to promote cancer metastasis. Nature. 2010 Apr 15;464(7291):1071-6.

47. Rinn JL, Kertesz M, Wang JK, Squazzo SL, Xu X, Brugmann SA, et al. Functional demarcation of active and silent chromatin domains in human HOX loci by noncoding RNAs. Cell. 2007 Jun 29;129(7):1311-23.

48. Messaoudi-Aubert SE, Nicholls J, Maertens GN, Brookes S, Bernstein E, Peters G. Role for the MOV10 RNA helicase in polycomb-mediated repression of the INK4a tumor suppressor. Nat Struct Mol Biol. 2010 Jul;17(7):862-8.

49. Yap KL, Li S, Munoz-Cabello AM, Raguz S, Zeng L, Mujtaba S, et al. Molecular interplay of the noncoding RNA ANRIL and methylated histone H3 lysine 27 by

polycomb CBX7 in transcriptional silencing of INK4a. Mol Cell. 2010 Jun 11;38(5):662-74.

50. Chu C, Qu K, Zhong FL, Artandi SE, Chang HY. Genomic maps of long noncoding RNA occupancy reveal principles of RNA-chromatin interactions. Mol Cell. 2011 Sep 29.

51. Lister R, Pelizzola M, Dowen RH, Hawkins RD, Hon G, Tonti-Filippini J, et al. Human DNA methylomes at base resolution show widespread epigenomic differences. Nature. 2009 Nov 19;462(7271):315-22.

52. Goll MG, Bestor TH. Eukaryotic cytosine methyltransferases. Annu Rev Biochem. 2005;74:481-514.

53. Jones PA, Liang G. Rethinking how DNA methylation patterns are maintained. Nat Rev Genet. 2009 Nov;10(11):805-11.

54. Gardiner-Garden M, Frommer M. CpG islands in vertebrate genomes. J Mol Biol. 1987 Jul 20;196(2):261-82.

55. Herman JG, Baylin SB. Gene silencing in cancer in association with promoter hypermethylation. N Engl J Med. 2003 Nov 20;349(21):2042-54.

56. Meissner A, Mikkelsen TS, Gu H, Wernig M, Hanna J, Sivachenko A, et al. Genome-scale DNA methylation maps of pluripotent and differentiated cells. Nature. 2008 Aug 7;454(7205):766-70.

57. Henderson IR, Jacobsen SE. Epigenetic inheritance in plants. Nature. 2007 May 24;447(7143):418-24.

58. Cokus SJ, Feng S, Zhang X, Chen Z, Merriman B, Haudenschild CD, et al. Shotgun bisulphite sequencing of the arabidopsis genome reveals DNA methylation patterning. Nature. 2008 Mar 13;452(7184):215-9.

59. Ito S, Shen L, Dai Q, Wu SC, Collins LB, Swenberg JA, et al. Tet proteins can convert 5-methylcytosine to 5-formylcytosine and 5-carboxylcytosine. Science. 2011 Jul 21.

60. He YF, Li BZ, Li Z, Liu P, Wang Y, Tang Q, et al. Tet-mediated formation of 5-carboxylcytosine and its excision by TDG in mammalian DNA. Science. 2011 Aug 4.

61. Williams K, Christensen J, Pedersen MT, Johansen JV, Cloos PA, Rappsilber J, et al. TET1 and hydroxymethylcytosine in transcription and DNA methylation fidelity. Nature. 2011 Apr 13.

62. Epsztejn-Litman S, Feldman N, Abu-Remaileh M, Shufaro Y, Gerson A, Ueda J, et al. De novo DNA methylation promoted by G9a prevents reprogramming of embryonically silenced genes. Nat Struct Mol Biol. 2008 Nov;15(11):1176-83.

63. Vire E, Brenner C, Deplus R, Blanchon L, Fraga M, Didelot C, et al. The polycomb group protein EZH2 directly controls DNA methylation. Nature. 2006 Feb 16;439(7078):871-4.

64. Widschwendter M, Fiegl H, Egle D, Mueller-Holzner E, Spizzo G, Marth C, et al. Epigenetic stem cell signature in cancer. Nat Genet. 2007 Feb;39(2):157-8.

65. Corcione A, Benvenuto F, Ferretti E, Giunti D, V C, Cazzanti F, et al. Human mesenchymal stem cells modulate B-cell functions. Blood. 2006 Jan 1;107(1):367-72.

66. McGarvey KM, Greene E, Fahrner JA, Jenuwein T, Baylin SB. DNA methylation and complete transcriptional silencing of cancer genes persist after depletion of EZH2. Cancer Res. 2007 Jun 1;67(11):5097-102.

67. Kondo Y, Shen L, Cheng AS, Ahmed S, Boumber Y, Charo C, et al. Gene silencing in cancer by histone H3 lysine 27 trimethylation independent of promoter DNA methylation. Nat Genet. 2008 Jun;40(6):741-50.

68. Ohm JE, McGarvey KM, Yu X, Cheng L, Schuebel KE, Cope L, et al. A stem cell-like chromatin pattern may predispose tumor suppressor genes to DNA hypermethylation and heritable silencing. Nat Genet. 2007 Feb;39(2):237-42.

69. Bernstein BE, Mikkelsen TS, Xie X, Kamal M, Huebert DJ, Cuff J, et al. A bivalent chromatin structure marks key developmental genes in embryonic stem cells. Cell. 2006 Apr 21;125(2):315-26.

70. Easwaran H, Johnstone SE, Van Neste L, Ohm J, Mosbruger T, Wang Q, et al. A DNA hypermethylation module for the stem/progenitor cell signature of cancer. Genome Res. 2012 May;22(5):837-49.

71. Wood LD, Parsons DW, Jones S, Lin J, Sjoblom T, Leary RJ, et al. The genomic landscapes of human breast and colorectal cancers. Science. 2007 Nov 16;318(5853):1108-13.

72. Yi JM, Dhir M, Van Neste L, Downing SR, Jeschke J, Glockner SC, et al. Genomic and epigenomic integration identifies a prognostic signature in colon cancer. Clin Cancer Res. 2011 Mar 15;17(6):1535-45.

73. Weisenberger DJ, Siegmund KD, Campan M, Young J, Long TI, Faasse MA, et al. CpG island methylator phenotype underlies sporadic microsatellite instability and is

tightly associated with BRAF mutation in colorectal cancer. Nat Genet. 2006 Jul;38(7):787-93.

74. Hegi ME, Liu L, Herman JG, Stupp R, Wick W, Weller M, et al. Correlation of O6-methylguanine methyltransferase (MGMT) promoter methylation with clinical outcomes in glioblastoma and clinical strategies to modulate MGMT activity. J Clin Oncol. 2008 Sep 1;26(25):4189-99.

75. Jones S, Wang TL, Shih I, Mao TL, Nakayama K, Roden R, et al. Frequent mutations of chromatin remodeling gene ARID1A in ovarian clear cell carcinoma. Science. 2010 Oct 8;330(6001):228-31.

76. Figueroa ME, Abdel-Wahab O, Lu C, Ward PS, Patel J, Shih A, et al. Leukemic IDH1 and IDH2 mutations result in a hypermethylation phenotype, disrupt TET2 function, and impair hematopoietic differentiation. Cancer Cell. 2010 Dec 14;18(6):553-67.

77. Coussens LM, Werb Z. Inflammation and cancer. Nature. 2002 Dec 19-26;420(6917):860-7.

78. O'Hagan HM, Mohammad HP, Baylin SB. Double strand breaks can initiate gene silencing and SIRT1-dependent onset of DNA methylation in an exogenous promoter CpG island. PLoS Genet. 2008 Aug 15;4(8):e1000155.

79. O'Hagan HM, Wang W, Sen S, Destefano Shields C, Lee SS, Zhang YW, et al. Oxidative damage targets complexes containing DNA methyltransferases, SIRT1, and polycomb members to promoter CpG islands. Cancer Cell. 2011 Nov 15;20(5):606-19.

80. Berman BP, Weisenberger DJ, Aman JF, Hinoue T, Ramjan Z, Liu Y, et al. Regions of focal DNA hypermethylation and long-range hypomethylation in colorectal cancer coincide with nuclear lamina-associated domains. Nat Genet. 2011 Nov 27;44(1):40-6.

81. Pardal R, Clarke MF, Morrison SJ. Applying the principles of stem-cell biology to cancer. Nat Rev Cancer. 2003 Dec;3(12):895-902.

82. Spivakov M, Fisher AG. Epigenetic signatures of stem-cell identity. Nat Rev Genet. 2007 Apr;8(4):263-71.

83. Florek M, Haase M, Marzesco AM, Freund D, Ehninger G, Huttner WB, et al. Prominin-1/CD133, a neural and hematopoietic stem cell marker, is expressed in adult human differentiated cells and certain types of kidney cancer. Cell Tissue Res. 2005 Jan;319(1):15-26.

84. Singh SK, Hawkins C, Clarke ID, Squire JA, Bayani J, Hide T, et al. Identification of human brain tumour initiating cells. Nature. 2004 Nov 18;432(7015):396-401.

85. Liu S, Dontu G, Mantle ID, Patel S, Ahn NS, Jackson KW, et al. Hedgehog signaling and bmi-1 regulate self-renewal of normal and malignant human mammary stem cells. Cancer Res. 2006 Jun 15;66(12):6063-71.

86. Shimono Y, Zabala M, Cho RW, Lobo N, Dalerba P, Qian D, et al. Downregulation of miRNA-200c links breast cancer stem cells with normal stem cells. Cell. 2009 Aug 7;138(3):592-603.

87. Eppert K, Takenaka K, Lechman ER, Waldron L, Nilsson B, van Galen P, et al. Stem cell gene expression programs influence clinical outcome in human leukemia. Nat Med. 2011 Aug 28;17(9):1086-93.

88. Kern SE, Shibata D. The fuzzy math of solid tumor stem cells: A perspective. Cancer Res. 2007 Oct 1;67(19):8985-8.

89. Pietersen AM, Evers B, Prasad AA, Tanger E, Cornelissen-Steijger P, Jonkers J, et al. Bmi1 regulates stem cells and proliferation and differentiation of committed cells in mammary epithelium. Curr Biol. 2008 Jul 22;18(14):1094-9.

90. Jagani Z, Wiederschain D, Loo A, He D, Mosher R, Fordjour P, et al. The polycomb group protein bmi-1 is essential for the growth of multiple myeloma cells. Cancer Res. 2010 Jul 1;70(13):5528-38.

91. Varambally S, Dhanasekaran SM, Zhou M, Barrette TR, Kumar-Sinha C, Sanda MG, et al. The polycomb group protein EZH2 is involved in progression of prostate cancer. Nature. 2002 Oct 10;419(6907):624-9.

92. Sharma SV, Lee DY, Li B, Quinlan MP, Takahashi F, Maheswaran S, et al. A chromatin-mediated reversible drug-tolerant state in cancer cell subpopulations. Cell. 2010 Apr 2;141(1):69-80.

93. Baylin SB. Resistance, epigenetics and the cancer ecosystem. Nat Med. 2011 Mar;17(3):288-9.

94. Jones PA, Taylor SM. Cellular differentiation, cytidine analogs and DNA methylation. Cell. 1980 May;20(1):85-93.

95. Fenaux P, Mufti GJ, Hellstrom-Lindberg E, Santini V, Finelli C, Giagounidis A, et al. Efficacy of azacitidine compared with that of conventional care regimens in the treatment of higher-risk myelodysplastic syndromes: A randomised, open-label, phase III study. Lancet Oncol. 2009 Mar;10(3):223-32.

96. Juergens RA, Wrangle J, Vendetti FP, Murphy SC, Zhao M, Coleman B, et al. Combination epigenetic therapy has efficacy in patients with refractory advanced non-small cell lung cancer. Cancer Discov. 2011 Dec;1(7):598-607.

97. Gao Z, Zhang J, Bonasio R, Strino F, Sawai A, Parisi F, et al. PCGF homologs, CBX proteins, and RYBP define functionally distinct PRC1 family complexes. Mol Cell. 2012 Feb 10;45(3):344-56.

98. Bernstein E, Duncan EM, Masui O, Gil J, Heard E, Allis CD. Mouse polycomb proteins bind differentially to methylated histone H3 and RNA and are enriched in facultative heterochromatin. Mol Cell Biol. 2006 Apr;26(7):2560-9.

99. Vincenz C, Kerppola TK. Different polycomb group CBX family proteins associate with distinct regions of chromatin using nonhomologous protein sequences. Proc Natl Acad Sci U S A. 2008 Oct 28;105(43):16572-7.

100. Ren X, Vincenz C, Kerppola TK. Changes in the distributions and dynamics of polycomb repressive complexes during embryonic stem cell differentiation. Mol Cell Biol. 2008 May;28(9):2884-95.

101. O'Loghlen A, Munoz-Cabello AM, Gaspar-Maia A, Wu HA, Banito A, Kunowska N, et al. MicroRNA regulation of Cbx7 mediates a switch of polycomb orthologs during ESC differentiation. Cell Stem Cell. 2012 Jan 6;10(1):33-46.

102. Morey L, Pascual G, Cozzuto L, Roma G, Wutz A, Benitah SA, et al. Nonoverlapping functions of the polycomb group cbx family of proteins in embryonic stem cells. Cell Stem Cell. 2012 Jan 6;10(1):47-62.

103. Gil J, Bernard D, Martinez D, Beach D. Polycomb CBX7 has a unifying role in cellular lifespan. Nat Cell Biol. 2004 Jan;6(1):67-72.

104. Scott CL, Gil J, Hernando E, Teruya-Feldstein J, Narita M, Martinez D, et al. Role of the chromobox protein CBX7 in lymphomagenesis. Proc Natl Acad Sci U S A. 2007 Mar 27;104(13):5389-94.

105. Pallante P, Federico A, Berlingieri MT, Bianco M, Ferraro A, Forzati F, et al. Loss of the CBX7 gene expression correlates with a highly malignant phenotype in thyroid cancer. Cancer Res. 2008 Aug 15;68(16):6770-8.

106. Federico A, Pallante P, Bianco M, Ferraro A, Esposito F, Monti M, et al. Chromobox protein homologue 7 protein, with decreased expression in human carcinomas, positively regulates E-cadherin expression by interacting with the histone deacetylase 2 protein. Cancer Res. 2009 Aug 25.

107. Mohammad HP, Cai Y, McGarvey KM, Easwaran H, Van Neste L, Ohm JE, et al. Polycomb CBX7 promotes initiation of heritable repression of genes frequently silenced with cancer-specific DNA hypermethylation. Cancer Res. 2009 Aug 1;69(15):6322-30.

108. Andrews PW. Teratocarcinomas and human embryology: Pluripotent human EC cell lines. review article. APMIS. 1998 Jan;106(1):158,67; discussion 167-8.

109. Andrews PW. Retinoic acid induces neuronal differentiation of a cloned human embryonal carcinoma cell line in vitro. Dev Biol. 1984 Jun;103(2):285-93.

110. Andrews PW, Damjanov I, Simon D, Banting GS, Carlin C, Dracopoli NC, et al. Pluripotent embryonal carcinoma clones derived from the human teratocarcinoma cell line tera-2. differentiation in vivo and in vitro. Lab Invest. 1984 Feb;50(2):147-62.

111. Mohammad HP, Baylin SB. Linking cell signaling and the epigenetic machinery. Nat Biotechnol. 2010 Oct;28(10):1033-8.

112. Saadeddin A, Babaei-Jadidi R, Spencer-Dene B, Nateri AS. The links between transcription, beta-catenin/JNK signaling, and carcinogenesis. Mol Cancer Res. 2009 Aug;7(8):1189-96.

113. Reya T, Clevers H. Wnt signalling in stem cells and cancer. Nature. 2005 Apr 14;434(7035):843-50.

114. Hayakawa J, Mittal S, Wang Y, Korkmaz KS, Adamson E, English C, et al. Identification of promoters bound by c-Jun/ATF2 during rapid large-scale gene activation following genotoxic stress. Mol Cell. 2004 Nov 19;16(4):521-35.

115. Hernandez JM, Floyd DH, Weilbaecher KN, Green PL, Boris-Lawrie K. Multiple facets of junD gene expression are atypical among AP-1 family members. Oncogene. 2008 Aug 14;27(35):4757-67.

116. Aguilera C, Nakagawa K, Sancho R, Chakraborty A, Hendrich B, Behrens A. c-jun N-terminal phosphorylation antagonises recruitment of the Mbd3/NuRD repressor complex. Nature. 2011 Jan 13;469(7329):231-5.

117. Weiss C, Schneider S, Wagner EF, Zhang X, Seto E, Bohmann D. JNK phosphorylation relieves HDAC3-dependent suppression of the transcriptional activity of c-jun. EMBO J. 2003 Jul 15;22(14):3686-95.

118. Angel P, Hattori K, Smeal T, Karin M. The jun proto-oncogene is positively autoregulated by its product, Jun/AP-1. Cell. 1988 Dec 2;55(5):875-85.

119. Rivat C, Le Floch N, Sabbah M, Teyrol I, Redeuilh G, Bruyneel E, et al. Synergistic cooperation between the AP-1 and LEF-1 transcription factors in activation of the matrilysin promoter by the src oncogene: Implications in cellular invasion. FASEB J. 2003 Sep;17(12):1721-3.

120. Wei W, Jin J, Schlisio S, Harper JW, Kaelin WG,Jr. The v-jun point mutation allows c-jun to escape GSK3-dependent recognition and destruction by the Fbw7 ubiquitin ligase. Cancer Cell. 2005 Jul;8(1):25-33.

121. Vogt PK, Bader AG. Jun: Stealth, stability, and transformation. Mol Cell. 2005 Aug 19;19(4):432-3.

122. Sato N, Meijer L, Skaltsounis L, Greengard P, Brivanlou AH. Maintenance of pluripotency in human and mouse embryonic stem cells through activation of wnt signaling by a pharmacological GSK-3-specific inhibitor. Nat Med. 2004 Jan;10(1):55-63.

123. Hochedlinger K, Yamada Y, Beard C, Jaenisch R. Ectopic expression of oct-4 blocks progenitor-cell differentiation and causes dysplasia in epithelial tissues. Cell. 2005 May 6;121(3):465-77.

124. Silva J, Barrandon O, Nichols J, Kawaguchi J, Theunissen TW, Smith A. Promotion of reprogramming to ground state pluripotency by signal inhibition. PLoS Biol. 2008 Oct 21;6(10):e253.

125. Marson A, Foreman R, Chevalier B, Bilodeau S, Kahn M, Young RA, et al. Wnt signaling promotes reprogramming of somatic cells to pluripotency. Cell Stem Cell. 2008 Aug 7;3(2):132-5.

126. Davidson KC, Adams AM, Goodson JM, McDonald CE, Potter JC, Berndt JD, et al. Wnt/beta-catenin signaling promotes differentiation, not self-renewal, of human embryonic stem cells and is repressed by Oct4. Proc Natl Acad Sci U S A. 2012 Mar 20;109(12):4485-90.

127. Bone HK, Nelson AS, Goldring CE, Tosh D, Welham MJ. A novel chemically directed route for the generation of definitive endoderm from human embryonic stem cells based on inhibition of GSK-3. J Cell Sci. 2011 Jun 15;124(Pt 12):1992-2000.

128. Snow GE, Kasper AC, Busch AM, Schwarz E, Ewings KE, Bee T, et al. Wnt pathway reprogramming during human embryonal carcinoma differentiation and potential for therapeutic targeting. BMC Cancer. 2009 Oct 29;9:383.

129. Watanabe K, Meyer MJ, Strizzi L, Lee JM, Gonzales M, Bianco C, et al. Cripto-1 is a cell surface marker for a tumorigenic, undifferentiated subpopulation in human embryonal carcinoma cells. Stem Cells. 2010 Aug;28(8):1303-14.

130. Rhee I, Bachman KE, Park BH, Jair KW, Yen RW, Schuebel KE, et al. DNMT1 and DNMT3b cooperate to silence genes in human cancer cells. Nature. 2002 Apr 4;416(6880):552-6.

131. Moasser MM, Khoo KS, Maerz WJ, Zelenetz A, Dmitrovsky E. Derivation and characterization of retinoid-resistant human embryonal carcinoma cells. Differentiation. 1996 Jul;60(4):251-7.

132. Roesch A, Fukunaga-Kalabis M, Schmidt EC, Zabierowski SE, Brafford PA, Vultur A, et al. A temporarily distinct subpopulation of slow-cycling melanoma cells is required for continuous tumor growth. Cell. 2010 May 14;141(4):583-94.

133. Zoller M. CD44: Can a cancer-initiating cell profit from an abundantly expressed molecule? Nat Rev Cancer. 2011 Apr;11(4):254-67.

134. Teramoto H, Castellone MD, Malek RL, Letwin N, Frank B, Gutkind JS, et al. Autocrine activation of an osteopontin-CD44-rac pathway enhances invasion and transformation by H-RasV12. Oncogene. 2005 Jan 13;24(3):489-501.

135. Suzuki H, Watkins DN, Jair KW, Schuebel KE, Markowitz SD, Chen WD, et al. Epigenetic inactivation of SFRP genes allows constitutive WNT signaling in colorectal cancer. Nat Genet. 2004 Apr;36(4):417-22.

136. Zhang W, Glockner SC, Guo M, Machida EO, Wang DH, Easwaran H, et al. Epigenetic inactivation of the canonical wnt antagonist SRY-box containing gene 17 in colorectal cancer. Cancer Res. 2008 Apr 15;68(8):2764-72.

137. Wielenga VJ, Smits R, Korinek V, Smit L, Kielman M, Fodde R, et al. Expression of CD44 in apc and tcf mutant mice implies regulation by the WNT pathway. Am J Pathol. 1999 Feb;154(2):515-23.

138. Nateri AS, Spencer-Dene B, Behrens A. Interaction of phosphorylated c-jun with TCF4 regulates intestinal cancer development. Nature. 2005 Sep 8;437(7056):281-5.

139. Clements EG, Mohammad HP, Leadem BR, Easwaran H, Cai Y, Van Neste L, et al. DNMT1 modulates gene expression without its catalytic activity partially through its interactions with histone-modifying enzymes. Nucleic Acids Res. 2012 May;40(10):4334-46.

140. Tiwari VK, McGarvey KM, Licchesi JD, Ohm JE, Herman JG, Schubeler D, et al. PcG proteins, DNA methylation, and gene repression by chromatin looping. PLoS Biol. 2008 Dec 2;6(12):2911-27.

141. Toyota M, Ahuja N, Suzuki H, Itoh F, Ohe-Toyota M, Imai K, et al. Aberrant methylation in gastric cancer associated with the CpG island methylator phenotype. Cancer Res. 1999 Nov 1;59(21):5438-42.

142. Toyota M, Ahuja N, Ohe-Toyota M, Herman JG, Baylin SB, Issa JP. CpG island methylator phenotype in colorectal cancer. Proc Natl Acad Sci U S A. 1999 Jul 20;96(15):8681-6.

143. Noushmehr H, Weisenberger DJ, Diefes K, Phillips HS, Pujara K, Berman BP, et al. Identification of a CpG island methylator phenotype that defines a distinct subgroup of glioma. Cancer Cell. 2010 May 18;17(5):510-22.

144. Holm K, Hegardt C, Staaf J, Vallon-Christersson J, Jonsson G, Olsson H, et al. Molecular subtypes of breast cancer are associated with characteristic DNA methylation patterns. Breast Cancer Res. 2010;12(3):R36.

145. Mack SC, Witt H, Piro RM, Gu L, Zuyderduyn S, Stutz AM, et al. Epigenomic alterations define lethal CIMP-positive ependymomas of infancy. Nature. 2014 Feb 27;506(7489):445-50.

146. Toole BP. Hyaluronan: From extracellular glue to pericellular cue. Nat Rev Cancer. 2004 Jul;4(7):528-39.

147. Al-Hajj M, Wicha MS, Benito-Hernandez A, Morrison SJ, Clarke MF. Prospective identification of tumorigenic breast cancer cells. Proc Natl Acad Sci U S A. 2003 Apr 1;100(7):3983-8.

148. Su YJ, Lai HM, Chang YW, Chen GY, Lee JL. Direct reprogramming of stem cell properties in colon cancer cells by CD44. EMBO J. 2011 Jun 24;30(15):3186-99.

149. Zhang S, Balch C, Chan MW, Lai HC, Matei D, Schilder JM, et al. Identification and characterization of ovarian cancer-initiating cells from primary human tumors. Cancer Res. 2008 Jun 1;68(11):4311-20.

150. van der Voort R, Taher TE, Wielenga VJ, Spaargaren M, Prevo R, Smit L, et al. Heparan sulfate-modified CD44 promotes hepatocyte growth factor/scatter factor-induced signal transduction through the receptor tyrosine kinase c-met. J Biol Chem. 1999 Mar 5;274(10):6499-506.

151. Miyake H, Hara I, Yamanaka K, Gohji K, Arakawa S, Kamidono S. Expression patterns of CD44 adhesion molecule in testicular germ cell tumors and normal testes. Am J Pathol. 1998 May;152(5):1157-60.

152. Mani SA, Guo W, Liao MJ, Eaton EN, Ayyanan A, Zhou AY, et al. The epithelial-mesenchymal transition generates cells with properties of stem cells. Cell. 2008 May 16;133(4):704-15.

153. Schwartz DR, Wu R, Kardia SL, Levin AM, Huang CC, Shedden KA, et al. Novel candidate targets of beta-catenin/T-cell factor signaling identified by gene expression profiling of ovarian endometrioid adenocarcinomas. Cancer Res. 2003 Jun 1;63(11):2913-22.

154. Zeilstra J, Joosten SP, Dokter M, Verwiel E, Spaargaren M, Pals ST. Deletion of the WNT target and cancer stem cell marker CD44 in apc(min/+) mice attenuates intestinal tumorigenesis. Cancer Res. 2008 May 15;68(10):3655-61.

155. Kuhl M, Sheldahl LC, Park M, Miller JR, Moon RT. The Wnt/Ca2+ pathway: A new vertebrate wnt signaling pathway takes shape. Trends Genet. 2000 Jul;16(7):279-83.

156. Vijayaragavan K, Szabo E, Bosse M, Ramos-Mejia V, Moon RT, Bhatia M. Noncanonical wnt signaling orchestrates early developmental events toward hematopoietic cell fate from human embryonic stem cells. Cell Stem Cell. 2009 Mar 6;4(3):248-62.

157. Sugimura R, Li L. Noncanonical wnt signaling in vertebrate development, stem cells, and diseases. Birth Defects Res C Embryo Today. 2010 Dec;90(4):243-56.

158. Talmadge JE, Singh RK, Fidler IJ, Raz A. Murine models to evaluate novel and conventional therapeutic strategies for cancer. Am J Pathol. 2007 Mar;170(3):793-804.

159. Nieto MA. Epithelial plasticity: A common theme in embryonic and cancer cells. Science. 2013 Nov 8;342(6159):1234850.

160. McDonald OG, Wu H, Timp W, Doi A, Feinberg AP. Genome-scale epigenetic reprogramming during epithelial-to-mesenchymal transition. Nat Struct Mol Biol. 2011 Jul 3;18(8):867-74.

161. Yang MH, Wu KJ. TWIST activation by hypoxia inducible factor-1 (HIF-1): Implications in metastasis and development. Cell Cycle. 2008 Jul 15;7(14):2090-6.

162. Yang MH, Wu MZ, Chiou SH, Chen PM, Chang SY, Liu CJ, et al. Direct regulation of TWIST by HIF-1alpha promotes metastasis. Nat Cell Biol. 2008 Mar;10(3):295-305.

163. Peinado H, Olmeda D, Cano A. Snail, zeb and bHLH factors in tumour progression: An alliance against the epithelial phenotype? Nat Rev Cancer. 2007 Jun;7(6):415-28.

164. Eades G, Yao Y, Yang M, Zhang Y, Chumsri S, Zhou Q. miR-200a regulates SIRT1 expression and epithelial to mesenchymal transition (EMT)-like transformation in mammary epithelial cells. J Biol Chem. 2011 Jul 22;286(29):25992-6002.

165. Gregory PA, Bracken CP, Smith E, Bert AG, Wright JA, Roslan S, et al. An autocrine TGF-beta/ZEB/miR-200 signaling network regulates establishment and maintenance of epithelial-mesenchymal transition. Mol Biol Cell. 2011 May 15;22(10):1686-98.

166. Shapiro IM, Cheng AW, Flytzanis NC, Balsamo M, Condeelis JS, Oktay MH, et al. An EMT-driven alternative splicing program occurs in human breast cancer and modulates cellular phenotype. PLoS Genet. 2011 Aug;7(8):e1002218.

167. Chiou SH, Wang ML, Chou YT, Chen CJ, Hong CF, Hsieh WJ, et al. Coexpression of Oct4 and nanog enhances malignancy in lung adenocarcinoma by inducing cancer stem cell-like properties and epithelial-mesenchymal transdifferentiation. Cancer Res. 2010 Dec 15;70(24):10433-44.

168. Kamiya D, Banno S, Sasai N, Ohgushi M, Inomata H, Watanabe K, et al. Intrinsic transition of embryonic stem-cell differentiation into neural progenitors. Nature. 2011 Feb 24;470(7335):503-9.

169. Li R, Liang J, Ni S, Zhou T, Qing X, Li H, et al. A mesenchymal-to-epithelial transition initiates and is required for the nuclear reprogramming of mouse fibroblasts. Cell Stem Cell. 2010 Jul 2;7(1):51-63.

170. Samavarchi-Tehrani P, Golipour A, David L, Sung HK, Beyer TA, Datti A, et al. Functional genomics reveals a BMP-driven mesenchymal-to-epithelial transition in the initiation of somatic cell reprogramming. Cell Stem Cell. 2010 Jul 2;7(1):64-77.

171. Hanahan D, Weinberg RA. The hallmarks of cancer. Cell. 2000 Jan 7;100(1):57-70.

172. Hanahan D, Weinberg RA. Hallmarks of cancer: The next generation. Cell. 2011 Mar 4;144(5):646-74.

173. Meshorer E, Yellajoshula D, George E, Scambler PJ, Brown DT, Misteli T. Hyperdynamic plasticity of chromatin proteins in pluripotent embryonic stem cells. Dev Cell. 2006 Jan;10(1):105-16.

174. Azad N, Zahnow CA, Rudin CM, Baylin SB. The future of epigenetic therapy in solid tumours--lessons from the past. Nat Rev Clin Oncol. 2013 May;10(5):256-66.

175. Esteller M, Garcia-Foncillas J, Andion E, Goodman SN, Hidalgo OF, Vanaclocha V, et al. Inactivation of the DNA-repair gene MGMT and the clinical response of gliomas to alkylating agents. N Engl J Med. 2000 Nov 9;343(19):1350-4.

176. Ahuja N, Easwaran H, Baylin SB. Harnessing the potential of epigenetic therapy to target solid tumors. J Clin Invest. 2014 Jan 2;124(1):56-63.

177. Campbell RM, Tummino PJ. Cancer epigenetics drug discovery and development: The challenge of hitting the mark. J Clin Invest. 2014 Jan 2;124(1):64-9.

178. Simhadri C, Daze KD, Douglas SF, Quon TT, Dev A, Gignac MC, et al. Chromodomain antagonists that target the polycomb-group methyllysine reader protein chromobox homolog 7 (CBX7). J Med Chem. 2014 Mar 13.

Tables and Table Legends

Gene		Primer Sequence (5'->3')
CD44	Forward	AGCCTGGCGCAGATCGATTTGA
	Reverse	GGCCTCCGTCCGAGAGATGC
Integrin B1	Forward	GCCAAAGCGAAGGCATCCCTGA
	Reverse	CGCCCTTCATTGCACCTGCAC
Osteopontin	Forward	CAAATACCCAGATGCTGTGGCCAC
	Reverse	CAGCATTCTGTGGGGCTAGGAGAT
	Forward	GGAAGTTCTGAGGAAAAGCAGCTTTACAA
	Reverse	GGGCTAGGAGATTCTGCTTCTGAGATG
	Forward	GCAGACCTGACATCCAGTACCCTGA
	Reverse	GGGATGGCCTTGTATGCACCATTCA
JUN	Forward	TGCGCGCAGCCCAAACTAAC
	Reverse	GCTCTCGGACGGGAGGAACG
JUNB	Forward	CGATCTGCACAAGATGAACCACGTGA
	Reverse	CTGCTGAGGTTGGTGTAAACGGGA
LEF1	Forward	CTCCAGGATCACACCCGTCACACA
	Reverse	TGTCCAACACCACCCGGAGACAA
TCF4	Forward	TACTACGAGCTGGCCCGGAAGGA
	Reverse	ATTGGTCTCTCCCGGCTGCTTGTC

Table 2.1: Sequences for quantitative Real-Time PCR primers.

Gene		Sequence (5'->3')
CD44	Set 1F	CCCGGGAGGGCTGCTACTTCTTAA
	Set 1R	AGTGACCTAAGACGGAGGGAGGGA
	Set 2F	CCGATTATTTACAGCCTCAGCAGAGCA
	Set 2R	TGCCTCGGAAGTTGGCTGCA
	Set 3F	CTCACCAGGCAAGAAGTCCATGCA
	Set 3R	TTTCTCCCATCTTTCCTACCCAGCAGA
	Set 4F	CGGGAGGGCTGCTACTTCTTA
	Set 4R	CAGTGACCTAAGACGGAGGGA
	Set 5F	AGGGATCCTCCAGCTCCTTT
	Set 5R	CAGACAGCTCACTTGACTCCA
	Set 6F	ATTTACAGCCTCAGCAGAGCA
	Set 6R	TCGGAAGTTGGCTGCAGTT
	Set 7F	AACTGCAGCCAACTTCCGA
	Set 7R	CTTGTCCATGGTGTCCGGA
	Set 8F	TCAAGTGAGCTGTCTGCGAA
	Set 8R	GCATCCGGGAGAACGGTTA
c-JUN	Set 1F	CTGTAGGAGGGCAGCGGAGCA
	Set 1R	CGAGCTCAACACTTATCTGCTACCAGTCAA
	Set 2F	GACCAAACATTTGGTGAACAGAAAGGGAGA
	Set 2R	TGCCCATACATCATTGGCCAAAGCA
	Set 3F	CCTGATGTACCTGATGCTATGGTCAGGTTA
	Set 3R	AATGGTCACAGCACATGCCACTTGA
	Set 4F	GTGTTTCGGGAGTGTCCAGA
	Set 4R	GAGAAGCCTAAGACGCAGGAA
	Set 5F	GAGAGCCACGCAAGAGAAGA
	Set 5R	CGAACTCACTTCCCAGAGCA
	Set 6F	GCGCGAGTCGACAAGTAAGA
	Set 6R	CCGTCACTTCACGTGAGGTTA
	Set 7F	TGTTGAGCTCGGGCTGGATA
	Set 7R	TGGGCAGTTAGAGAGAAGGTGA

Table 2.2: Sequences for Chromatin Immunoprecipitation quantitative PCR primers.

LEF1	Set 1F	CGGGCAGCCAAGGAGAGCTAGA
	Set 1R	CCTGGTTCCTCGGCCCGAGA
	Set 2F	AGCCGGGCACTAGTCCTGCA
	Set 2R	GGTGACCAGTGGAGTGTCGGGTA
	Set 3F	CAGAGCCACAGGCGGGAGGAA
	Set 3R	GGGCGGTACAGCCAGGGTGTA
	Set 4F	GCTGCACGAACCCTTCCA
	Set 4R	GATCGCCCTCGTCCTTGAA
	Set 5F	CAGCGGAGCGGAGATTACA
	Set 5R	CTGGCCGGGATGATTTCAGA
	Set 6F	TCTCCGCGAAGCGGGAAA
	Set 6R	AGAGTTGGAAGGGTTCGTGCA
	Set 7F	CGGACCCTCCTCTGCACTTT
	Set 7R	TTTCCCGCTTCGCGGAGA

Table 2.2 (continued): Sequences for quantitative Real-Time PCR and Chromatin

Immunoprecipitation

Label	TRC ID	Sequence (5' → 3')
shCD44-1	57563	CCGGGCCCTATTAGTGATTTCCAAACTCGAGTTTGGAAATCACTAATAGGGCTTTTTG
shCD44-2	289308	CCGGCGCTATGTCCAGAAAGGAGAACTCGAGTTCTCCTTTCTGGACATAGCGTTTTTG
shCD44-3	308110	CCGGCCGTTGGAAACATAACCATTACTCGAGTAATGGTTATGTTTCCAACGGTTTTTG
shCD44-4	289233	CCGGCCTCCCAGTATGACACATATTCTCGAGAATATGTGTCATACTGGGAGGTTTTTG
shCD44-5	296191	CCGGGGACCAATTACCATAACTATTCTCGAGAATAGTTATGGTAATTGGTCCTTTTTG

Table 2.3: Sequences for lentivirus-mediated CD44 knockdown.

All Down	CpG	PcG	All Down	CpG	PcG
CD44	CD44	CD44	ICAM1	ICAM1	ICAM1
CDH1	CDH1	CDH1	IGFBP2	IGFBP2	IGFBP2
CDH11	CDH11	CDH11	IGFBP7	IGFBP7	IGFBP7
COL1A1	COL1A1		LAMA1	LAMA1	
COL2A1	COL2A1	COL2A1	LAMA5	LAMA5	
COL3A1			LAMB1	LAMB1	LAMB1
COL4A1	COL4A1		LAMB3		
COL4A2	COL4A2		LAMC1	LAMC1	
COL4A5		COL4A5	LOX	LOX	LOX
COL4A6		COL4A6	LOXL1	LOXL1	
COL5A1	COL5A1		LOXL3	LOXL3	
COL5A2			LOXL4	LOXL4	
COL8A1		COL8A1	MMP2	MMP2	MMP2
COL11A1			MMP11	MMP11	
COL12A1	COL12A1	COL12A1	NID1	NID1	
COL16A1			NTN1	NTN1	NTN1
COL27A1	COL27A1	COL27A1	NTN4	NTN4	NTN4
EVL			PLAU	PLAU	
FBN2	FBN2	FBN2	SDC2	SDC2	SDC2
FBN1	FBN1	FBN1	TGFB2	TGFB2	TGFB2
FLNC	FLNC		THBS1	THBS1	THBS1
FN1	FN1		THBS3	THBS3	
FNDC3B	FNDC3B		TIMP3		TIMP3
			SNAI2	SNAI2	SNAI2
			TWIST1	TWIST1	TWIST1

Table 2.4: Extracellular Matrix proteins with reduced expression in Cbx7-overexpressing Tera2. Gene expression differences between empty vector control and Cbx7-overexpressing Tera2 were measured by Agilent Gene Expression microarray data, as described previously by Mohammad et al. {{137}}. "All down" represents genes downregulated in Cbx7-overexpressing Tera2 relative to empty vector control. "CpG" denotes genes with CpG island-containing promoters, as determined by UCSC criteria.

Figures and Figure Legends
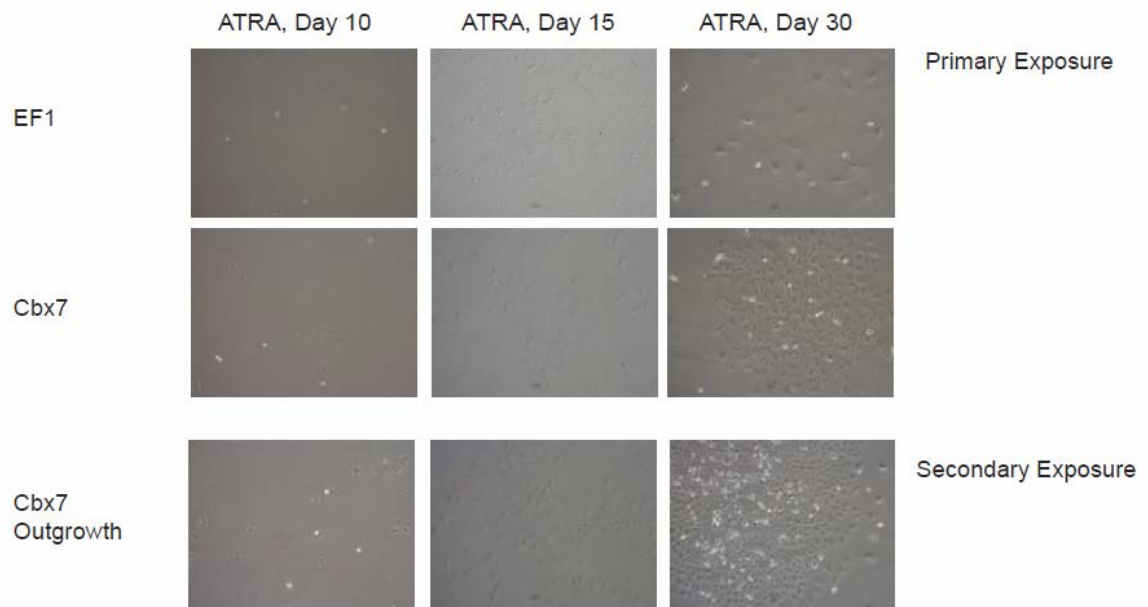
Figure 2.1: Formation of retinoid-resistant Cbx7-overexpressing Tera2 and Tera2 Cbx7 Outgrowth cells. Empty vector, Cbx7 Tera2, Cbx7 Outgrowth Tera2 were exposed to all-*trans* retinoic acid (ATRA). Cells were shown at Day 15, and Day 30 of treatment, with media and ATRA changed every 3 days.
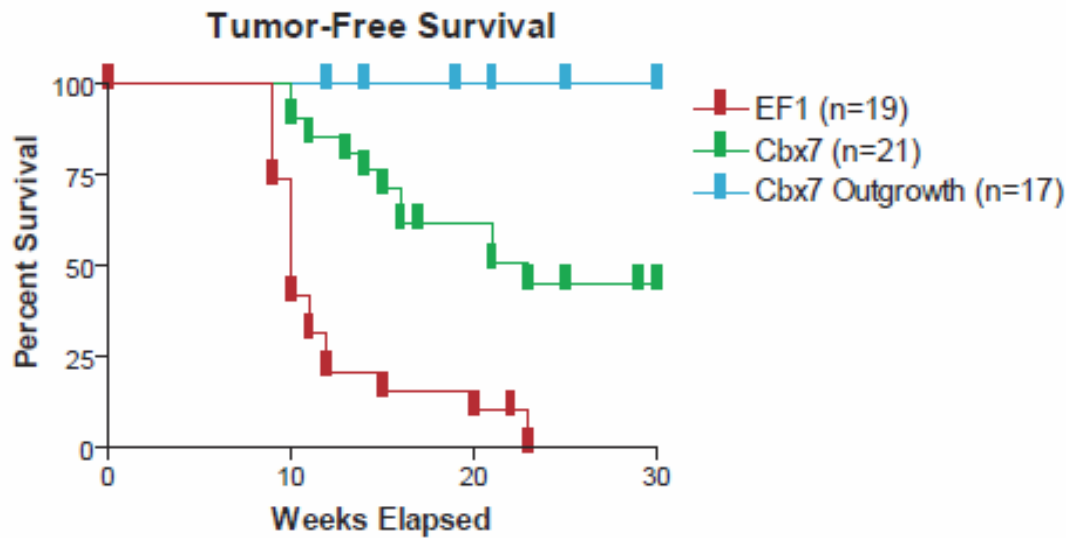
Figure 2.2: Tumor formation in empty-vector control Tera2, Cbx7-overexpressing Tera2 and ATRA-exposed Cbx7 Outgrowth population. 5 million cells were injected subcutaneously in NOD/SCID mice 1:1 with MatriGel (100ul volume). Empty Vector EF1, Cbx7-overexpressing Tera2, and retinoid-exposed Cbx7 Outgrowth Tera2. Y-axis value represents tumor-free survival; each decrease represents time of first detection of palpable subcutaneous tumors in xenografted animals. Data represents totals from three independent series of injections with empty vector, Cbx7, and Cbx7 Outgrowth.
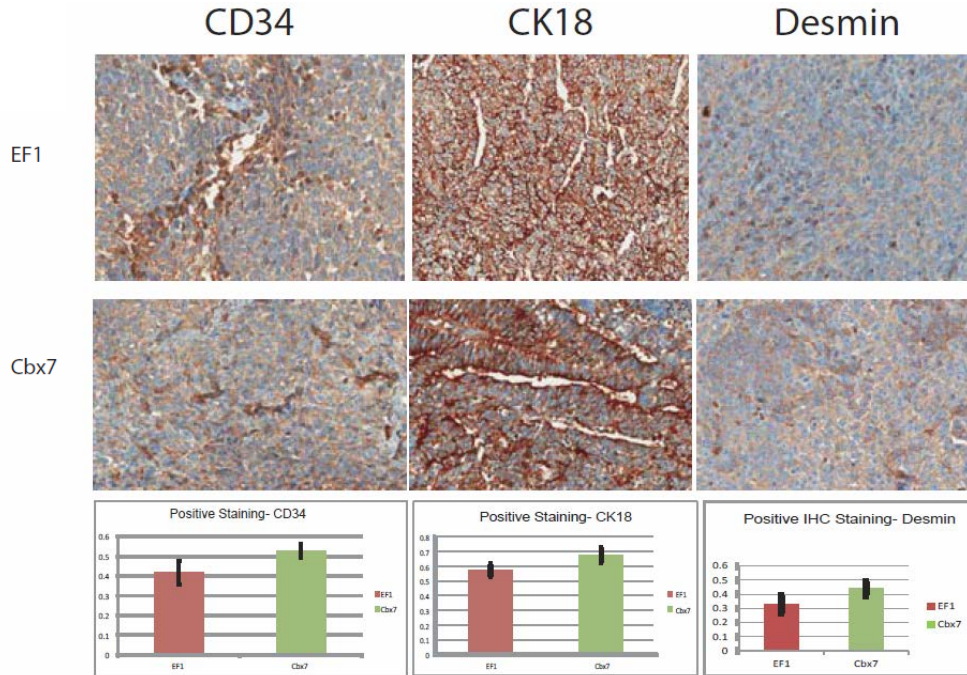
Figure 2.3: Immunohistochemistry for lineage markers on xenografted empty vector, Cbx7, and Cbx7 Outgrowth Tera2 teratocarcinomas. IHC image for EF1 (top panel), Cbx7 (middle panel) and comparison of positive staining in empty vector Tera2 xenograft and Cbx7-overexpressing Tera2 (bottom panel) for markers CD34, CK18, Desmin, GFAP, Chromogranin, S100. Xenografted mice were sacrificed when subcutaneous tumors reached 2cm in size, according to animal protocol guidelines. Dissected tumors were fixed overnight in 4% formaldehyde.
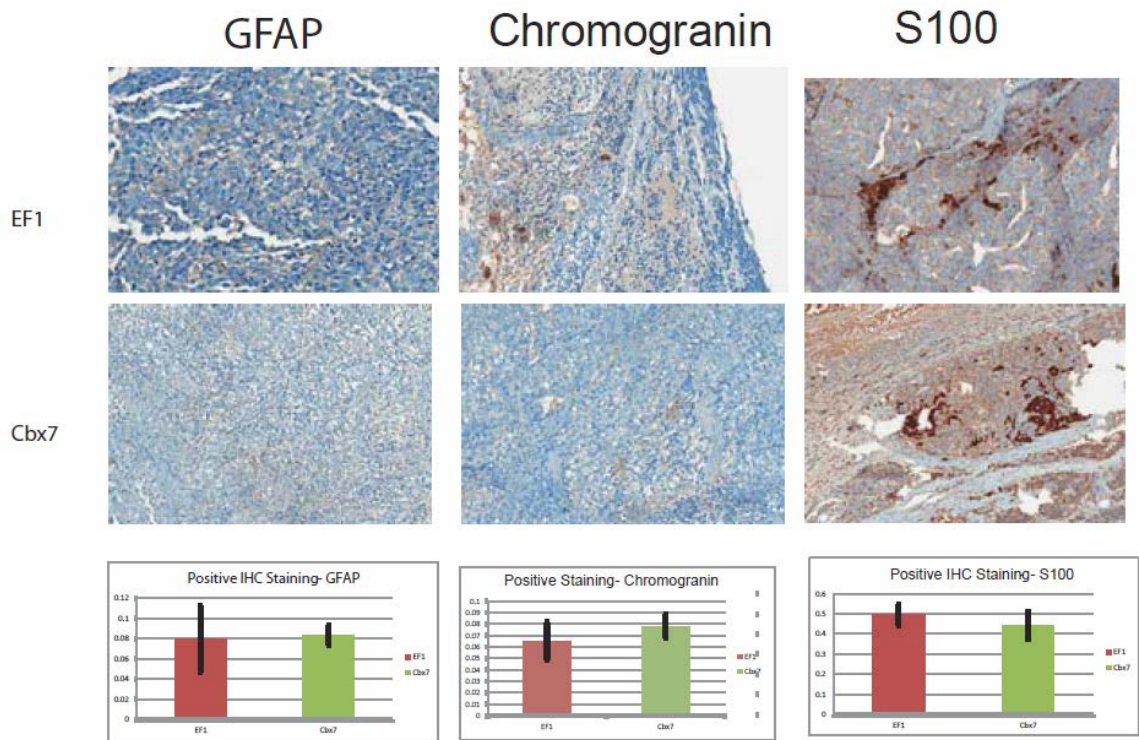
Figure 2.3 (cont.) IHC image for EF1 (top panel), Cbx7 (middle panel) and comparison of positive staining in empty vector Tera2 xenograft and Cbx7-overexpressing Tera2 (bottom panel) for markers CD34 (A), CK18 (B), and Desmin (C).
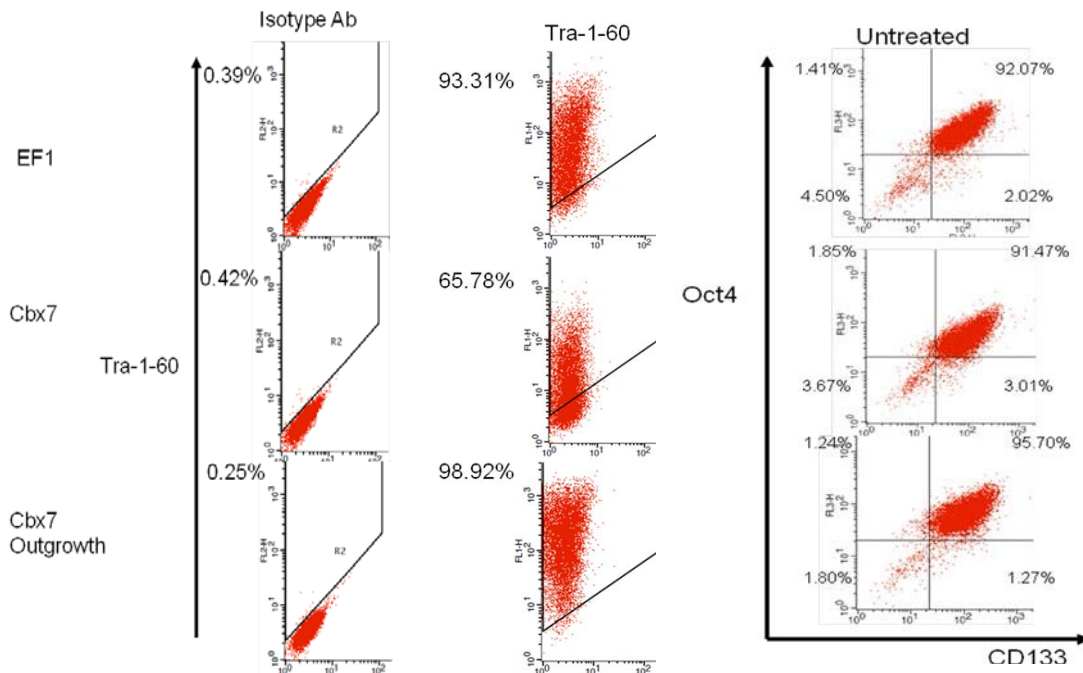
Figure 2.4: **Measurement of stem cell markers Oct4, CD133, and Tra-1-60**.

Pluripotent cell surface markers Tra-1-60 were measured by flow cytometry. Non-specific Isotype antibody or anti-Tra-1-60 antibody was incubated with Empty Vector, Cbx7, and Cbx7 Outgrowth cells.
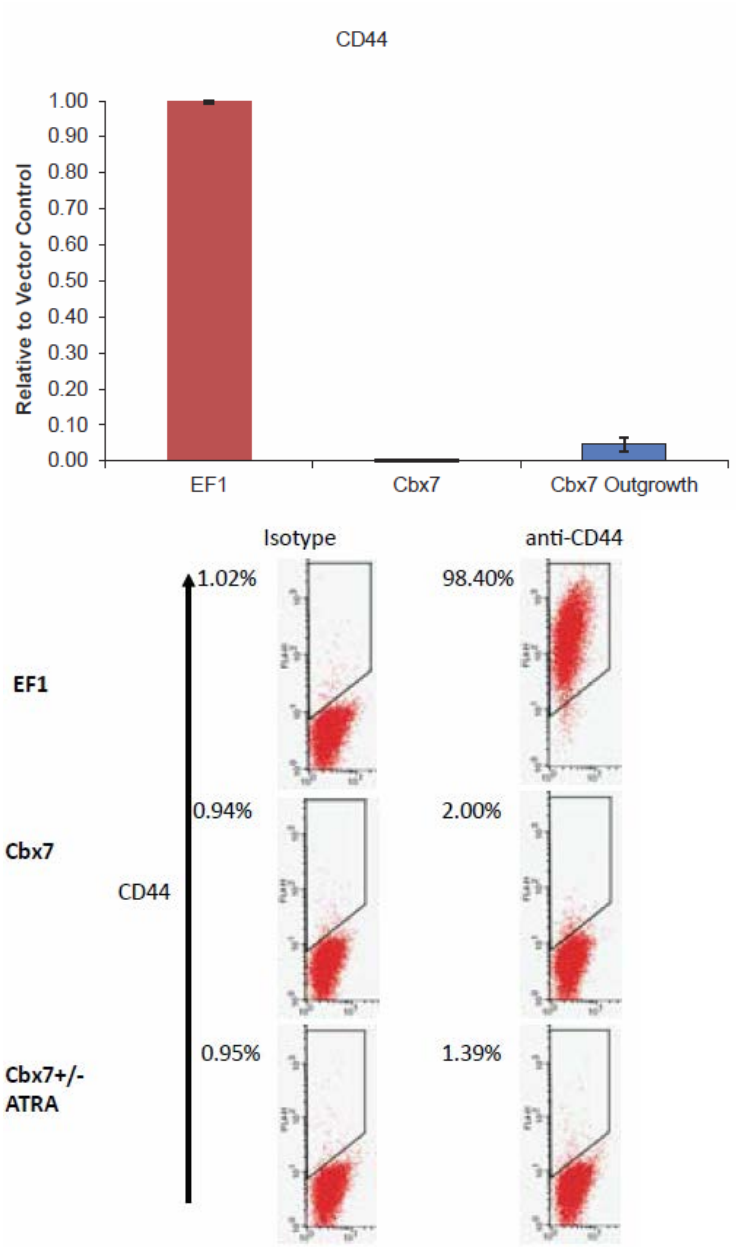
Figure 2.5: Validation of microarray results for loss of CD44 mRNA and protein.

Real-time quantitative PCR was used to measure levels of CD44 in empty vector, Cbx7, and Cbx7 Outgrowth cells. Flow cytometry with anti-CD44 and conjugated secondary antibody. Isotype represents incubation with fluorophore-conjugated secondary antibody only.
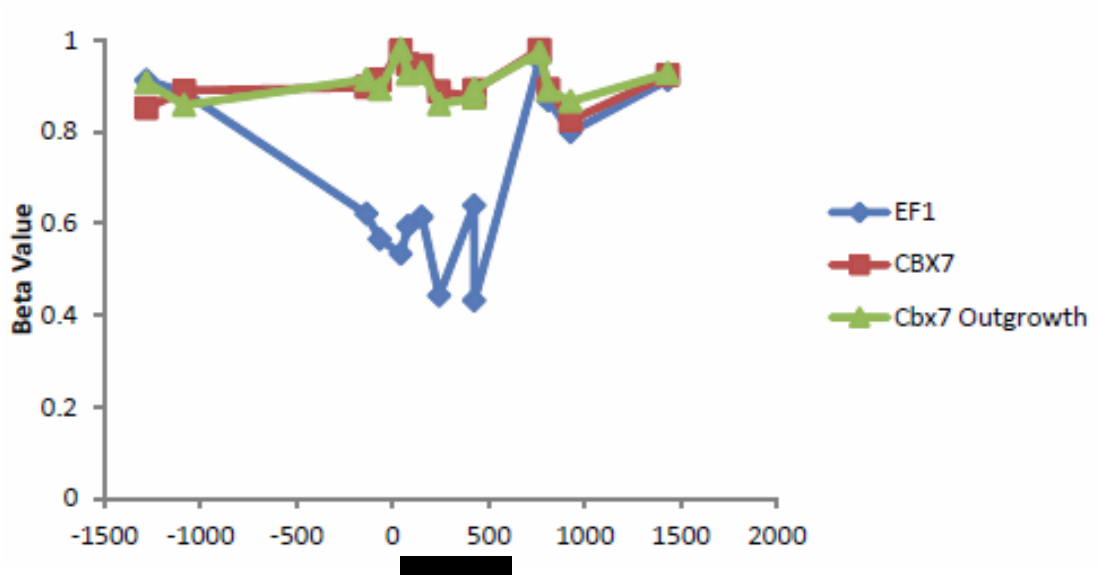
Figure 2.6: Increase in DNA methylation at the CD44 promoter. Promoter DNA methylation was measured by Illumina Infinium 450K microarray with empty vector, Cbx7, and Cbx7 Outgrowth cells. X-axis shows location relative to the CD44 transcriptional start site. Y-values represent beta values (Methylation signal/Total signal).
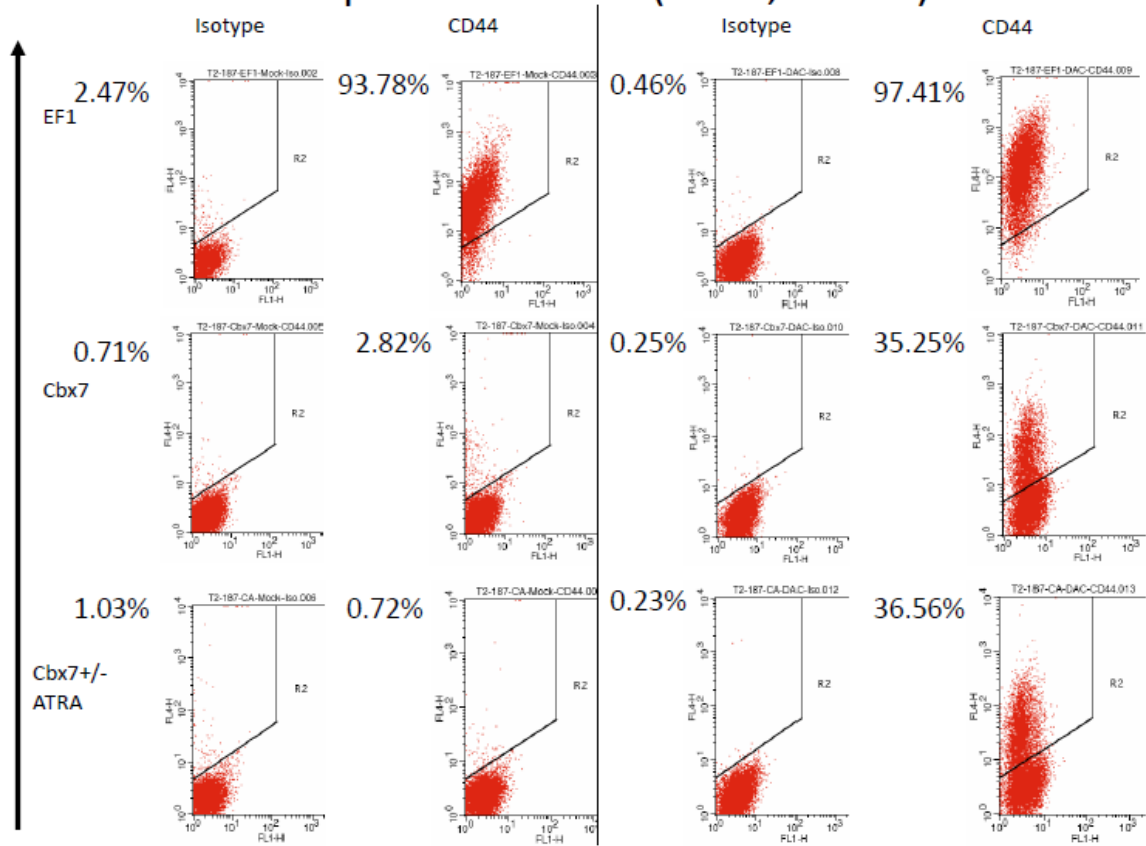
Figure 2.7: Re-expression of CD44 with 1uM demethylating agent 2'-deoxy-5-azacytidine (DAC, decitabine). 72 hour treatment of empty vector, Cbx7, and Cbx7 Outgrowth cells with 1uM DAC (fresh media with DAC changed at 24-hour intervals). Cells were incubated with primary rabbit anti-CD44 antibody and anti-rabbit APC-conjugated secondary or anti-rabbit APC-conjugated antibody only (Isotype) prior to flow cytometry. Percentages represent cells positive in the defined region.

Osteopontin (OPN, SPP1)
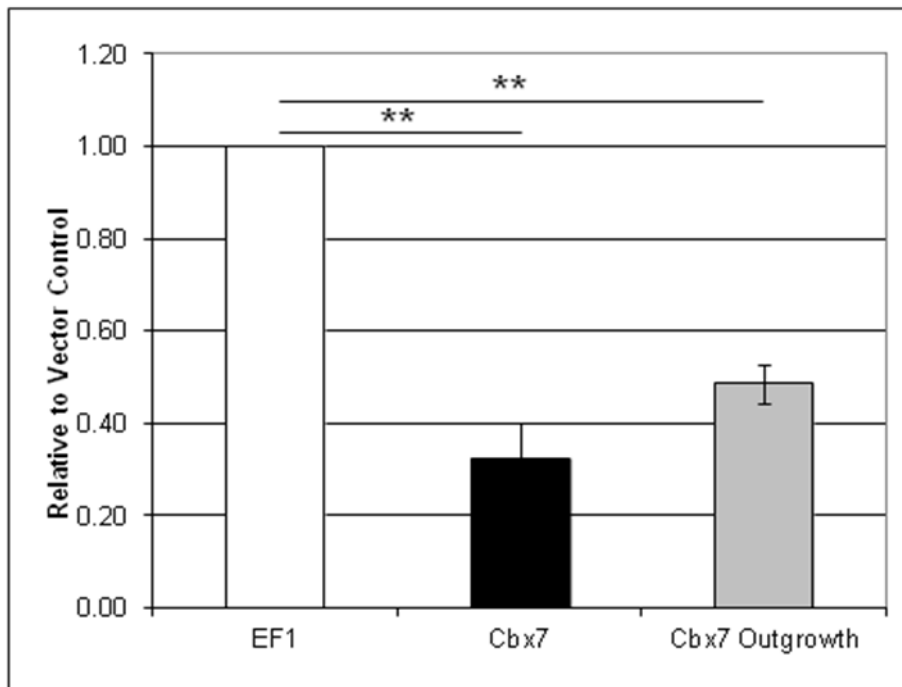
Integrin β2
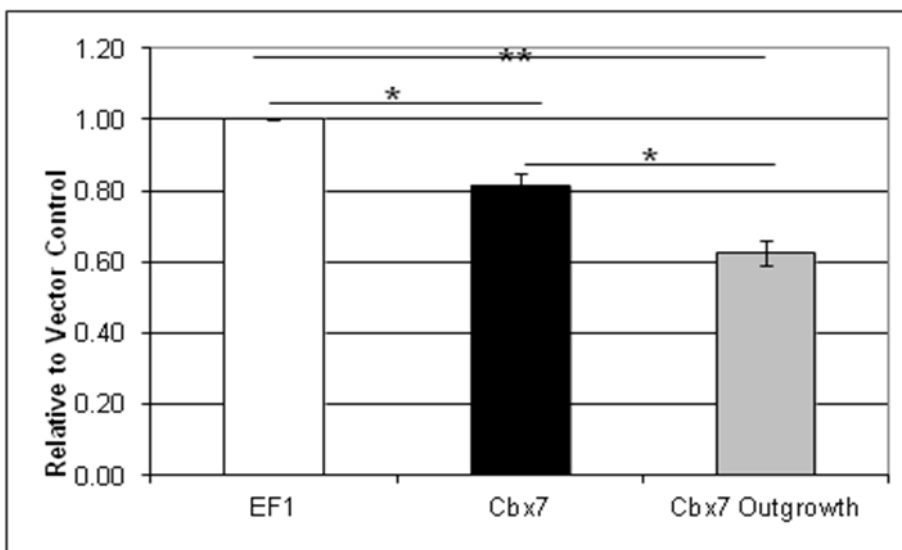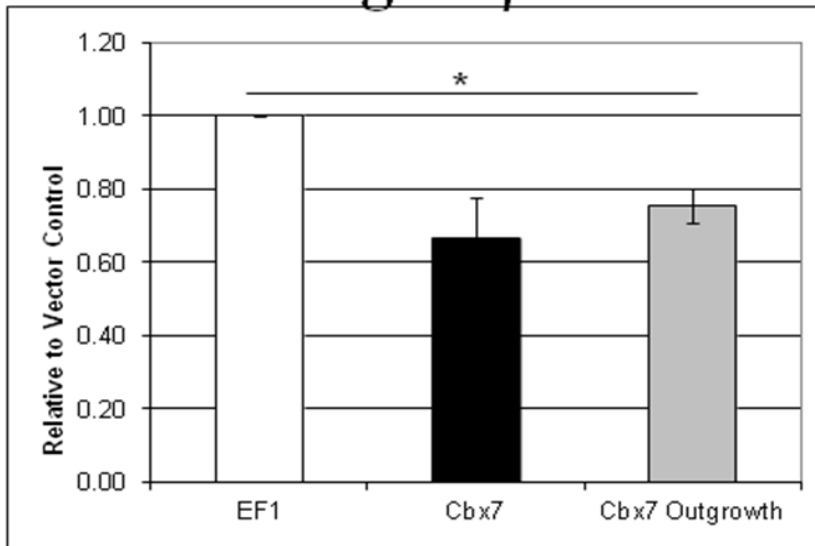
Integrin β1
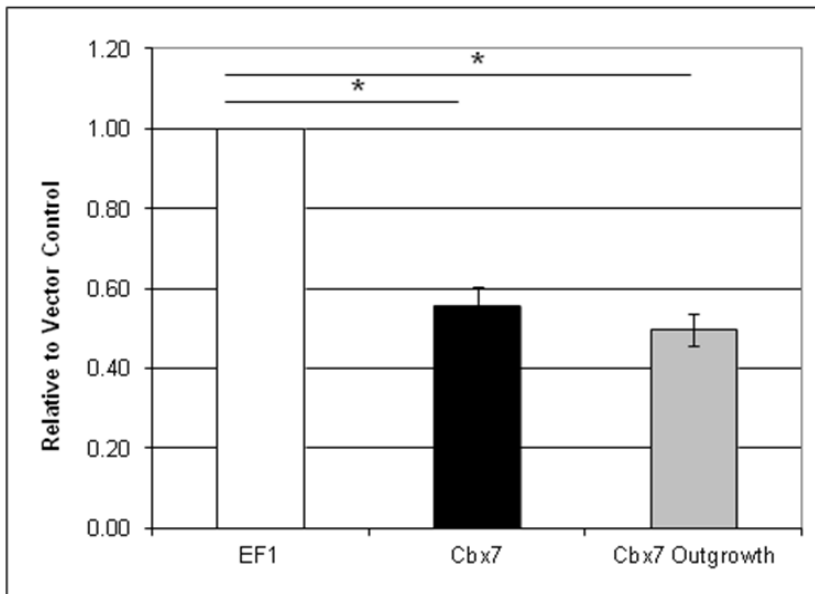
Integrin α7

Figure 2.8: Reductions in transcripts associated with CD44-mediated signaling.

Expression of osteoponin and several integrins were reduced in Cbx7 and Cbx7

Outgrowth populations, as measured by quantitative real-time PCR.

EF1   Cbx7   Cbx7 Outgrowth

phospho-Src

Src (total)

GAPDH
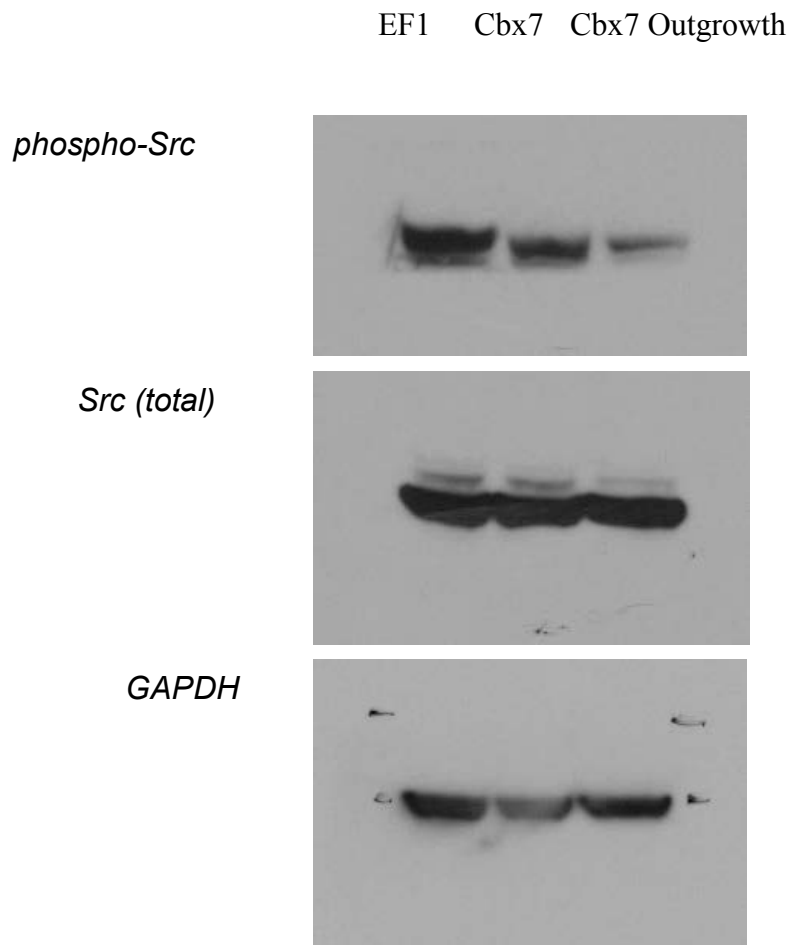
Figure 2.9: Measurement of c-Src total expression and phosphorylation status.

Immunoblots of Phosphorylated c-Src were measured by Western Blot.
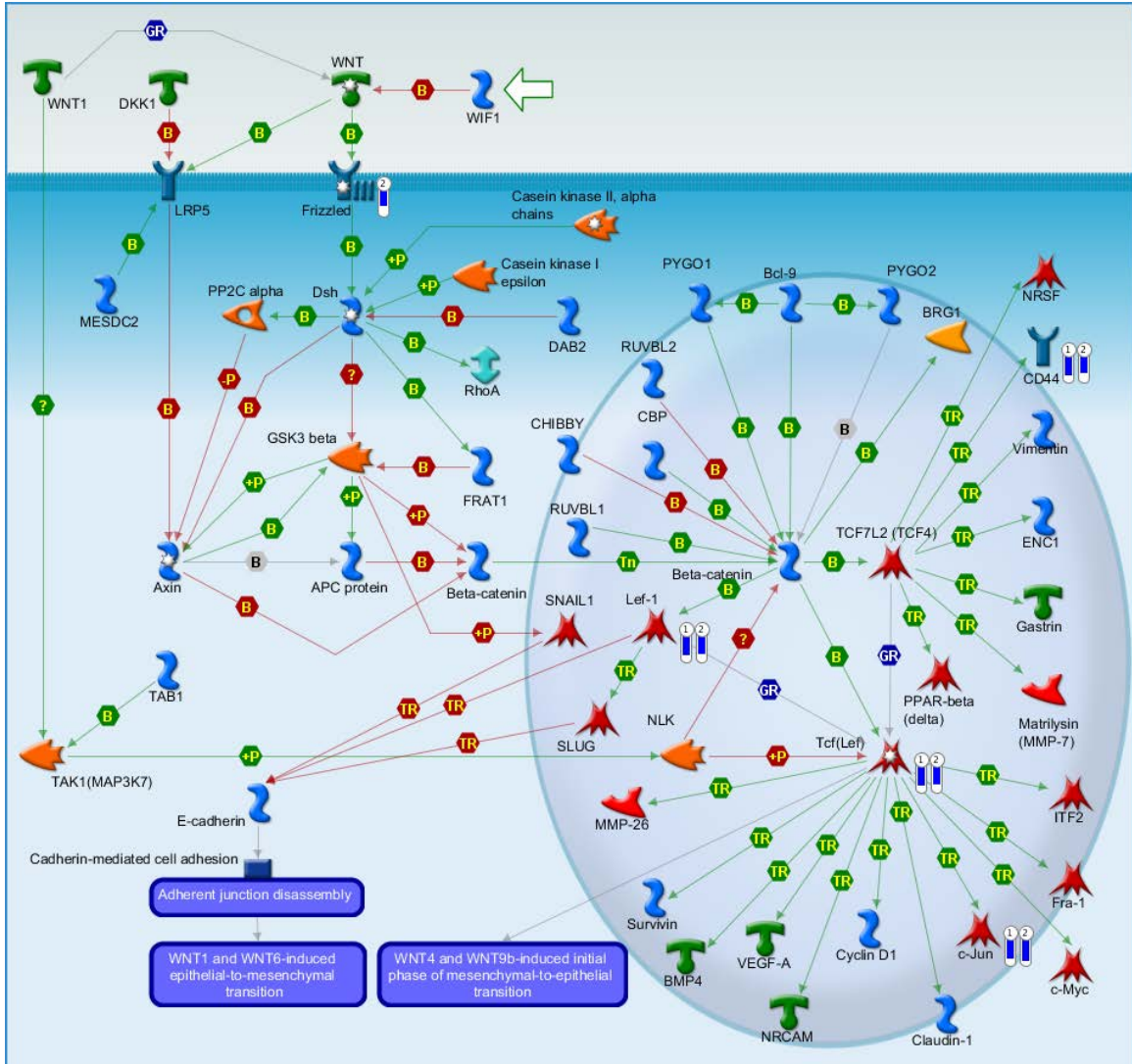
Figure 2.10 MetaCore Analysis on gene expression comparison of empty vector, Cbx7-overexpressing Tera2, and Cbx7 Outgrowth populations. Agilent Gene expression microarray data comparison of empty vector vs. Cbx7 (thermometer 1) and Empty vector vs. Cbx7 Outgrowth populations (thermometer 2) were analyzed via MetaCore pathway analysis.
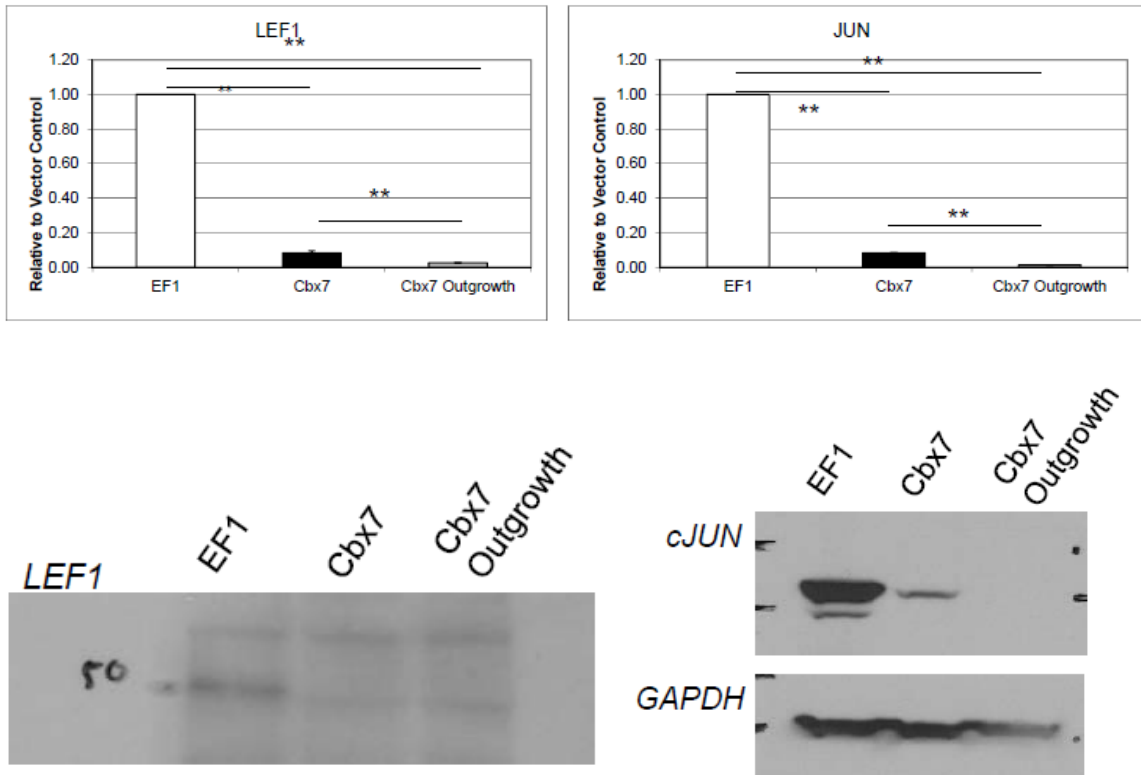
Figure 2.11: Validation of reduction in LEF1 and cJUN DNA binding proteins.

Comparison of LEF1 and cJUN mRNA expression levels were measured by cDNA

synthesis followed by real-time PCR. Immunoblots were used to confirm reductions in

LEF1 levels. **: p<0.01 (by Student's t-test)

A
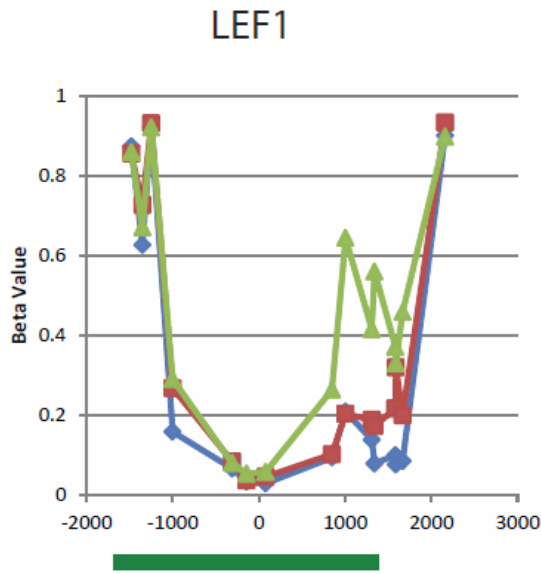
B
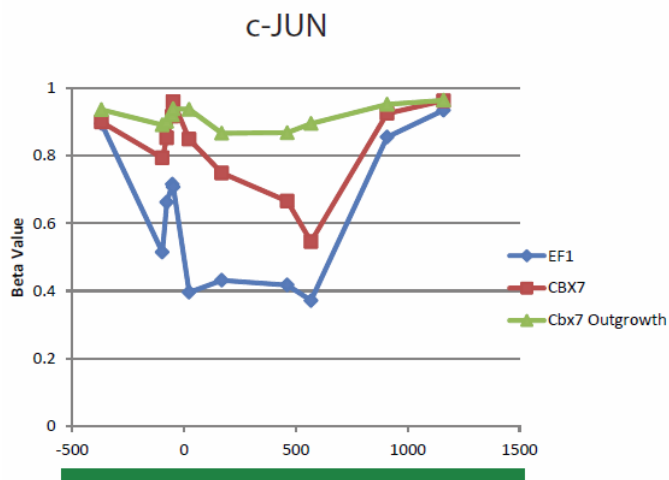
Figure 2.12: Analysis of CpG DNA methylation at LEF1 and cJUN genomic loci by microarray. Global methylation analysis was performed by Illumina Infinim450K array for LEF1 (A) and JUN (B). Values along the X-axis represent location relative to gene transcriptional start site. Y-axis values represent beta values. Dark bars below the X-axis represent location of CpG island(s).
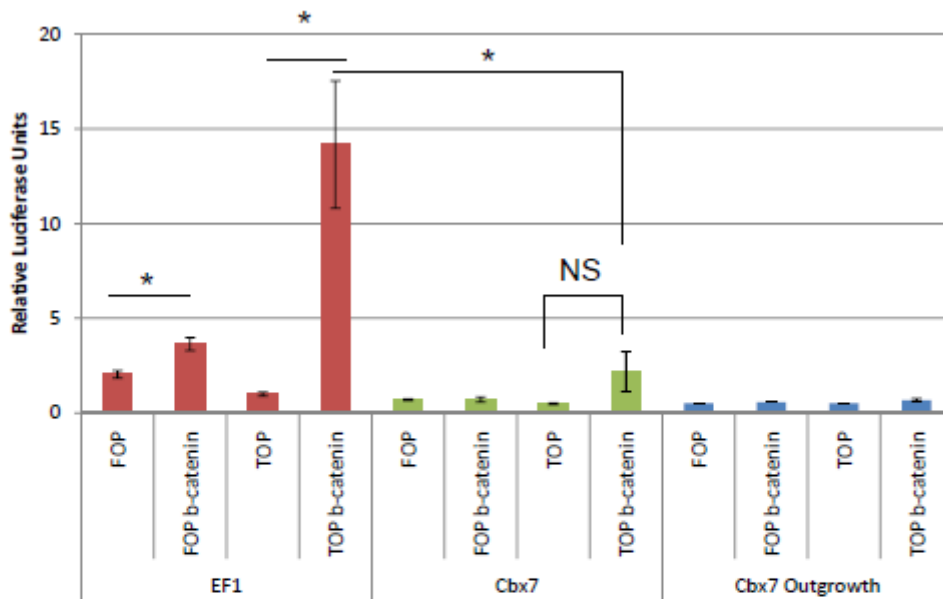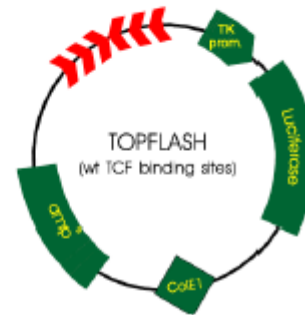
Figure 2.13: Study of Wnt pathway analysis by TOPFLASH LEF/TCF reporter assay. Empty vector, Cbx7, and Cbx7 Outgrowth populations were co-transfected with b-catenin, pRL-TK constitutive *Renilla* luciferase control and either the TOPFLASH (WT consensus LEF/TCF binding sites) or FOPFLASH (mutant LEF/TCF binding sites) *Photinus* firefly luciferase reporter vectors. Cell lysates were analyzed for luciferase activity after 48 hours with DualGlo Dual Luciferase Assay Kit (Promega). *: $p<0.05$ (by Student's t-test)
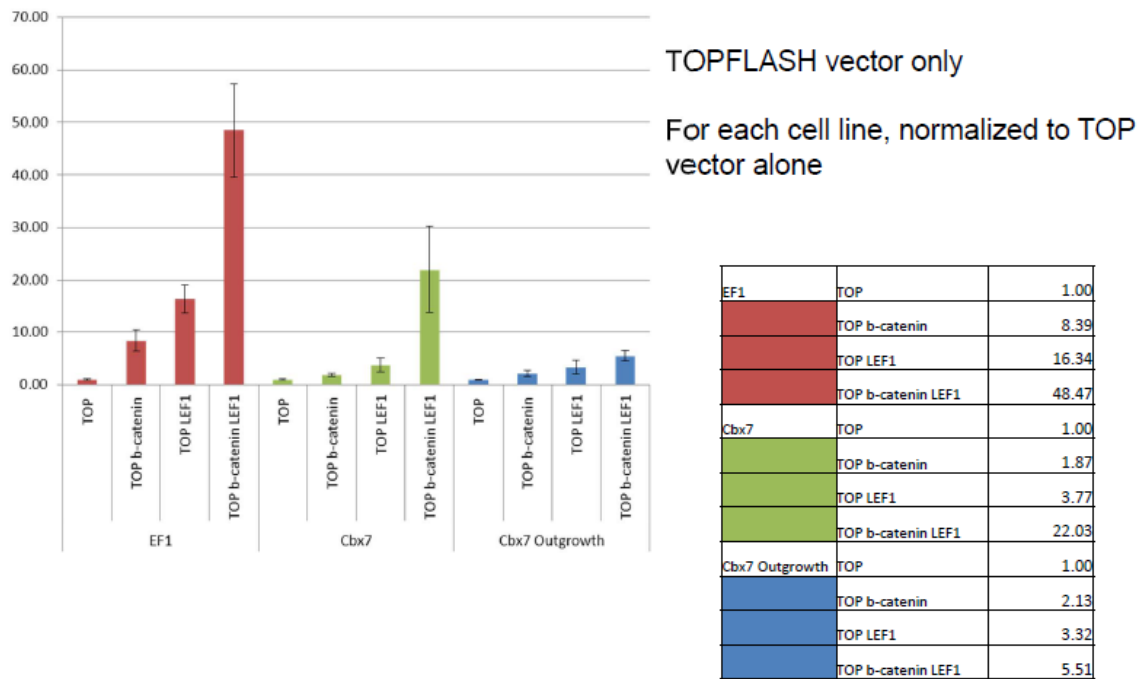
Figure 2.14: Luciferase reporter constructs with co-transfection with LEF1. Empty vector, Cbx7, and Cbx7 Outgrowth populations were co-transfected with TOPFLASH and LEF1, b-catenin, or both. Cell lysates were analyzed for luciferase activity after 48 hours with DualGlo Dual Luciferase Assay Kit (Promega).

phosho-GSK3b   *GSK3b*

GAPDH
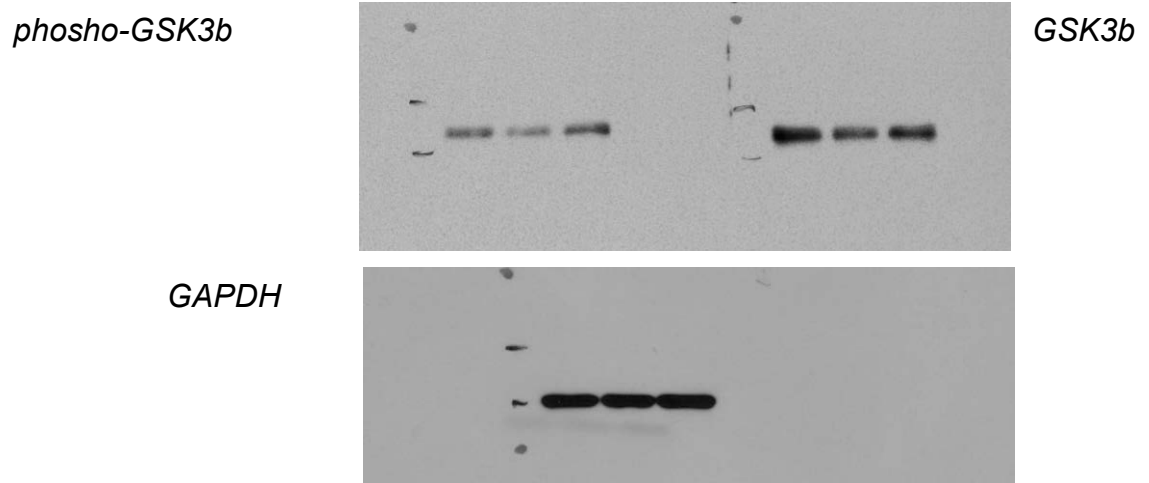
Figure 2.15: Protein expression and activity status of Glycogen Synthase Kinase (GSK)-3β. Immunoblotting was used to measure total expression levels of GSK3β, as well as the phosphorylation status of GSK3β.
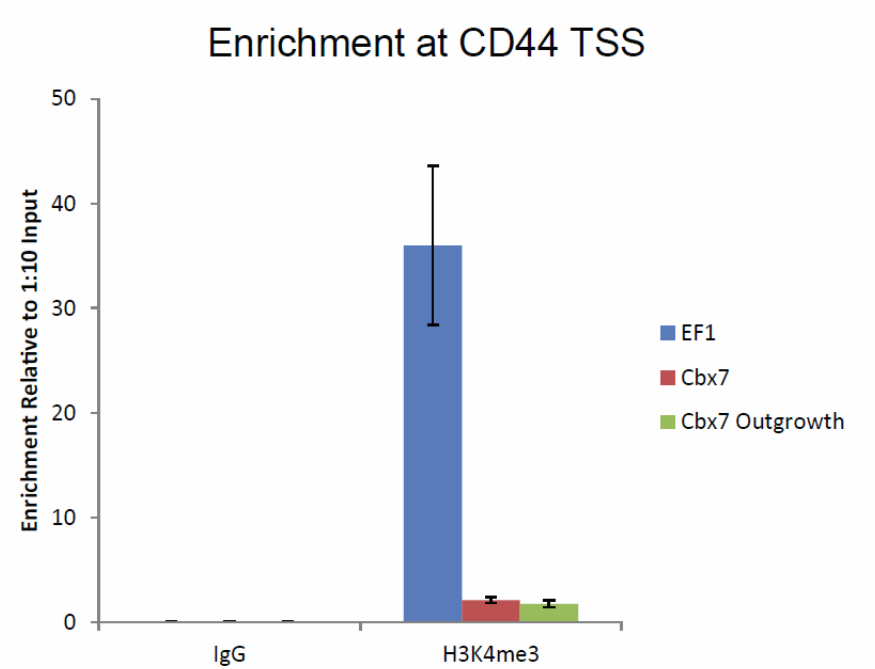
Figure 2.16: Chromatin immunoprecipitation (ChIP) of H3K4me3 at the CD44 transcriptional start site. ChIP for H3K4me3, associated with active genes, and repressive histone marks H3K9me2 were performed at the CD44 transcriptional start sites.
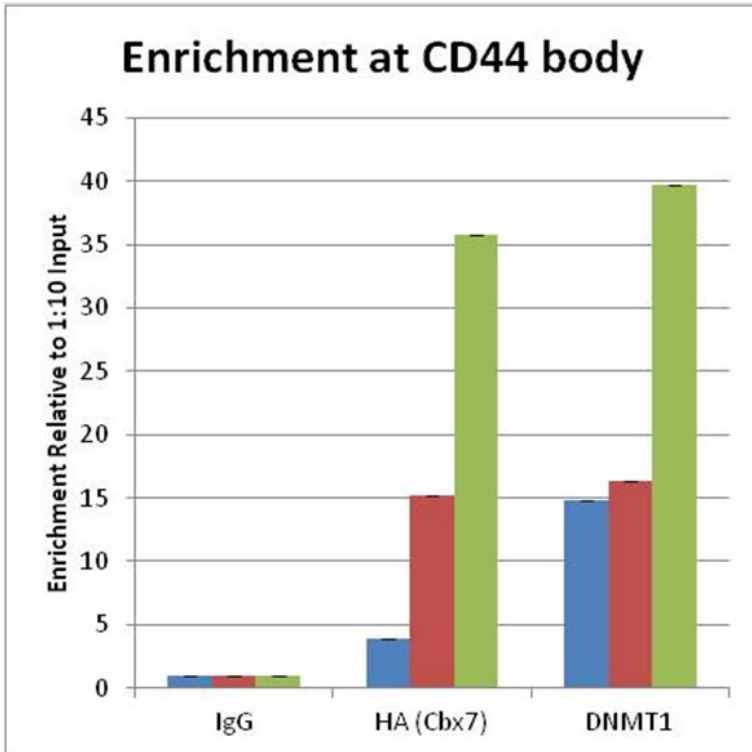
Figure 2.17: Recruitment of HA-Cbx7 and DNMT1 to the CD44 CpG island within gene body. ChIP using anti-HA was used to show recruitment of the tagged Cbx7 protein at genes that gain CpG DNA methylation. Enrichment values relative to non-immunoprecipitated input were calculated by real-time PCR. Primers used for ChIP are listed in Table 2.1
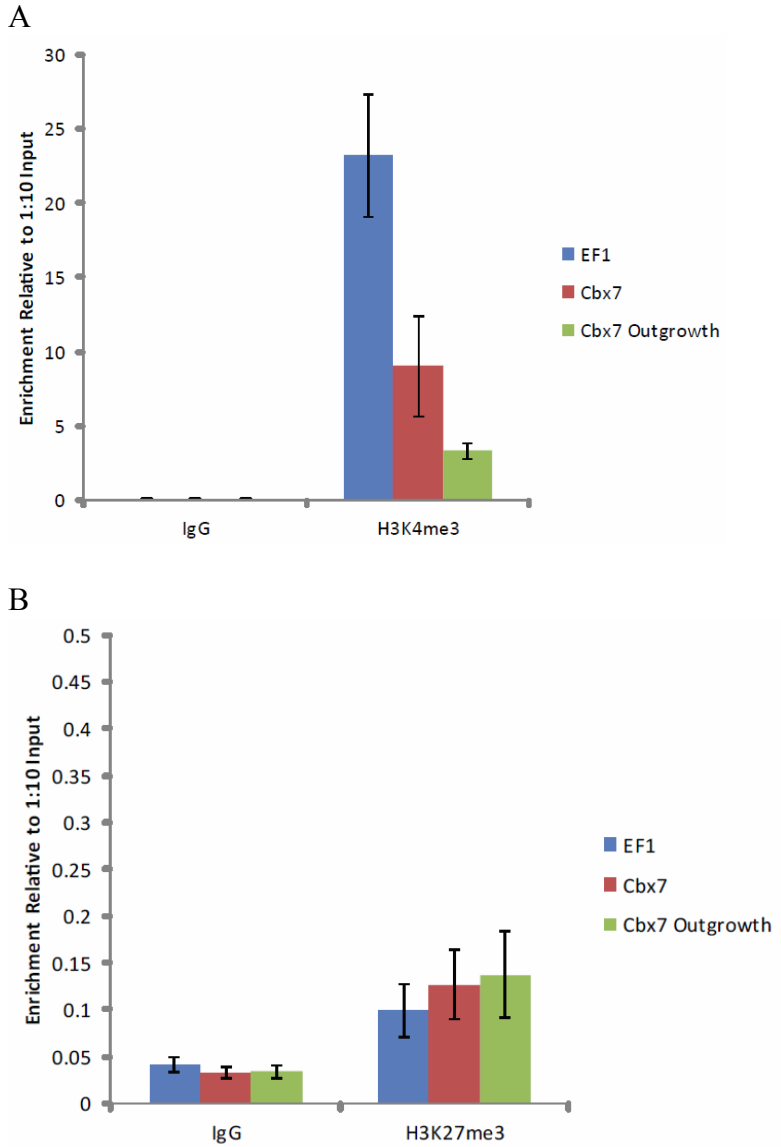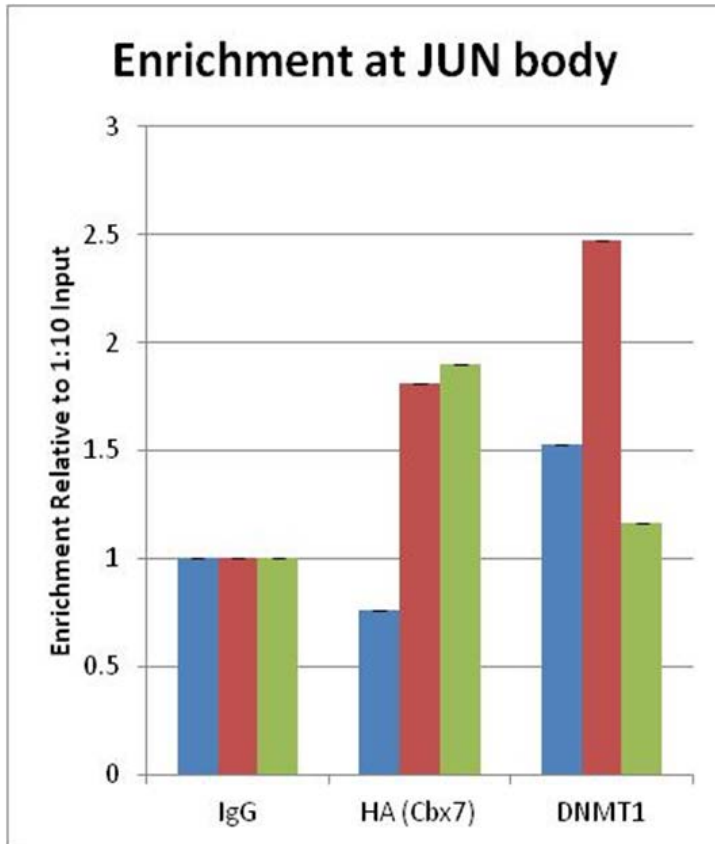
.
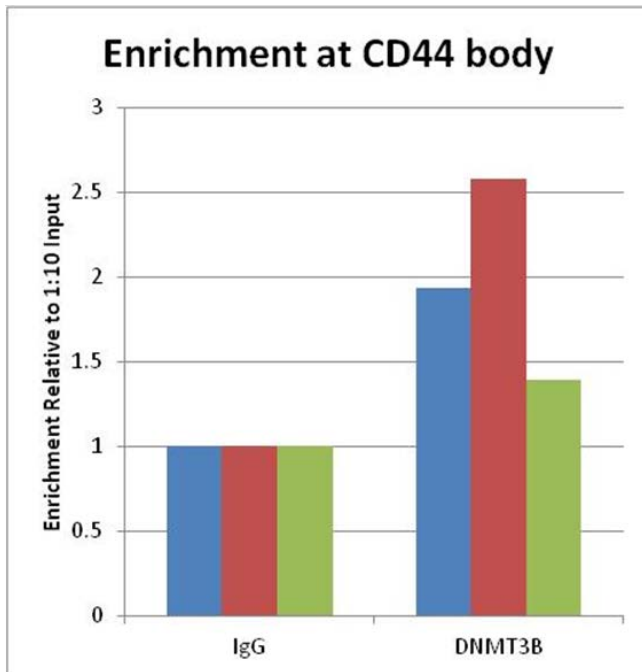
Figure 2.18: Recruitment of DNMT3 to the CD44 CpG island within gene body.

ChIP using anti-HA was used to show recruitment of the tagged Cbx7 protein at genes that gain CpG DNA methylation. Enrichment values relative to non-immunoprecipitated input were calculated by real-time PCR. Primers used for ChIP are listed in Table 2.1

A

B

Figure 2.19: Chromatin immunoprecipitation (ChIP) of H3K4me3 and H3K9me3 at the *JUN* locus. ChIP for H3K4me3, associated with active genes, and repressive histone marks H3K9me2 were performed within the *JUN* gene body.
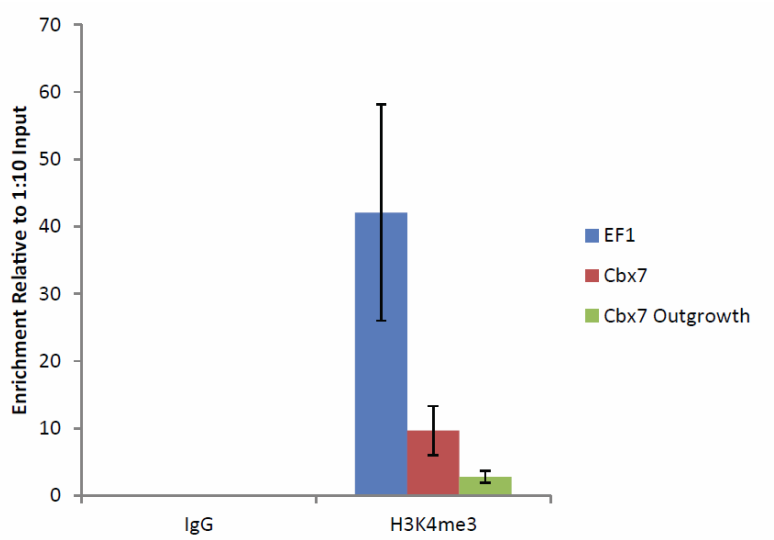
Figure 2.20: Recruitment of HA-Cbx7 and DNMT1 near the JUN CpG island promoter. ChIP using anti-HA was used to show recruitment of the tagged Cbx7 protein at genes that gain CpG DNA methylation. Enrichment values relative to non-immunoprecipitated input were calculated by real-time PCR. Primers used for ChIP are listed in Table 2.1
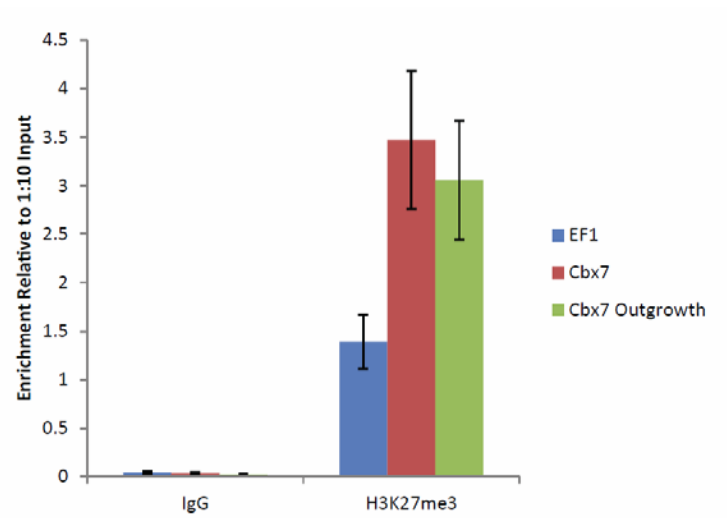
A

B

Figure 2.21: Chromatin immunoprecipitation (ChIP) of H3K4me3 at the LEF1 transcriptional start site. ChIP for H3K4me3, associated with active genes, and repressive histone marks H3K9me2 were performed within the *JUN* gene body.
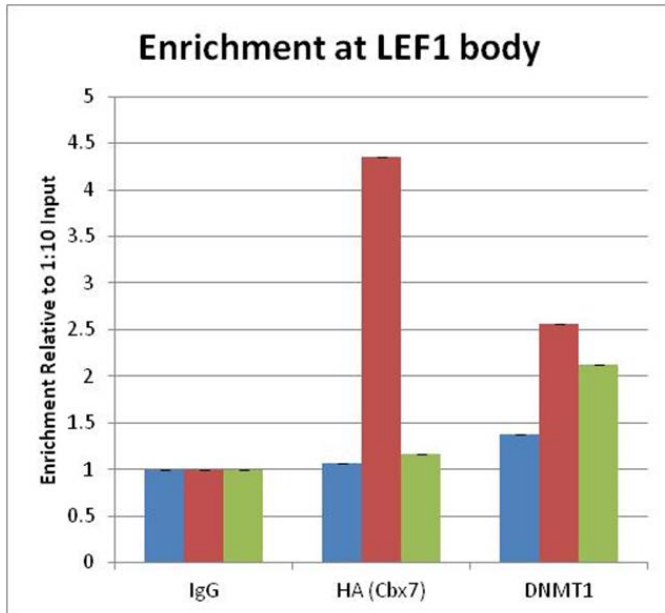
Figure 2.22: Recruitment of HA-Cbx7 and DNMT1 in the LEF1 CpG island gene body. ChIP using anti-HA was used to show recruitment of the tagged Cbx7 protein at genes that gain CpG DNA methylation. Enrichment values relative to non-immunoprecipitated input were calculated by real-time PCR. Primers used for ChIP are listed in Table 2.1

Figure 2.23: Recruitment of DNMT3b LEF1 CpG island within gene body. ChIP

using anti-HA was used to show recruitment of the tagged Cbx7 protein at genes that

gain CpG DNA methylation. Enrichment values relative to non-immunoprecipitated

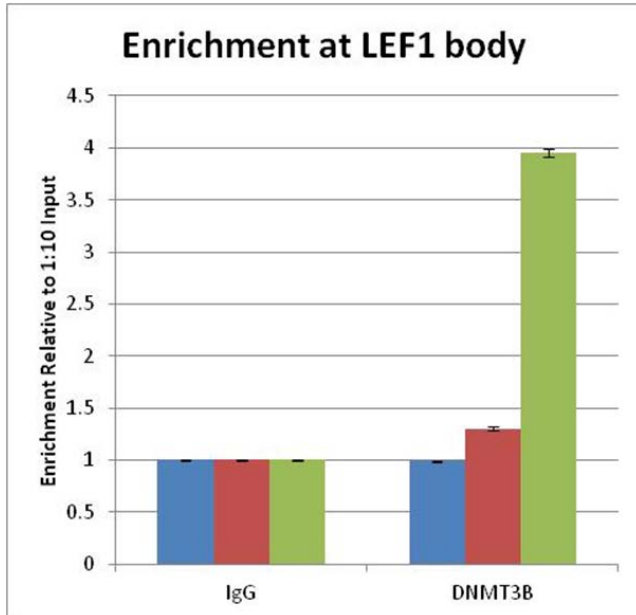input were calculated by real-time PCR. Primers used for ChIP are listed in Table 2.1
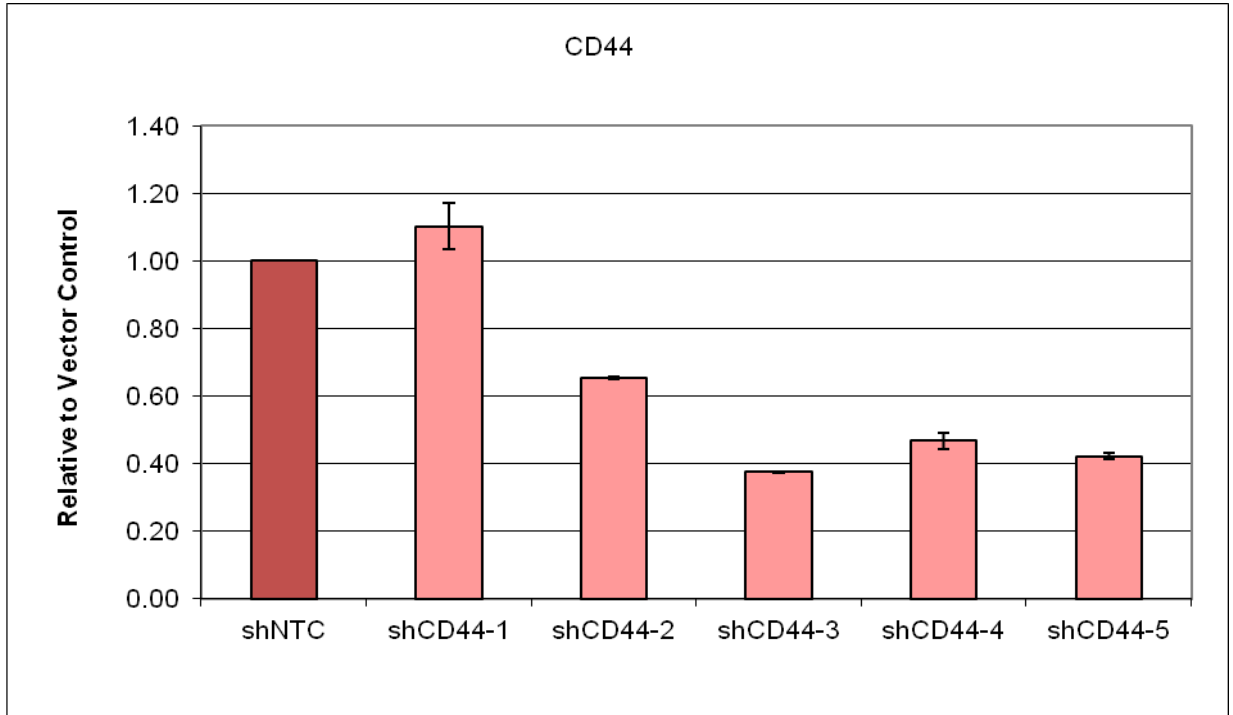
Figure 2.24: Short-hairpin RNA-mediated reduction in CD44 levels. Empty vector cells were transduced with lentivirus particles carrying anti-CD44 shRNA sequences or scrambled sequence ("NTC"). Transduced cells were placed under dual selection for puromycin (for Cbx7-HA selection) and geneticin (for stably-transduced cells). For each shRNA sequence, real-time PCR was performed after approximately 2 weeks after transduction. Sequences targeted by lentiviral constructs are listed in Table 2.2.
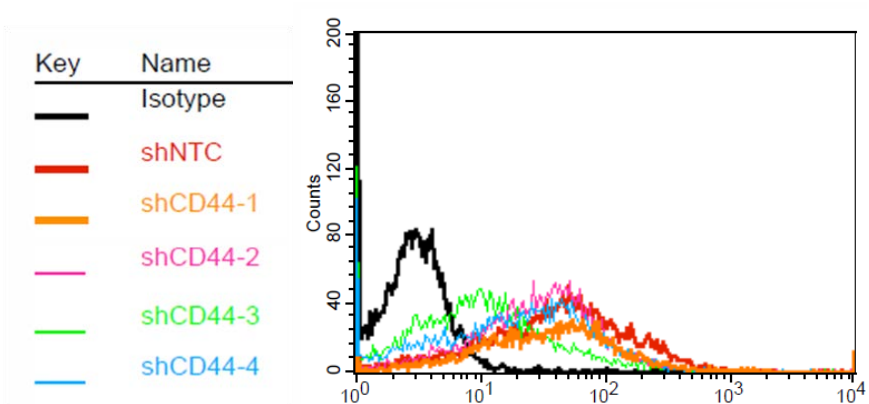
Figure 2.25: Flow cytometry of lentiviral mediated knockdown of CD44. Empty vector, Cbx7, and Cbx7 Outgrowth were transduced with lentivirus particles carrying anti-CD44 shRNA sequences. Transduced cells were placed under dual selection for puromycin (for Cbx7-HA selection) and geneticin (for stably-transduced cells). Flow cytometry was used to validate reduction in surface expression of CD44.
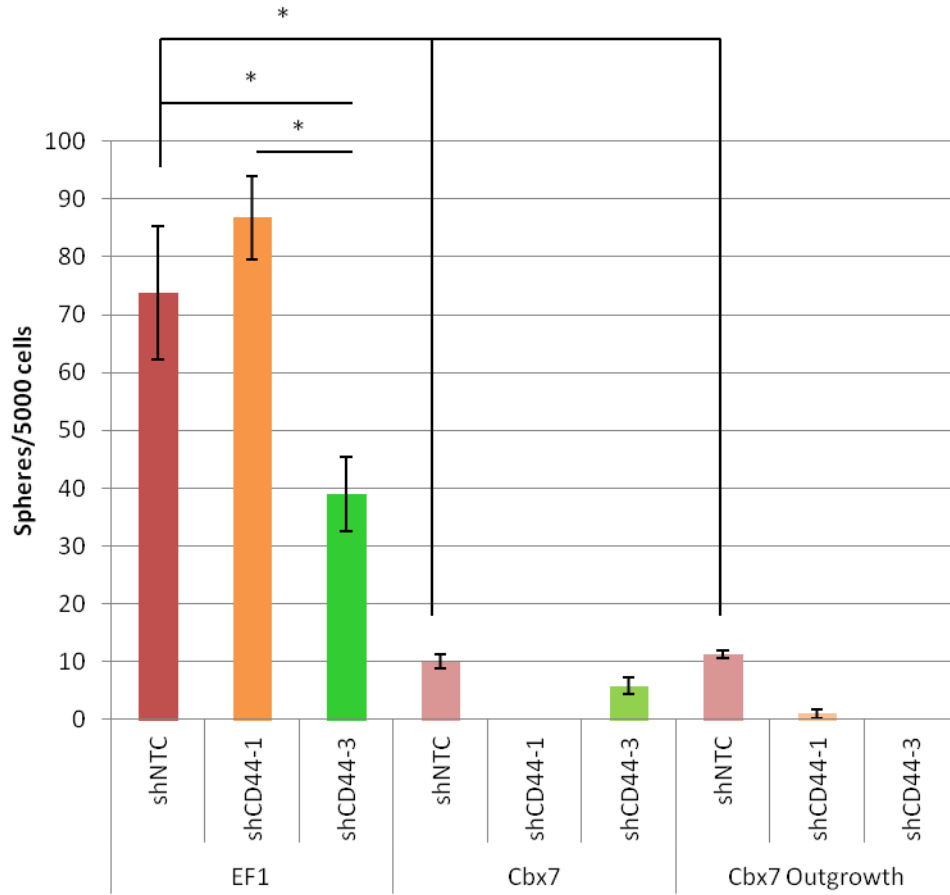
Figure 2.26: Reduction of sphere formation in CD44-reduced Tera2 population.

Non-targeting negative control (shNTC), ineffective CD44 shCD44-1, and effective

CD44 knockdown lentivirus shCD44-3 were analyzed by tumor sphere formation as

previously described {{228}}. Spheres were photographed on AxioCam for

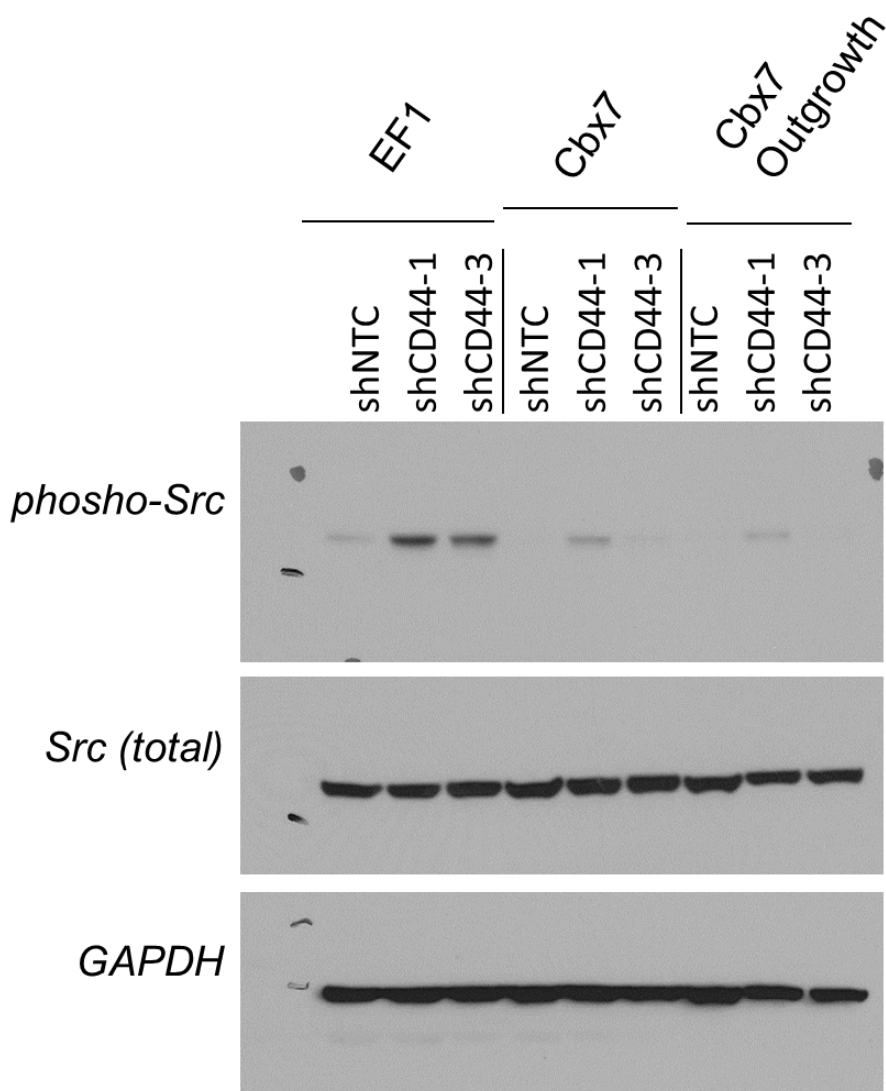measurements, and spheres greater than 50um were counted.

Figure 2.27: Reduction in Src activity in CD44-knock down cells. Immunoblots for phosphorylated Src kinase and total Src kinase levels were performed for Empty vector, Cbx7, and Cbx7 Outgrowth cells for non-targeting control (shNTC), shCD44-1 (ineffective CD44 knockdown), and shCD44-3 (effective CD44 knockdown).
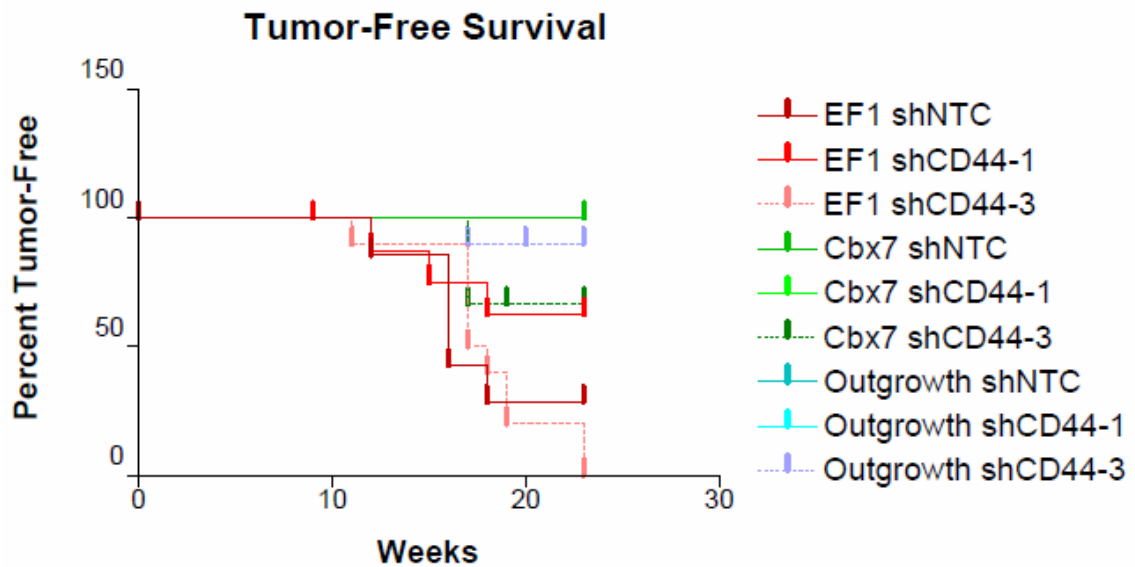
Figure 2.28: Xenografts of EF1, Cbx7, and Cbx7 Outgrowth with CD44 lentiviral knockdown. EF1, Cbx7, and Cbx7 Outgrowth were transduced with non-targeting control shNTC, shCD44-1 (ineffective CD44 knockdown) or shCD44-3 (effective CD44 knockdown), followed by selection for stable clones with antibiotic selection.
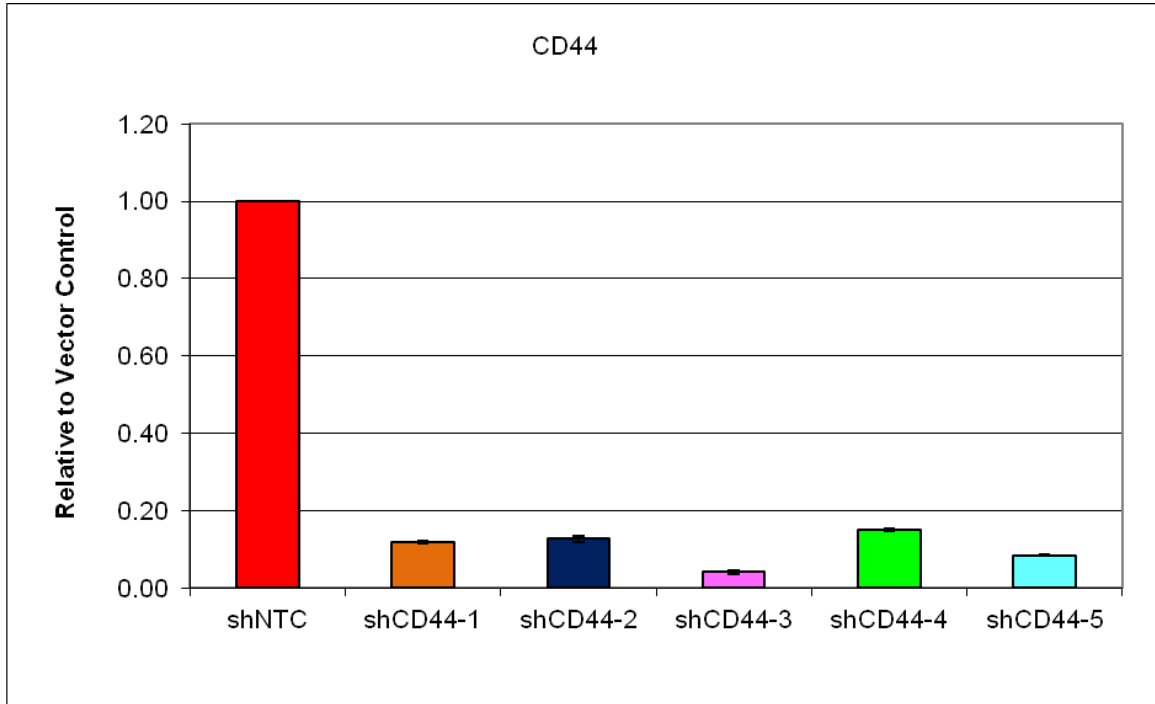
Figure 2.29: Short-hairpin RNA-mediated reduction in CD44 levels in WT Tera2.
Wild-type Tera2 cells were transduced with lentivirus particles carrying anti-CD44
shRNA sequences. Transduced cells were placed under single selection for geneticin (for
stably-transduced cells). For each shRNA sequence, real-time PCR was performed after
approximately 2 weeks after transduction. Sequences targeted by lentiviral cconstructs
are listed in Table 2.2.
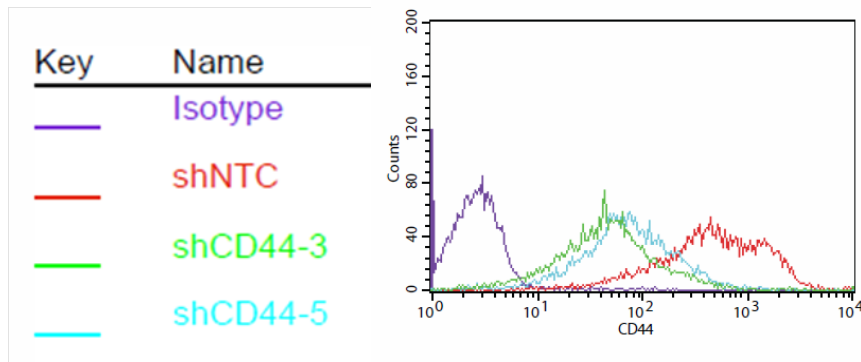
Figure 2.30: Flow cytometry of lentiviral mediated knockdown of CD44. Wild-type Tera2 cells were transduced with lentivirus particles carrying anti-CD44 shRNA sequences. Transduced cells were placed under single antibiotic selection for geneticin (for stably-transduced cells). Flow cytometry was used to validate reduction in surface expression of CD44.
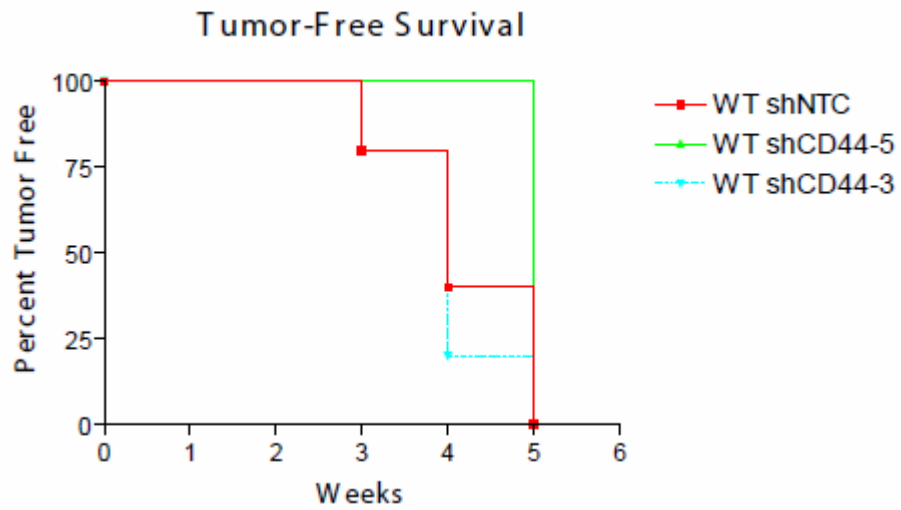
Figure 2.31: Xenografts of WT Tera2 with CD44 lentiviral knockdown. Wild-Type

Tera2 cells were transduced with non-targeting control shRNA sequence (shNTC) or

anti-CD44 shRNA (shCD44-5 or shCD44-3, both effective CD44 protein knockdown),

followed by selection for stable clones with antibiotic selection

A

B
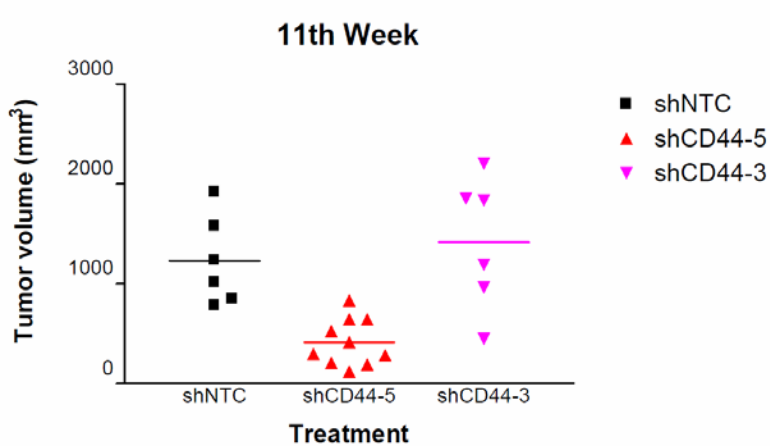
Figure 2.32: Xenografts of WT Tera2 with CD44 lentiviral knockdown. WT Tera2 were transduced with non-targeting control shRNA sequence or anti-CD44 shRNA (shCD44-3 or shCD44-5, both of which demonstrate effective CD44 knockdown), followed by selection for stable clones with geneticin. A.) Average tumor volume (in mm3; n=10 for each group). B.) Tumor volumes of individual tumors in each group.

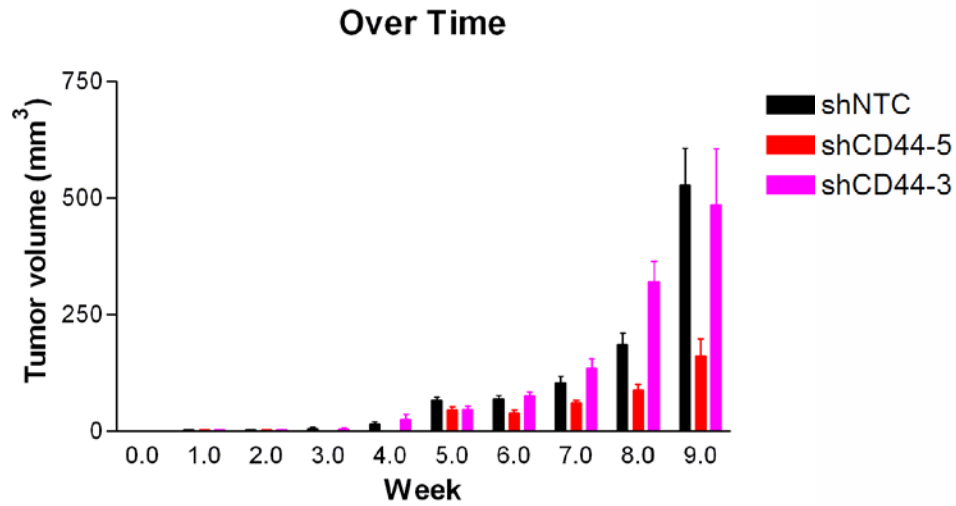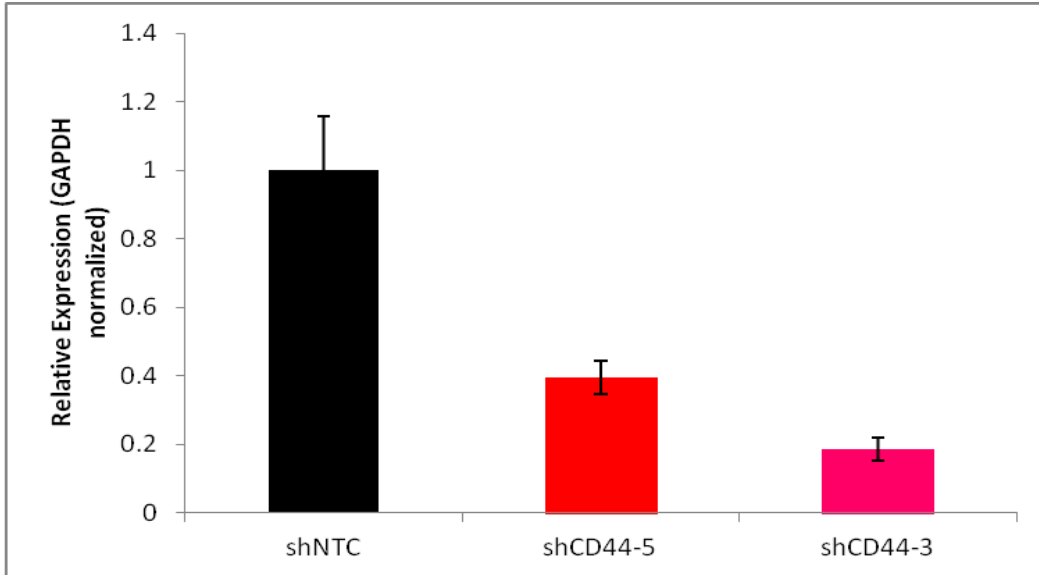**Figure 2.33: CD44 knockdown persistence in excised tumor tissue.** Wild-type Tera2 cells were transduced with lentivirus particles carrying either scrambled shNTC or anti-CD44 shRNA sequences (shCD44-3 or shCD44-5). Transduced cells were placed under single selection for geneticin (for stably-transduced cells) during *in vitro* culture prior to injection into NOD-SCID mice. Xenografted cells were not subject to geneticin selection during growth *in vivo*. For each shRNA sequence, real-time PCR was performed after approximately 2 weeks after transduction. Sequences targeted by lentiviral cconstructs are listed in Table 2.2.
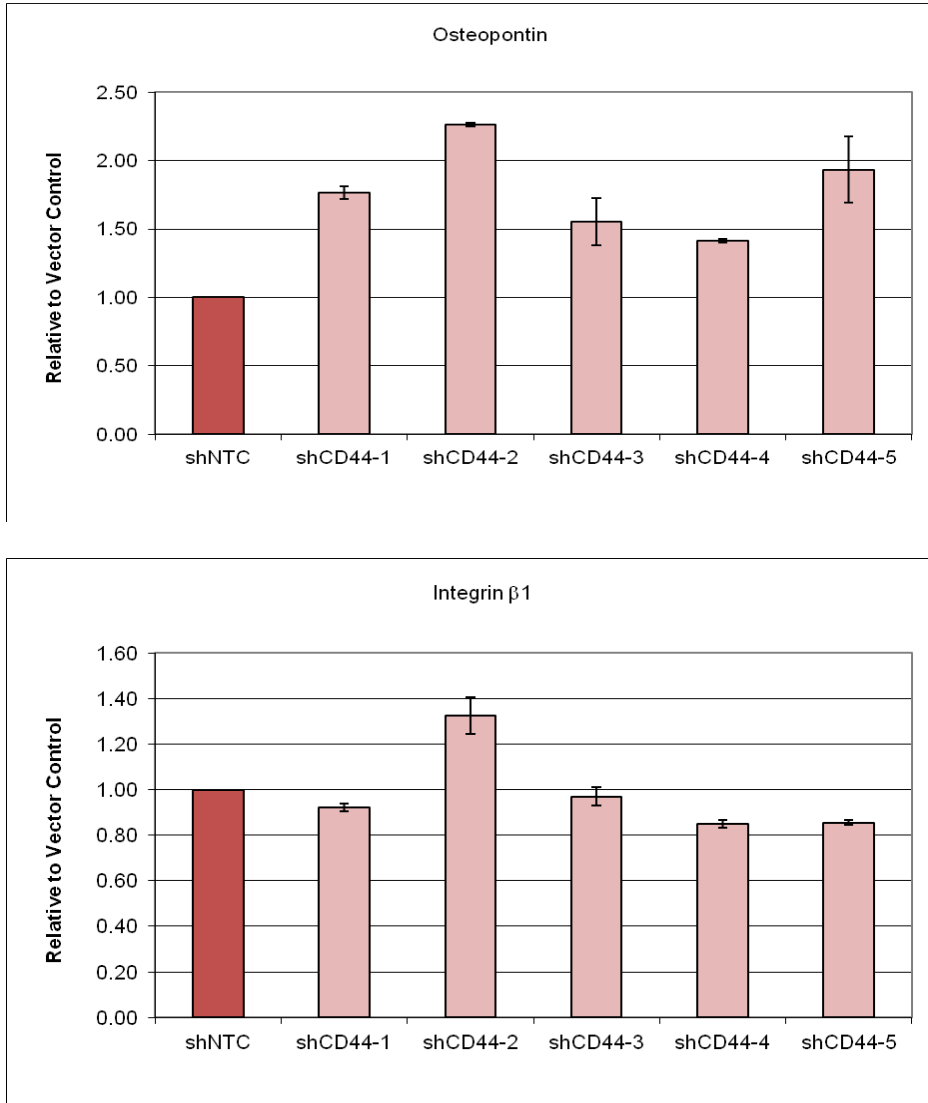
Figure 2.34: Expression levels of integrins in CD44-knockdown empty-vector Tera2 cells. Real-time PCR for osteopontin and integrin β1 in empty vector cells transduced with non-targeting control (shNTC) or anti-CD44 shRNA lentivirus followed by long-term selection for stable clones.

Figure 2.35: MetaCore analysis on gene expression changes in Cbx7 and Cbx7 Outgrowth populations. Orange bars represent comparison of empty vector to Cbx7-overexpressing Tera2 cells, while blue bars represent the comparison of empty vector to Cbx7 Outgrowth populations. Gene expression changes were based on Agilent Gene Expression.

Curriculum Vitae

André Rashad Kydd

akydd1@jhmi.edu

EDUCATION

2004-Present   **Johns Hopkins University School of Medicine**   Baltimore, MD
Doctor of Medicine, Anticipated 2014
Doctor of Philosophy, Anticipated 2014
Cellular and Molecular Medicine Graduate Program

2000-2004   **Harvard College**   Cambridge, MA
Bachelor of Arts, *Magna cum Laude*

HONORS & AWARDS

Johns Hopkins University School of Medicine
2004   Medical Scientist Training Program (MSTP) Training Grant

Harvard College
2004   Honorable Mention, T. Thomas Hoopes Prize for Excellence in Honors Thesis in Biochemical Sciences

2003   National Institutes of Health (NIH) Undergraduate Scholarship Program (UGSP)
- National scholarship for students "committed to careers in biomedical, behavioral, and social science health-related research"

RESEARCH EXPERIENCE

2006-Present   **Interaction of chromatin remodeling complexes and DNA methylation machinery in cancer biology**. Mentor: Stephen B. Baylin, M.D. (Chairman of Department of Tumor Biology, JHUSOM)
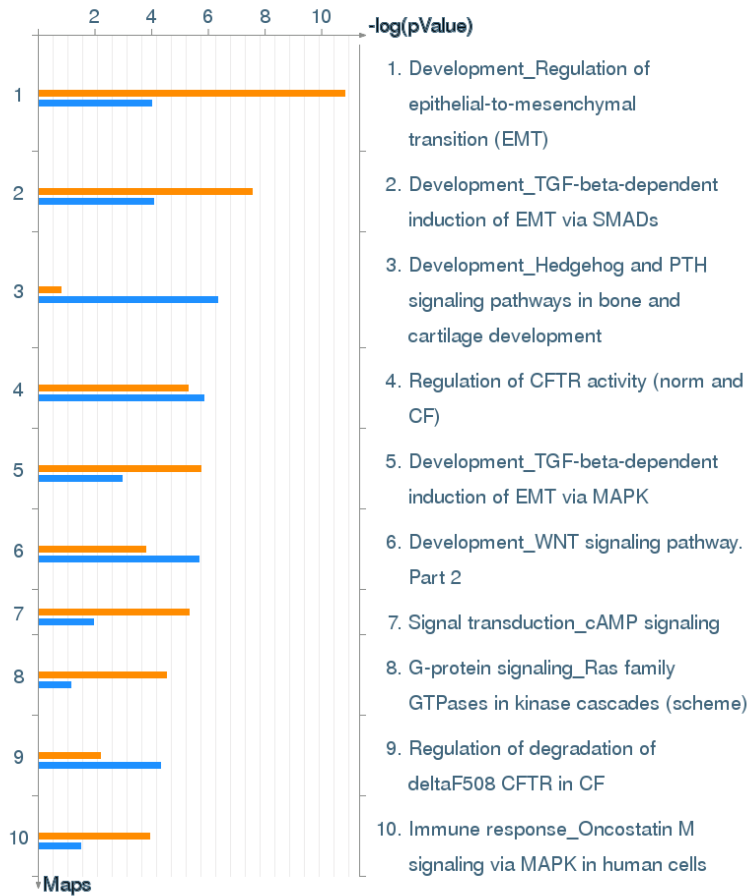*JHUSOM, Baltimore, MD*
- PhD Project: Role of Polycomb Repressive Complex 1 (PRC1) overexpression in DNA promoter hypermethylation and reduced tumorigenicity in teratocarcinoma model
- Genomewide evaluation of DNA methylation patterns by Illumina Infinium450K array, *in vitro* and *in vivo* models of tumorigenicity

2003-2004   **Identification of genomic DNA elements repressed in HTLV-1 infection.**
Mentor: Wayne A. Marasco, M.D., Ph.D. (Tumor Immunology Department- Dana-Farber Cancer Institute/ Harvard University School of Medicine)
Dana-Farber Cancer Institute, Boston, MA
- Senior Honors Thesis: Investigation of virus-associated constitutive activation of leukocyte signaling pathways associated with leukemia

- Use of serial promoter truncation fragments, DNase footprinting assay, electrophoretic mobility shift assay (EMSA), and luciferase reporter assays to identify binding sites for regulatory proteins

2003, 2004 **Tumor-specific antigens for cancer immunotherapy**. Mentor: Ira Pastan, M.D. (Head, Laboratory of Molecular Biology, National Cancer Institute)
National Cancer Institute, Bethesda, MD
- UGSP Summer Project: Identification of proteins with cancer-specific expression as potential targets for immune-targeted therapy

PUBLICATIONS

Cheng J, **Kydd AR**, Nakase K, Noonan KM, Murakami A, Tao H, Dwyer M, Xu C, Zhu Q, Marasco WA. Negative regulation of the SH2-homology containing protein-tyrosine phosphatase-1 (SHP-1) P2 promoter by the HTLV-1 Tax oncoprotein. Blood. 110(6): 2110-20, Sept, 2007

Bera TK, Saint Fleur A, Lee Y, **Kydd A**, Hahn Y, Popescu NC, Zimonjic DB, Lee B, Pastan I. POTE paralogs are induced and differentially expressed in many cancers. Cancer Res. 66 (1):52-56,2006.

PRESENTATIONS AND POSTERS

2004 **Oral Presentation**: "Differential expression of POTE Paralogs in Prostate Cancers." Biomedical Sciences Career Program's New England Science Symposium, Boston, MA.